VARIOUS ASPECTS OF GRAVITY

By

Marcin Jankiewicz

Dissertation

Submitted to the Faculty of the

Graduate School of Vanderbilt University

in partial fulfillment of the requirements

for the degree of

DOCTOR OF PHILOSOPHY

in

Physics

May, 2007

Nashville, Tennessee

Approved:

Thomas W. Kephart

Thomas J. Weiler

Robert J. Scherrer

Volker E. Oberacker

John G. Ratcliffe

PHYSICS

VARIOUS ASPECTS OF GRAVITY

MARCIN JANKIEWICZ

Dissertation under the direction of Professor Thomas W. Kephart

This thesis summarizes research projects that I have been involved in during my graduate studies at Vanderbilt University. My research spanned different areas of theoretical high energy physics with gravity as a common denominator. I explore both fundamental and phenomenological aspects of: (i) mathematical physics where I have studied relations between partition functions of certain class of conformal field theories and Fischer-Griess Monster group; (ii) cosmology, where I performed a numerical study of a horizon size modes of scalar field; (iii) a black hole physics project involving possible extensions of the non-hair theorem in a presence of exotic types of scalar field; and (iv) a study of phenomenological space-time foam models and their relation to Planck scale physics.

Approved_____ Date_____

ACKNOWLEDGMENTS

It is a pleasure to thank first and foremost, Dr. Thomas W. Kephart and Dr. Thomas J. Weiler for this great time and all of these research and life experiences. I would also like to thank the other members of my Ph.D. committee: Dr. Volker E. Oberacker, Dr. John G. Ratcliffe and Dr. Robert J. Scherrer. And finally, I would like to thank my family, friends and collaborators: Dr. Anjan Sen, Dr. Ralf Lehnert (dude), Dr. Liguo Song, Dr. James Dent, Dr. Arjun Berera, Dr. Roman V. Buniy, Dr. Sergio Palomarez-Ruiz, Mr. Matthew Weippert and Ms. Martha J. Holmes, for their love and support.

To my parents: Ta praca jest dedykowana dla was kochani rodzice.

TABLE OF CONTENTS

LIST OF TABLES

LIST OF FIGURES

CHAPTER I

INTRODUCTION TO EVERYTHING

1.1 Overview of The Field

This thesis is a collection of the theoretical investigations that I participated in during my graduate tenure. The title of this work is a compromise, since, some of our findings are tenuously related to a theory of gravity. However, additional review material is presented tying everything together.

1.1.1 History of the Standard Model of Particle Interactions and Beyond

Currently, there are three types of interactions: electro-weak, strong and gravitational. Historically, unification is something to be expected. But this argument, which is somewhat appealing, is an aesthetic one. Beauty is definitely an important argument, however it might not be sufficient if one decides to choose it as a primary motivation for further research in the fundamental sciences. There are however clues of unification; such as running coupling constants of electromagnetic, weak and strong interactions, that together with a concept of supersymmetry suggest that unification of interactions may be a fact. Moreover, we have electrons, muons, neutrinos, quarks, W bosons, gluons etc., the list is rather large and the whole collection begins to look like a zoo. The Standard Model of particle interactions, excluding gravity, is described by one ugly direct product of three gauge groups (modulo some finite groups)

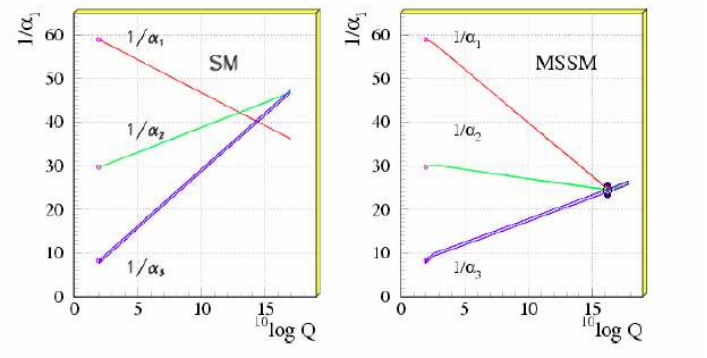

Figure 1: Unification of gauge coupling constants in the Standard Model (SM) and its superymmetric extension (MSSM).

$SU(3)_C \times SU(2)_L \times U(1)_Y$, therefore unification could simplify this complicated picture. However, Standard Model works, it correctly describes electroweak and strong interactions. Gravity is absent in this picture; a fully satisfactory theory of quantum gravity does not currently exist. There are clues that give insight into the form of quantum gravity. We seem to understand gravity at a classical level. In this regime, Einstein's theory of general relativity seems to be a working theory. Furthermore, observationally general relativity is the most successful theory so far.

One of the main goals of fundamental physics of the 21th century is the quantization of gravity. Despite decades of research, a comprehensive theory has not been obtained. There are couple of reasons of why this is the case. First, gravitation is a difficult subject to study, for example because classical gravitational field theory is described by a nonlinear theory. Second, contrary to other field theories which are defined on a fixed background space-time manifold, space-time geometry itself becomes dynamical in general relativity. Third, if you want to quantize Einstein's

theory of gravity then one has to face a problem of non-renormalizability, in contrast to all particle interactions described by the Standard Model. Fourth, gravity is weak in comparison to other interactions making it challenging to test and measure in the high-energy regime.

There are several approaches to gravitational interactions at the quantum level. We list only the ones that have drawn recent attention: string/M-theory [1]-[5]; loop quantum-gravity [6]; causal sets [7]; dynamical triangulations [8]; twistor theory [9]; non-commutative geometry [10]; supergravity; cellular networks; approaches based on analogies with condensed matter physics; foamy structure of quantum spacetime. However, none of these theories seem to completely describe Nature.

We want a theory which describes all fundamental forces. There are a couple of examples of successful attempts of unification. Maxwell unified electricity to include magnetism; and optics the first time in the history of physics that three "distinct" theories where unified, i.e. described by a single set of equations related to each other. At this point in history, electricity, magnetism and gravity were the only types of interactions known to physicists. Then during Einstein's era, Theodor Kaluza [11] and Oscar Klein [12] made an attempt to unify electromagnetism to include gravity. The unification, however, required the introduction of an extra spatial dimension. Moreover, it was impossible to quantize their theory. Kaluza and Klein's ideas were forgotten for more then 50 years.

In the first half of the twentieth century, under heavy influence of quantum mechanics and easily accessible experimental data, quantum electrodynamics (QED) was born as a practical realization of what came to be called quantum field theory. For the first time in history, through the work of R.P. Feynman, J. Schwinger, I. Tomonaga and others, a fully satisfactionary quantum theory of electrodynamics was formulated. QED is an example of a gauge theory with a $U(1)_{em}$ gauge symmetry containing a single generator, which physically corresponds to a single interaction boson, the photon.

In the 60s, Sheldon Glashow [14], Steven Weinberg [15], Abdus Salam [16] proposed a unifying model of electromagnetic and weak interactions. This was accomplished under an $SU(2) \times U(1)_Y$ gauge group. The theory can be spontaneously broken, through a Higgs mechanism to the $U(1)_{em}$ electromagnetic gauge group. The theory of electroweak interactions contains three electroweak bosons called $W^{\pm}$ and Z which mediate weak interactions, and a photon corresponding to electromagnetic interactions. Moreover it was shown by Gerard 't Hooft and Martinus Veltman [17] that the electroweak theory is renormalizable, if the Lagrangian of the theory is not allowed to contain combinations of the field operators of dimension higher then four in energy units, and so the number of counter-terms required to cancel all divergences is finite.

Later, together with the use of group theory and the discovery of color $SU(3)$ symmetry, physicists were finally prepared to take the next step towards unification. Both strong and weak interactions were discovered from experiments, and quantum

chromodynamics (QCD) was developed in the 70s to successfully describe strong interactions. In QCD, interactions are mediated by eight gluons. Moreover, QCD is renormalizable, and possesses a property of asymptotic freedom, which means that at high energies strongly interacting quarks and gluons are nearly non-interacting ("free").

Finally, quantum theories of all interactions but gravity were present in the picture. Following the success of earlier unification attempts such as Maxwell's electromagnetism, and using techniques developed for electroweak theory, i.e., spontaneous symmetry breaking, physicists pushed the idea of unification even further. In the 1970s, physicists tried to unify the two fundamental particle interactions: electroweak and strong. Physicists, were looking for a simple gauge group, G that would break to a Standard Model gauge group at high energy scales, yet agree with experiments. There is some theoretical and experimental evidence for unification at low energies, in particular the coupling constants of the interactions run, i.e., the coupling "constants" of all of the gauge interactions depend on the energy scale, and when extrapolated to high energies possibly meet. There are a lot of gauge groups G that could in principle serve as a grand unifying (GU) group. We list some of them: minimal left-right model $SU(3)_c \times SU(2)_L \times SU(2)_R \times U(1)_{B-L}$; Georgi-Glashow model SU(5); SO(10); flipped $SU(5) \sim SU(5) \times U(1)$, Pati-Salam model $SU(4) \times SU(2) \times SU(2)$; flipped $SO(10) \sim SO(10) \times U(1)$; trinification $SU(3) \times SU(3) \times SU(3)$; $SU(6)$ and E_6 gauge symmetry. But GU as a stand alone theory ran into difficulties. The theory possesses

a "hierarchy problem" i.e., the unification scale is much higher than the masses of familiar elementary particles, such as electrons or quarks. Hence a natural question to ask would be the following: Why are these particles so much lighter then the GU scale? The discrepancy between these scales is roughly 16 orders of magnitude! Current GU theories predict the unification scale to be somewhere around $10^{16}GeV$. Moreover, unless supplemented by supersymmetry, unification of GU theories at high energies is not exact, meaning that the energy-scale, where the unification occurs, isn't a well defined point, i.e., values of the running coupling constants at a unification point don't exactly match each other. Supersymmetry solves the hierarchy problem (although not entirely) by stabilization of the electroweak Higgs boson mass against radiative corrections. But, even supersymmetric GU theories seem not to be fully accepted by the scientific community.

In the early 70s, string theory was proposed as an explanation for the symmetry between the scattering amplitudes in the $s-$ and $t-$channels of the scattering processes of strongly interacting mesons. In the presence of more satisfying and experimentally appealing QCD, string models of the strong interactions were abandoned. However, a certain class of the string models (bosonic strings) can serve as a quantum theory of gravity. Moreover, in the early 80s it was realized that all of the Standard Model interactions and gravity can be accommodated in the eleven dimensional supergravity and ten dimensional superstring theories, and many techniques were developed to reduce the dimensionality of this theory to our familiar four space-time dimensions. There are several other reasons why we consider superstring theory [1]-[5] as a pos-

sible candidate for the theory of all interactions. Superstring theory gains control over divergences that enter traditional quantum field theory. The following is a short overview of string theory.

One can distinguish two types of strings, open and closed. In order to have a consistent quantum string theory, which would describe physical reality, strings have to propagate on a higher dimensional (higher then four dimensional) manifold. This is related to cancellation of gauge anomalies in D dimensions. In its simplest form, bosonic string models are free of anomaly in Lorentz algebra in $D = 26$, and for superstring/heterotic models anomalies are canceled in $D = 10$. Since the Standard Model gauge interactions are stuck on the physical four dimensional manifold, they cannot penetrate extra dimensions. As a result, it is necessary to divide space-time into two parts, one where Standard Model interactions can propagate, and one in which they cannot. The simplest way is to compactify the extra dimensions on a torus. Realistic string models use more complicated compactification manifolds, like six dimensional Calabi-Yau manifolds, etc. However, it is not clear which is the right compactification space. There are too many choices, since there are many possible moduli, i.e., sets of scalar fields that parametrize the shape of the compact space. One ends up with many possible solutions, each corresponding to a different set of physical laws and realities. We know only that a final theory should have a four dimensional space-time where all interactions should be properly described.

1.1.2 History of Standard Model of Cosmology and Beyond

The universe appears to be both homogeneous and isotropic. This fact is an approximation that becomes better and better as cosmological length scale increases. In other words, the universe can be described by the Robertson-Walker metric at large scales. There are other interesting observations, for example observational evidence of the acceleration of the universe, which follows from the observations in high redshift surveys of type Ia supernovae [13]. Acceleration is also independently implied from the cosmic microwave background experiment WMAP (The Wilkinson Microwave Anisotropy Probe). The favored explanation for this behavior is that the universe is presently dominated by some form of dark energy density, contributing 74% of the critical energy density, i.e., density required for the universe to be flat (curvature of the space-time goes to zero on large scales). The remaining matter is thought to be 22% non-baryonic dark matter, and 4% of the ordinary baryonic matter.

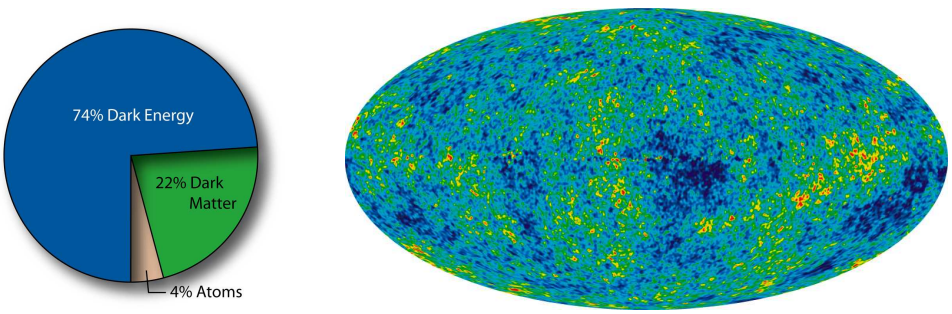

Figure 2: Content of the universe according to WMAP data. Full-sky WMAP image of the fluctuations in Cosmic Microwave Background. Credit: NASA/WMAP Science Team.

The idea of cosmic inflation is regarded as a breakthrough in modern cosmology: it solves the horizon[1], flatness[2] and monopole[3] problems, and provides a mechanism for the generation of density perturbations needed to seed the formation of structure in the universe. Moreover, even today, i.e., after radiation and matter domination epochs, dark energy which is broadly similar to inflation, is responsible for the acceleration of the universe.

The cosmological constant[4] is in many respects the most economical solution to the problem of cosmic acceleration. It successfully explains a multitude of observations. The current standard model of cosmology, the Lambda-CDM model, includes the cosmological constant as an essential feature. Alternatively, dark energy might arise from the particle-like excitations in some type of dynamical field, like quintessence, a self-interacting scalar field with a potential acting as a negative pressure source. Quintessence differs from the cosmological constant in that it can vary in space and time. In order for it not to clump and form structure like matter, it must be very light and so have a large Compton wavelength.

No evidence of quintessence is yet available, but it cannot be ruled out either. It generally predicts a slightly slower acceleration of the expansion of the universe than the cosmological constant. Some think that the best evidence for quintessence will

[1]Causally disconnected regions of the universe have the same temperature and other physical properties; this is the horizon problem.

[2]Energy density of the universe today is very close to the critical energy density; this is the flatness problem.

[3]Monopoles created early in the universe haven't been observed today; this is the monopole problem.

[4]The cosmological constant Λ is a term that can be added to Einstein's equations: $G_{\mu\nu} + \Lambda g_{\mu\nu} = T_{\mu\nu}$.

come from violations of Einstein's equivalence principle and/or variations of fundamental constants in space or time.

The cosmic coincidence problem asks why cosmic acceleration began just recently. If cosmic acceleration began earlier in the universe, structures such as galaxies would never have had time to form, and life, at least as we know it, would never have had a chance to exist. Proponents of the anthropic principle view this as support for their arguments. However, many models of quintessence have a so-called tracker behavior, which solves this problem. In these models, the quintessence field has a density which closely tracks the radiation density until matter-radiation equality, which triggers quintessence to start behaving as dark energy and ultimately causes it to dominate the universe. This mechanism sets the low energy scale of the dark energy.

Some special cases of quintessence are phantom energy, in which the energy density of quintessence actually increases with time, and k-essence (short for kinetic quintessence) which has a non-standard form of kinetic energy. They can have unusual properties: phantom energy, for example, can cause a Big Rip, i.e., all matter, from galaxies to atoms will be torn apart by the expansion of the universe.

1.2 The Plan

This dissertation represents research performed between 2001 and 2006 at Vanderbilt University. Herein we address several fundamental problems related to the understanding of the theory of gravity in all of its aspects, i.e., phenomenological

and formal. The goal was approached in an indirect way, i.e., none of our research projects focused directly on gravitation. However, indirect correlations to the subject are clearly stated.

In Chapter II we discuss space-time foam, a phenomenological model of the behavior of space-time at the Planck scale. We will represent some numerical results and tests performed to explain some astrophysical data. The major goal of Chapter III is to discuss the relevance of scalar fields with modes of the size of the universe's horizon. Numerical results will be presented, and we will discuss the relevance of the results to current observations in cosmology. In Chapter IV we will switch gears to black hole physics. We discuss possible expansions of the no-hair theorem for black holes. In Chapter V we discuss conformal field theories and their relationship to the Monster group. Finally in Chapter VI we will summarize the results and conclude.

This thesis results from collaborations and discussions with Thomas W. Kephart, Thomas J. Weiler, Anjan Sen, and is based on the following articles and preprints:

- M. Jankiewicz, Anjan A. Sen, "Black Holes and Generalized Scalar Field", submitted to Physics Letters B [gr-qc/0602085].
- M. Jankiewicz, T.W. Kephart, "Long Wavelength Modes of Cosmological Scalar Fields", published in Physical Review D 73, 123514, 2006, [hep-ph/0510009].
- M. Jankiewicz, T.W. Kephart, "Transformations Among Large c Conformal Field Theories", published in Nuclear Physics B 744, 380, 2006, [hep-th/0502190].

- M. Jankiewicz, R.V. Buniy, T.W. Kephart, T.J. Weiler: "Space-Time Foam and Cosmic Ray Interactions" published in Astroparticle Physics vol. 21/6 pp. 651-666, [hep-ph/0312221].

Before we proceed further let us briefly introduce our research topics, and discuss the obtained results and their relevance.

1.2.1 Space-Time Foam and Lorentz Invariance

The physics of space-time at the classical level is described by General Relativity. This theory is supported by at least three arguments. First, we impose an equivalence principle, which states that freely falling bodies accelerate at the same rate in the gravitational field independent on their compositions, also known as the principle of universality of free fall. Second, in General Relativity we assume that local Lorentz invariance holds. Third, we impose local position invariance. Violation of any of these principles leads to interesting physical theories with new phenomenology. We expect that violations of the fundamental classical principles would be present at an extremely high energy scale, possibly the Planck scale $M_P \equiv \frac{1}{\sqrt{G_N}}$ (where G_N is a four dimensional Newton's constant) where we expect quantum gravity effects to be present as well. However, quantum gravity and violations of the fundamental symmetries could in principle modify physics at low energies. Although this possibility still remains only a speculation, we want to list a couple of potential manifestations of quantum gravity in the low-energy regime, i.e., energy scales currently accessible

by present and near-future experiments[5].

Lorentz violation could introduce new energy threshold for reactions, for example photon decay or vacuum Cerenkov radiation[6]. At the same time, existing thresholds of some processes can be shifted, like in photon annihilation from blazars[7], and so-called Greisen-Zatsepin-Kuzmin[8] (GZK) threshold in the cosmic ray spectrum [40]. For decay processes without a threshold we also can infer the effects of Lorentz violation, for example decay of a particle from one helicity to the other. Other possible incarnations of Lorentz violating effects include the modification of dispersion relations (between energy and momentum) for certain species of particles, or violation of couplings at cosmological (horizon) scales.

Lorentz and related CPT invariance are cornerstones of our present description of the fundamental model of the Universe. Invariance under Lorentz transformations states that the laws of physics are independent of the reference frame. This is an underlying symmetry of all current physical theories. Some evidence recently found in the context of string field theory indicates that this symmetry can be spontaneously broken. That is why, one can think about theories with broken Lorentz invariance in much broader context, i.e., from the point of view of pure phenomenology of physics at the Planck scale. The experimental verification of broken Lorentz symmetry poses a

[5]For more complete list refer to a nice review by A. Kostelecky [18].

[6]Cerenkov radiation is electromagnetic radiation emitted when a charged particle passes through a medium with velocity higher then a speed of light in this medium.

[7]A very compact and highly variable energy source at the center of the host galaxy, possibly related to the existence of supermassive black hole.

[8]Theoretical upper limit, calculated from the interactions between cosmic rays and cosmic microwave bacground, on the energy of cosmic rays originating from distant sources.

significant challenge. As a part of our original motivation, we listed the non-existence of a proper formulation of the unified quantum theory of fundamental interactions including gravity. We do believe that such a theory would become present at the Planck scale, but this scale is not accessible by current or and future accelerators. This is a problem. Moreover, one has to understand fundamental symmetries at these energy scales, since their conservation is an assumption that has to be experimentally verified. It has already been pointed out that astrophysical observations of distant sources of gamma radiation could give insight into the nature of gravity-induced wave dispersion in vacuum, and therefore point toward physics beyond the Standard Model. Limits on Lorentz symmetry violation based on the observations of ultra high-energy cosmic rays with energies beyond $5 \times 10^{19} eV$, the GZK cut-off, have also been discussed in recent literature. First, let us discuss the problem. The production of pions from the interaction of ultra-high-energy cosmic rays with cosmic microwave background photons would continue until the energy of the protons would fall below the pion production threshold of $5 \times 10^{19} eV$. Calculation shows that extragalactic cosmic rays originating from sources at distances more than 50 Mpc from the Earth with energies greater than this threshold energy should never be observed on Earth, since there are no known sources within this distance that could produce them. A number of observations have been made by the AGASA experiment that appear to show cosmic rays from distant sources with energies above this limit, see Figure-3. The observation of these particles is the GZK paradox or cosmic ray paradox. As one can see from the Figure-3, only the AGASA experiment predicts extension of the

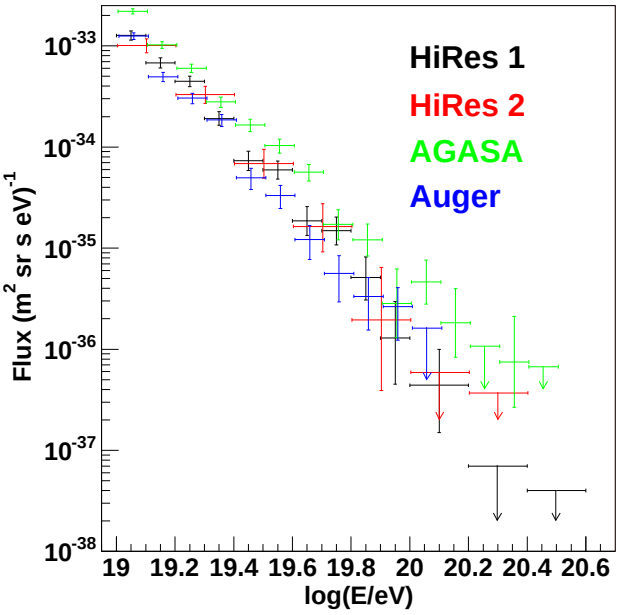

Figure 3: Ultra-high-energy cosmic ray spectra measured by AGASA [19], and other experiments, like Auger [20] and HiRes [21, 22]. For detailed comparison of these experiments refer to [23].

spectrum beyond GZK cutoff.

It has been proposed that propagation of cosmic rays at extreme-energy may be sensitive to Lorentz-violating metric fluctuations ("foam") [24]. We investigate the changes in interaction thresholds for cosmic-rays and gamma-rays interacting on the CMB and infrared (IR) backgrounds, for a class of stochastic models of space-time foam. The strength of the foam is characterized by the factor $(E_{th}/M_P)^a$, where a is a phenomenological suppression parameter and E_{th} is threshold energy of a given reaction. We find that there exists a critical value of a (dependent on the particular reaction: $a_{\rm crit} \sim 3$ for cosmic-rays, ~ 1 for gamma-rays), below which the threshold energy can only be lowered, and above which the threshold energy may be raised,

but at most by a factor of two. Thus, it does not appear possible in this class of models to extend cosmic-ray spectra significantly beyond their classical absorption energies. However, the lower thresholds resulting from foam may have signatures in the cosmic-ray spectrum. In the context of this foam model, we find that cosmic-ray energies cannot exceed the fundamental Planck scale, and so set a lower bound of 10^8 TeV for the scale of gravity. We also find that suppression of $p \to p\pi^0$ and $\gamma \to e^- e^+$ "decays" favors values $a \gtrsim a_{\rm crit}$. Finally, we comment on the apparent non-conservation of particle energy-momentum, and speculate on its re-emergence as dark energy in the foamy vacuum.

1.2.2 Cosmological Scalar Fields

Scalar fields have played a major role in attempts to model the early Universe. In particular, nearly every incarnation of the inflation scenario has relied on scalars to generate vacuum energy and in turn exponential expansion and density fluctuations. Many of these models rely on slow-roll potentials, i.e., potentials that are nearly flat where the scalar masses can be very small. Recently, horizon size and super horizon size density perturbations have been studied intensively, because of their importance for understanding low multipoles (ℓ modes) (see [41] and references therein) in the WMAP data [42]. The generic Lagrangian [25] for a scalar in a Friedmann-Robertson-Walker (FRW) Universe is

$$\mathcal{L} = g^{\mu\nu}\partial_\mu\phi\partial_\nu\phi + \xi\phi^2 R - V(\phi)\,. \tag{I.1}$$

If $V(\phi)$ contains no dimensionful parameters, then the scalar field is conformally[9] coupled when $\xi = 1/6$. Conformal invariance can be broken by including a mass term in $V(\phi)$. The other value that is encountered in the literature is $\xi = 0$ (minimal coupling). There have been proposals [26] which discuss the possibility of strong coupling, i.e., $|\xi| >> 0$. The presence of a non-minimally coupled scalar fields in a theory is not just convenient, it is forced upon us in many cosmological scenarios, like inflation. Moreover, non-minimally coupled scalar fields can appear as a quantum correction to the scalar theory, even if $\xi = 0$ was considered for the classical, unperturbed, theory. There is no definite answer to the question: what is the numerical value of the coupling constant ξ. The answer depends on a theory of gravity and the form of the scalar field. In most of the inflationary scenarios, the value of the coupling constant $\xi \neq 0$ cannot be avoided. Here we assume that the local (Minkowski limit) real ϕ^4 theory is renormalizable. While this is not completely general, it is sufficient for our purposes. One could easily generalize our analysis to complex fields or fields in irreducible representations of some continuous symmetry group. We give a numerical analysis of long-wavelength modes in the WKB approximation of cosmological scalar fields coupled to gravity via $\xi\phi^2 R$. Massless fields are coupled conformally at $\xi = 1/6$. Conformality can be preserved for fields of nonzero mass by shifting ξ. We discuss the implications for density perturbations.

Long wavelength scalar field modes have interesting properties when the wave-

[9] An n-dimensional theory is said to be conformal if it is invariant under $SO(n, 2)$ conformal group in n dimensions in the case of $n + 1$ dimensional Minkowski space-time and $SO(n + 1, 1)$ group in the Euclidean space. A presence of the mass term in the Lagrangian can conformal symmetry.

length is on the order of the horizon size cH_0^{-1}. One finds dispersion and diffraction effects that depend on the scalar mass and its coupling to gravity.

One expects scalars to be an integral part of any realistic model. For instance, if the overarching theory is based on strings with a local or global SUSY preserved down to some scale, then the scalars will be components of some superfield Φ contributing to the superpotential $W(\Phi)$. This will put constraints on $V(\phi)$. In particular, flat directions could result (regions of moduli space where the scalar mass vanishes) and lead to massless or nearly massless modes, where for example SUSY could be broken by nonperturbative effects. We give these comments as a justification for the study of scalar zero modes and modes of very small positive mass or modes of very small imaginary mass.

As the wavelength approaches the horizon size, the naive redshift formula no longer applies and one must refine the flat space analysis of the scalar field dispersion relation [43, 44]. We will carry out a numerical analysis of the behavior of long wavelength scalar field modes and investigate the dependence of the redshift on the scalar field mass, and its coupling to gravity.

1.2.3 Black Holes, Generalized Scalar Fields and No-Hair Theorem

Inspired by the uniqueness theorems for static and stationary asymptotically flat vacuum black holes in Einstein-Maxwell theory [63], Wheeler [64] famously conjectured that "black holes have no hair" in more general matter theories, in four dimensions.

The no-hair theorem states that black holes are completely characterized by three externally observable parameters: mass, electrical charge, and angular momentum. All other information about the matter which formed a black hole or fell into it, "disappears" behind the black-hole event horizon and is therefore permanently inaccessible to external observers. For example, there would be no way for an external observer to distinguish a black hole made of ordinary matter from one made of anti-matter.

Wheeler's idea is a conjecture. There exist some rigorous proofs of no-hair theorems, but they are limited to specific kinds of matter. On the other hand, Wheeler's hypothesis was proven wrong in Einstein-Yang-Mills [65] and Einstein-Skyrme theory [66], in various combinations with dilaton or Higgs fields [67]. Some, but not all, of these "hairy" black holes are unstable. For gravity coupled to scalar fields, possibly in combination with Abelian gauge fields, a precise formulation of the no-hair conjecture has not yet been given. In this area there still remains interesting ground to explore between several rigorous (but limited) no-hair theorems, and a number of explicit "hairy" black hole solutions which appear to disagree with Wheeler's conjecture in its most general form.

Here, we will study the possibility of scalar hair with a non-canonical kinetic term for a static, spherically symmetric asymptotically flat black hole space-time. We first obtain a general equation for this purpose and then consider various examples for the kinetic term $F(X)$ with $X = -\frac{1}{2}\partial^\mu\phi\partial_\mu\phi$. For example, our study shows that for a tachyon field with a positive potential, which naturally arises in open string theory, an asymptotically flat static black hole solution does not exist. However, we show

that for other types of scalar fields, the existence of the black hole solution with a corresponding scalar hair is guaranteed.

1.2.4 Conformal Field Theories, their Partition Functions, and the Monster Group

We show that there is a set of transformations that relates all of the 24-dimensional even self-dual (Niemeier) lattices[10], and also leads to non-lattice objects, some of which can perhaps be interpreted as a basis for the construction of holomorphic conformal field theories.

We extend our observations to higher dimensional conformal field theories built on so-called extremal partition functions, where we generate $c = 24 \cdot k$ theories, where c is a central charge of a given conformal field theory, that can be interpreted as a dimension of a given lattice, and k is a positive integer. We argue that there exists generalizations of the $c = 24$ models based on Niemeier lattices and of the non-Niemeier spin-1 theories. One of the reasons why we choose 24 dimensions as a staring point of our considerations is that the partition functions of the corresponding conformal field theories are simple, and can serve as toy models for more realistic theories. The extremal cases have spectra decomposable into the irreducible representations of the Fischer-Griess Monster group.

This group is the largest *sporadic* group. A group is called finite if it has finite number of elements. It's called simple if it doesn't have any *normal subgroups*[11]

[10]Every lattice in $\mathbb{R}^n$ can be generated from a basis of the vector space by forming all linear combinations with integral coefficients. More detailed introduction to the subject will be given in Chapter V.

[11]A normal subgroup is the one with elements being invariant under conjugation, i.e., $\forall_{n \in N}$ and

except for the subgroup consisting only of the identity element and the group itself. The classification of simple finite groups seems to be complete. There are 18 infinite families of finite simple group, and 26 sporadic groups that do not follow any pattern. The situation is similar to the Cartan classification for the continuous groups, where there are infinite families of A_n, B_n, C_n and D_n groups and 5 simple exceptional Lie groups G_2, F_4, E_6, E_7 and E_8. The Monster is the largest of sporadic groups. It has order

$$808017424794512875886459904961710757005754368000000000 \approx 8 \times 10^{53}\,.$$

It was proven by Richard Borcherds [27] in 1992, that the Monster group relates mathematical aspects of both finite and continuous groups, so-called Monstrous Moonshine. It can be shown that Monster group is a symmetry group of conformal field theory built on one of the Niemeier lattices, called the Leech lattice. The Leech lattice is special. It is the lattice on which the highest density packing of spheres in 24 dimensions can be obtained. Just like in two and three dimensions where a hexagonal lattice, with correspondingly 6 and 12 nearest neighbors, give the most efficient sphere packing, the Leech lattice with 196560 nearest neighbors is the densest lattice in 24 dimensions. This number can be read off the partition function of the lattice. The construction of the partition function giving best packing, so-called extremal partition function, will be presented in the general $24k$ dimensional case.

The relation between the coefficient of the partition function corresponding to the extremal configuration in 24 dimensions and dimensions of the irreducible rep-

$\forall_{g\in G}$, the element $gng^{-1} \in N$, where N is a normal subgroup of G.

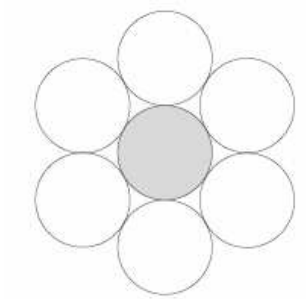

Figure 4: Densest sphere packing in two dimensions, with six nearest neighbors, is obtained in hexagonal configuration [28].

resentations of the Monster group, i.e., regular 24 dimensional moonshine, together with explicit construction of higher dimensional extremal cases, lead us to conjecture that these extremal theories, as well as the higher dimensional analogs of the group lattice based Niemeiers, will eventually yield to a full construction of their associated conformal field theories (CFTs).

We have obtained interesting patterns emerging from the construction of these theories together with new relations between corresponding partition functions and irreducible representations of the Monster group, a fact that can be seen as a generalization of the original Monster Moonshine. Moreover, we observe interesting periodicities in the coefficients of extremal partition functions.

CHAPTER II

PHENOMENOLOGICAL SPACE-TIME FOAM

In this chapter we present a family of phenomenological models of space-time foam with the scale induced by a Planck mass. First, we introduce the formalism and possible realizations of the foam. Second, we discuss the connections between the models and broken Lorentz invariance and how this fact relates to the particle kinematics and conservation of energy-momentum. We discuss possible experimental tests of these models with various of astroparticle processes. We also give a possible interpretation of the low energy effects of Planck scale induced by space-time foam. The result presented here was published in Astropart. Phys. **21**, 651 (2004).

2.1 Introduction of the model: metric fluctuations

The space-time metric tensor $g_{\mu\nu}$ becomes a dynamical variable when gravity is quantized, and space-time foam is the quantum mechanical uncertainty $\delta g_{\mu\nu}$ in this variable. We investigate the possibility that the foam has phenomenological consequences.

We work within the framework of foam models having a parameterization given by

$$\delta g_{\mu\nu} \geq \left(\frac{l_P}{l}\right)^a \sim \left(\frac{t_P}{t}\right)^a \ , \tag{II.1}$$

where $l_P \equiv \sqrt{\frac{\hbar G}{c^3}}$ is the Planck length and $t_P \equiv \frac{l_P}{c}$ is the Planck time in a four-

dimensional theory. In theories with more than four dimensions, these scales could be larger, in fact, much larger, than the Planck scales. The parameter "a" depends on the foam model [29, 30]. The covariance implicit in the fluctuation variable $\delta g_{\mu\nu}$ puts space and time uncertainties on an equal basis, in contrast to the situation in non-relativistic quantum mechanics where the length-momentum relation arises from operator commutators, and the energy-time relation from a less-compelling argument using the Fourier decomposition. The uncertainty relations given in Eq. (II.1), and those that follow below, are sometimes called "Generalized Uncertainty Principles" (GUP). We will use this name.

From (II.1) and the fact that $\delta l^2 = l^2 \delta g$, one obtains the uncertainties for length and time:

$$\delta l \geq \frac{l}{2} \left(\frac{l_P}{l}\right)^a , \qquad \text{and } \delta t \geq \frac{t}{2} \left(\frac{t_P}{t}\right)^a \tag{II.2}$$

The quantum mechanical relations between length and momentum, and time and energy, then lead to the equivalent expressions for the uncertainty:

$$\delta E \geq \frac{E}{2} \left(\frac{E}{M_P\, c^2}\right)^a , \qquad \text{and } \delta p \geq \frac{p}{2} \left(\frac{p}{M_P\, c}\right)^a , \tag{II.3}$$

where $M_P \sim 10^{28} eV$ denotes Planck mass. From here on we drop explicit mention of powers of c. These uncertain lengths, energies, etc., make the lengths of four-vectors uncertain, and so break Special Relativity. Accordingly, we must single out a frame in which these uncertainties are defined. It is common to assume that the special frame is the cosmic rest frame, in which the cosmic microwave background (CMB) is isotropic. We adopt this assumption.

The uncertainty relations defined above can effect violations of Lorentz invariance (LIV) even in the weak-field, flat-space limit. Two of the most studied cases are (i) modification of the energy-momentum conservation equations, $\Delta P^{\mu} = 0$, or (ii) modification of the energy-momentum dispersion relation, $p^{\mu}\, p_{\mu} = m^2$. Of course, LIV may also appear in both (i) and (ii) simultaneously. In this work, we study LIV of the energy-momentum conservation law at the scales defining the GUP, but maintain the usual dispersion relation $E_i^2 = p_i^2 + m_i^2$.

2.2 Modified threshold energy for $2 \rightarrow 2$ scattering reactions

Following many others [29]-[38], we investigate the role that LIV-kinematics may play on ultra-high energy cosmic rays (UHECRs). The UHECRs are gamma-rays at $E \sim$ tens of TeV, and nucleons at $E \sim 10^{20}\,\mathrm{eV}$. Standard particle and astrophysical arguments lead one to expect TeV gamma-rays and $10^{20}\,\mathrm{eV}$ nucleons to be just above their respective thresholds for absorption on cosmic radiation background fields. The annihilation reaction for TeV gamma-rays is $\gamma + \gamma_{IRB} \rightarrow e^+ + e^-$, where γ_{IRB} denotes a cosmic infrared background photon; the cms energy threshold is $\sqrt{s} = 2m_e$. The energy-loss reaction for $10^{20}\,\mathrm{eV}$ nucleons is dominated by $N + \gamma_{CMB} \rightarrow \Delta \rightarrow N' + \pi$ near threshold, where γ_{CMB} denotes a photon in the CMB; the cms threshold energy is $\sqrt{s} = m_{\Delta}$.

The generalized uncertainties can in principle raise or lower the energy thresholds of these reactions. Raising an annihilation or energy-loss threshold presents the possibility of extending the CR spectrum beyond expected cutoff energies. There have

been suggestions that such extended spectra do exist for both gamma-rays [36] and for nucleons [37]. Predictably, there have also been suggestions that LIV is the origin of the anomalous spectra [30].

Consider the general $2 \rightarrow 2$ scattering reaction $a + b \rightarrow c + d$. Let m_a, m_b, m_c and m_d label the particle masses, and E_a, E_b, E_c and E_d the particle energies. The unmodified dispersion relation reads

$$E_i = p_i + \frac{m_i^2}{2p_i} + \mathcal{O}\left(\frac{m_i^4}{p_i^3}\right) , \quad i = a, b, c, d \; . \tag{II.4}$$

However, the energy and momentum conservation laws *including GUP fluctuations* become

$$\begin{aligned} E_a + \delta E_a + E_b &= E_c + \delta E_c + E_d + \delta E_d \; , \\ p_a + \delta p_a + p_b &= p_c + \delta p_c + p_d + \delta p_d \; . \end{aligned} \tag{II.5}$$

According to Eq. (II.3), the energy and momentum fluctuations of the cosmic background photons, δE_b and δp_b, are very small since E_b and p_b are so small ($\sim$ meV for the CMB and a few tens of meV for the far-IRB). We have set them to zero. The magnitudes of the other uncertainties can be significant.

Subtracting the second of Eqs. (II.5) from the first, inserting (II.4) for the differences $E - p$, and realizing that $p_b = -E_b$, one gets for the energy of the background photon,

$$E_b = E_b^0 + \delta_{\text{Foam}} \, , \tag{II.6}$$

where

$$E_b^0 = \frac{1}{4}\left(\frac{m_c^2}{p_c} + \frac{m_d^2}{p_d} - \frac{m_a^2}{p_a}\right) \tag{II.7}$$

is the classical value, and

$$\delta_{\rm Foam} = \delta_c + \delta_d - \delta_a\,, \quad \text{with } \delta_j = \frac{1}{2}\left(\delta E_j - \delta p_j\right), \tag{II.8}$$

is the contribution from fluctuating foam. To first order in m_j^2, the p_j's in Eq. (II.7) can be replaced by E_j's. We remark at this point that $\delta_{\rm Foam}$ is sourced by δE and/or δp. Therefore, the origin of $\delta_{\rm Foam}$ is open to a broad interpretation. We discuss this a bit more in section (2.6). Also, since δp is a component of a three-vector, whereas δE is not, the relative sign in the combination $\delta E - \delta p$ appearing in the definition of $\delta_{\rm Foam}$ is not meaningful.

Next, consider the reaction at threshold, $\sqrt{s} = m_c + m_d$. In terms of the boost factor γ between the center of mass frame and the lab frame, one has $E_{\rm tot}^{LAB} = \gamma(m_c + m_d) = E_a + \mathcal{O}(E_b)$, $E_c = \gamma m_c$, and $E_d = \gamma m_d$, i.e., $\gamma = \frac{E_c}{m_c} = \frac{E_d}{m_d} = \frac{E_a}{m_c+m_d}$. These equalities allow the elimination of E_c and E_d in Eq. (II.7) in terms of E_a, which we write as $E_{\rm th}$ to remind ourselves that the kinematics are being calculated at threshold energies. The result is that Eq. (II.6) becomes

$$4\,E_b\,E_{\rm th} = (m_c + m_d)^2 - m_a^2 + E_{\rm th}\,\delta_{\rm Foam}\,. \tag{II.9}$$

Solving this equation for $E_{\rm th}$ then gives the modified threshold energy for the reaction. Of course, some model for the fluctuations must be introduced.

References [30, 31, 29] argued for the following form of the fluctuations:

$$\delta_j \equiv \frac{1}{2}\left(\delta E_j - \delta p_j\right) = -\frac{\epsilon}{4}\,p_j\,\left(\frac{p_j}{M_P}\right)^a \approx -\frac{\epsilon}{4}\,E_j\,\left(\frac{E_j}{M_P}\right)^a\,. \tag{II.10}$$

Different choices for a and ϵ parametrize different space-time foam models. With dimensionful mass-energy factors explicitly shown, ϵ is expected to be a number

roughly of order one. The exponent a is assumed to be positive such that fluctuations are suppressed below the Planck scale. Possibilities other than the particular form for the fluctuations given in Eq. (II.3) are certainly possible. For example, one may choose to parameterize the fluctuation $\delta_{\rm Foam}$ in Eq. (II.9) directly, with a parameterization of one's choosing. However, we will stay with the form given above.

As we have seen, the individual E_j's are linearly related to each other by mass ratios. Along with Eq. (II.10), this means that the δ_j's are also (nonlinearly) related to each other by mass ratios. This makes the result of inserting Eqs. (II.10) for each $j = a, b, c$ into Eq. (II.9) fairly simple. The result is a general and manageable equation for the reaction threshold energy, incorporating the correction from space-time foam:

$$4\,E_b\,E_{\rm th} = 4\,E_b\,E_{\rm class} + \epsilon\,E_{\rm th}^2\,\left(\frac{E_{\rm th}}{M_P}\right)^a\,\left[1 - \frac{m_c^{1+a} + m_d^{1+a}}{(m_c+m_d)^{1+a}}\right]\,, \qquad \text{(II.11)}$$

with $E_{\rm class} = \frac{(m_c+m_d)^2 - m_a^2}{4\,E_b}$ being the energy of the threshold when special relativity is not violated. When $\epsilon = 0$, the classical threshold $E_{\rm th} = E_{\rm class}$ of course obtains. When $a = 0$, the classical threshold $E_{\rm th} = E_{\rm class}$ also obtains, for any value of ϵ.

Before examining specific models for the meaning of a and ϵ, we can extract from Eq. (II.11) the number of real positive roots of $E_{\rm th}$. These roots are the candidate solutions for the modified threshold. Imagine plotting the LHS and RHS of the equation versus $E_{\rm th}$. The LHS of (II.11) rises linearly in $E_{\rm th}$ from zero, with a slope of $4\,E_b$. The RHS rises (falls) for positive (negative) ϵ at a higher power of $E_{\rm th}$, from a positive intercept of $(m_c+m_d)^2 - m_a^2$. For negative ϵ, the two curves will always cross once and only once, i.e., there is always a single positive root. For positive ϵ,

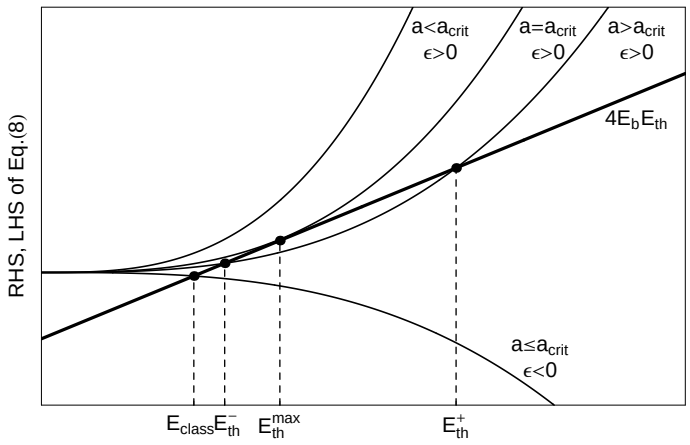

Figure 5: Schematic illustration of the classical and modified threshold energies.

the two curves may never cross, "kiss" once, or cross twice, giving none, one and two positive roots, respectively. There is a critical value of $a = a_{\rm crit}$, dependent on the particle masses and the positive value of ϵ, at which there is a single positive root, above which there are two, and below which there are none (since a is the exponent of a ratio less than one). These results are illustrated in Fig. (5).

When $\epsilon < 0$, the single positive solution for $E_{\rm th}$ is lower than the classical value $E_{\rm class}$. This leads to cutoffs in the CR spectra at energies lower than those predicted from classical physics. When $\epsilon > 0$ and $a < a_{\rm crit}$, there is no physical solution for $E_{\rm th}$, and so the absorption reaction does not happen at any energy. We return to this case briefly in §2.5. When $\epsilon > 0$ and $a \geq a_{\rm crit}$, then the solutions for $E_{\rm th}$ are always larger than $E_{\rm class}$. This leads to CR cutoff energies higher than those predicted from classical physics. However, as a increases, the influence of the foam term decreases, and for $a > a_{\rm crit}$, the lower of the two solutions, call it $E_{\rm th}^-$, approaches the classical value $E_{\rm class}$. The higher of the two solutions, call it $E_{\rm th}^+$, goes to M_P as a increases.

2.3 Foam dynamics

Not surprisingly, there exist several models for the foam dynamics of a and ϵ. We discuss some of these in this section.

2.3.1 Foam Model with Fixed Fluctuation Parameter ϵ

Since one interest of the particle-astrophysics community is to explain possibly extended CR spectra, we first discuss the higher cutoffs provided by the $E_{\rm th} > E_{\rm class}$ case, i.e., the $\epsilon > 0$, $a \geq a_{\rm crit}$ case. If there were a reason in Nature to reject the lower $E_{\rm th}^-$ solution (we know of none), then the arbitrarily-large value of $E_{\rm th} = E_{\rm th}^+$ would allow CR cutoffs to be arbitrarily extended. However, with both solutions operative, the reaction will occur when E rises to exceed either solution, i.e. to exceed $\min\{E_{\rm th}^-, E_{\rm th}^+\}$, which is just the lower-energy solution $E_{\rm th}^-$; the higher $E_{\rm th}^+$ solution seems irrelevant. So, how large can $E_{\rm th}^-$ be? The answer is that $E_{\rm th}^-$ is maximized at the single solution value occurring when $a = a_{\rm crit}$. Call this value $E_{\rm th}^{\rm max}$. These solutions and their labeling are shown in Fig. (5).

The critical a and the critical $E_{\rm th}$ can be found in principle by simultaneously solving two equations. The first is just (II.11), and the second is obtained from (II.11) by equating the first derivatives of the LHS and RHS with respect to $E_{\rm th}$. However, manipulation of these two equations does not lead to a useful analytic separation of $a_{\rm crit}$ and $E_{\rm th}^{\rm max}$. We content ourselves to use numerical techniques in the main text to determine $a_{\rm crit}$ and $E_{\rm th}^{\rm max}$, but present some accurate analytical approximations in the Appendix of [40]. There is however, one simple analytic relation that results from

manipulations of these two equations. It is

$$E_{\rm th}^{\rm max} = E_{\rm class} \left(\frac{a_{\rm crit} + 2}{a_{\rm crit} + 1} \right) . \qquad \text{(II.12)}$$

This result shows that $E_{\rm th}^{\rm max}$ depends on ϵ (assumed positive here) only implicitly through $a_{\rm crit}$, and that $E_{\rm th}^{\rm max}$ lies in the interval $[E_{\rm class}, 2\,E_{\rm class}]$ regardless of the value of $a_{\rm crit}$. $E_{\rm th}^{\rm max}$ approaches $2\,E_{\rm class}$ as $a_{\rm crit} \to 0^+$, and approaches $E_{\rm class}$ for $a_{\rm crit} \gg 2$. There are $E_{\rm th}^{+}$ solutions exceeding $2\,E_{\rm class}$, but these are inevitably accompanied by a second solution, $E_{\rm th}^{-}$, lying below $2\,E_{\rm th}$. This is our first new result. We repeat it: *For positive ϵ, the reaction threshold energy can be* **raised**, *but* **at most by a factor of 2**.

Let us comment on the foam-inspired extended CR spectra obtained in [29, 30, 31]. In this work a pre-desired value of $E_{\rm th}$ is input into Eq. (II.11), and from this the value of fixed, positive ϵ is extracted. This approach suffers from (at least) two drawbacks. The first is that it is oblivious to the existence of the second, lower-energy solution $E_{\rm th}^{-}$. The second drawback is that it is fine-tuned in the value of ϵ. The first drawback is much more serious, for we have just shown that the second solution raises the threshold energy by at most a factor of 2. The model of [29, 30, 31] appears to fail to raise threshold energies.

2.3.2 Foam Model with Gaussian Fluctuations

A healthier approach to foam dynamics is described in [32]. The parameter ϵ is treated as a stochastic variable, subject to some specified probability distribution. The stochastic assumption seems reasonable, in that space-time fluctuations at one

site would not depend on the fluctuations elsewhere. We follow this approach here, generalizing the results of [32].

When an interaction occurs, the kinematics are determined by the fixed parameter a and a single random value of ϵ. Since experiments sum over many events, the total data sample is best described by the most probable value of the threshold energy. This is determined by the Gaussian-distributed ϵ. In principle, some random occurrences will reduce the threshold for particular events even below the mean threshold. However, our numerical work reveals that the width in $E_{\rm th}$, resulting from the distribution in ϵ, is small. This is evident in Figs. (8)-(11).

In principle, the value of the fluctuation δ_i of each particle can be treated as independent stochastic variables. the effect of this on Eq. (II.11) is to replace the overall ϵ with an independent ϵ_a, ϵ_c, ϵ_d for the the respective three terms in the bracket. In the end, an overall Gaussian is probably a good approximation even for this more complicated case, given the generality of the central limit theorem. One might expect quantitative, but not qualitative, differences [32]. We will treat the overall ϵ as the single stochastic variable, and define the probability distribution of the single ϵ as $p(\epsilon)$. We will follow [32] and assume Gaussian statistics. Then

$$p(\epsilon) = \frac{1}{\sigma\sqrt{2\,\pi}}\, e^{-\frac{(\epsilon-\bar{\epsilon})^2}{2\,\sigma^2}}\ . \tag{II.13}$$

The stochastic ϵ's are then generated numerically via

$$\epsilon = \sigma\sqrt{2}\; erf^{-1}(r) + \bar{\epsilon}\ , \tag{II.14}$$

where r is a random number in the interval $[-1,\, 1]$, σ is the variance of a distribution,

and $\bar{\epsilon}$ is the average value of ϵ. We set $\sigma = a$ to avoid introducing a new parameter. Alternatively, one could for example choose a constant variance, say $\sigma = 1$, or any other value. This does not change the general behavior of our results, as we show in the next section. We choose $\bar{\epsilon} = 0$ based on a preference for symmetry, and to maintain the smallness of fluctuations. The same choice was made in [32]. A model with nonzero $\bar{\epsilon}$ was proposed in [33]. Obviously, this expresses a preference for negative ϵ (lowered threshold) over positive ϵ (raised threshold) or vice versa. While this asymmetrical choice may turn out to merit Nature's attention, it has not yet attracted our attention.

With the symmetrical choice for ϵ, half of the fluctuations present negative ϵ, and half present positive. For the negative half, each ϵ generates one solution for $E_{\rm th}$, with $E_{\rm th} < E_{\rm class}$. For the positive half, each ϵ generates no solution when $a < a_{\rm crit}$, and two solutions above $E_{\rm class}$ when $a > a_{\rm crit}$. The lower of these two solutions, $E_{\rm th}^{-}$, is relevant, while the higher solution is probably not.

2.4 Modified Thresholds in Detail

For gamma-rays incident on the IRB, Eq. (II.11) becomes

$$E_{IRB} E_{\rm th} = m_e^2 + \epsilon \, \frac{E_{\rm th}^{2+a}}{M_P^a} \, \frac{2^a - 1}{2^{2+a}} \,, \tag{II.15}$$

where m_e is the electron mass, and for definiteness we take $E_{IRB} = 0.025$ eV. For CR nucleons interacting on the CMB, Eq. (II.11) becomes

$$4 E_{CMB} E_{\rm th} = (m_p + m_\pi)^2 - m_p^2 + \epsilon \, \frac{E_{\rm th}^{2+a}}{M_P^a} \left[1 - \frac{m_p^{1+a} + m_\pi^{1+a}}{(m_p + m_\pi)^{1+a}} \right] , \tag{II.16}$$

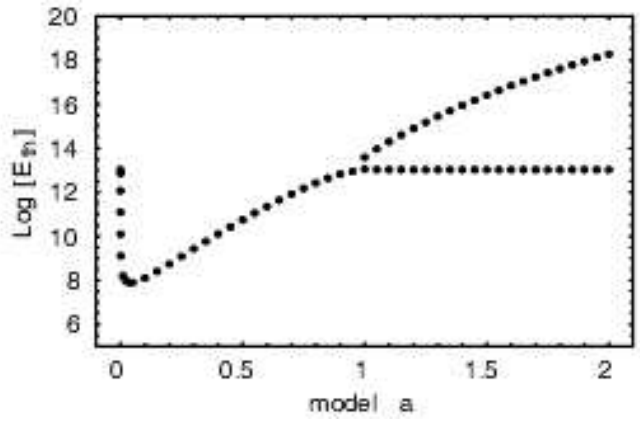

Figure 6: Most probable values of threshold energies (in eV) vs. foam models for γ-rays

with m_p and m_π the nucleon and pion masses. Here, for definiteness we take $E_{CMB} = 7.2 \times 10^{-4}$ eV, near the mean energy of the spectrum. Solving these equations numerically, we map the random Gaussian distribution of ϵ described in Eq. (II.14) onto a random fluctuation spectrum for $E_{\rm th}$.

Different choices of a characterize different foam models. The two choices $a = \frac{2}{3}$ and 1 are motivated by interesting plausibility arguments [30, 31]. Integral values of a are motivated by loop quantum gravity [34], and also by arguments for unbroken rotational invariance [35]. We take the agnostic approach and treat a as a continuous parameter to be explored from zero upward. In Figs. (6) and (7) we show the evolution of solutions with a. Each "solution" $E_{\rm th}$ is really the most probable value of $E_{\rm th}$ picked from a distribution.

The values of $a_{\rm crit}$ are evident in the critical points of these figures. Numerically, they are $a_{\rm crit} = 0.964$ for the gamma reaction, and $a_{\rm crit} = 2.87$ for the nucleon reaction. Numerical values of $a_{\rm crit}$ in general depend on the variance σ in the $p(\epsilon)$ distribution,

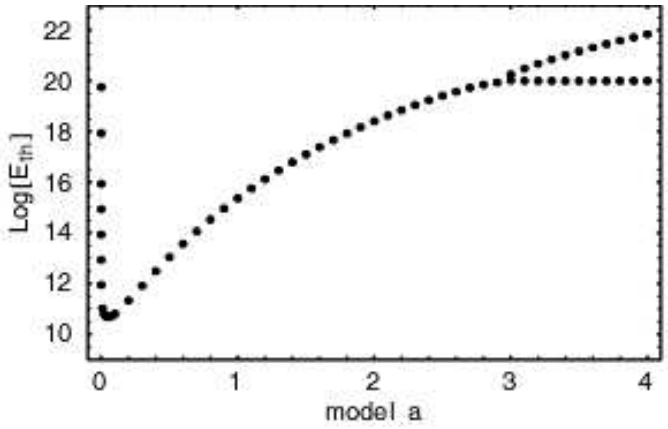

Figure 7: Most probable values of threshold energies (in eV) vs. foam models for UHECRs.

here set for simplicity to a. When σ is taken as a free parameter, we find that the following limiting values for $a_{\rm crit}$ would result: $a_{\rm crit} \to 0$ when $\sigma \to \infty$, and $a_{\rm crit} \to \infty$ when $\sigma \to 0$.

Below $a_{\rm crit}$, the single curve reveals the single solution accompanying negative ϵ fluctuations. Above $a_{\rm crit}$, and accepting both positive and negative ϵ fluctuations, three solutions are actually present. The two relevant solutions, $E_{\rm th}$ from negative ϵ fluctuations, and $E_{\rm th}^{-}$ from positive ϵ fluctuations, are nearly identical in value, clustered just below and just above, respectively, the classical solution $E_{\rm class}$. In the figure, these two near-classical solutions constitute the unresolvable horizontal branch of the curve to the right of the critical point, while the irrelevant solution $E_{\rm th}^{+}$ is the curve that rises to the right $a_{\rm crit}$.

In Figs. (8) and (9), the individual solution "packets" are shown, for different values of the parameter a. The area of each packet reflects how often a fluctuation in ϵ produces a physical solution. Below $a_{\rm crit}$, the total area in the packet is 50%,

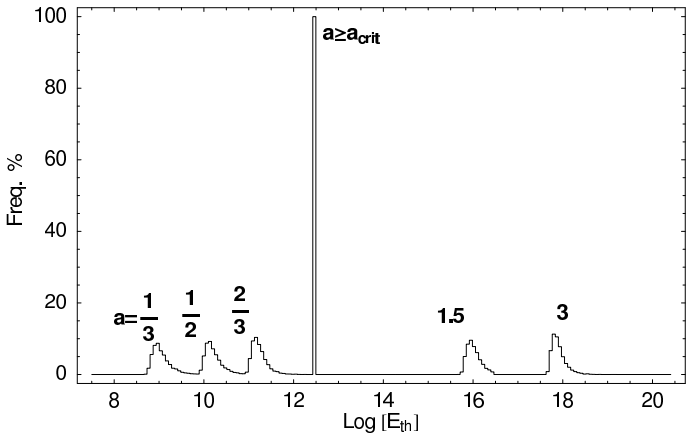

Figure 8: Distributions of threshold solutions for gamma-rays

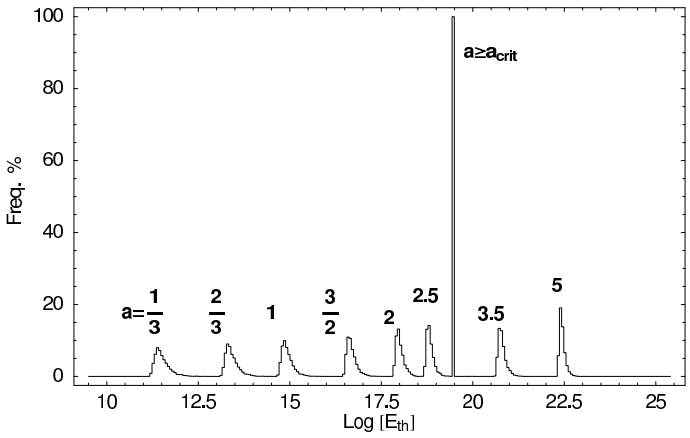

Figure 9: Distributions of threshold solutions for UHECRs

since only half of the fluctuations, the $\epsilon < 0$ ones, produce a physical solution. At $a_{\rm crit}$, the sharp packet has total area of 100%, reflecting one solution for each $\epsilon < 0$ and one for each $\epsilon > 0$. Above $a_{\rm crit}$, 100% of the area remains in the sharp peak labeled $a \geq a_{\rm crit}$, coming from the $\epsilon < 0$ solution and the $E_{\rm th}^-$ solution, plus another 50% area exists in the higher-energy $E_{\rm th}^+$ solution. Raising a reduces the magnitude of the space-time fluctuations, and so pushes the packets comprised of the $\epsilon < 0$ and $E_{\rm th}^-$ solutions closer to $E_{\rm class}$. Raising a also pushes the $E_{\rm th}^+$ solution ever higher, toward M_P.

We note that the width of the $\epsilon < 0$ packet decreases as $a \to a_{\rm crit}^-$. Above $a_{\rm crit}$, the $E_{\rm th}^-$ width and $\epsilon < 0$ solution width remain narrow, the former related to the bounding of $E_{\rm th}^-$ between $E_{\rm class}$ and $2\,E_{\rm class}$. The $E_{\rm th}^+$ width above $a_{\rm crit}$ gets narrower as a increases, or equivalently, as $E_{\rm th}^+ \to M_P$, due to the $\frac{1}{M_P^a}$ suppression of the fluctuation.

In Figs. (10) and (11) we show the $E_{\rm th}$ packets for gamma-ray reactions and nucleon reactions, for $a = \frac{2}{3}$ and $a = 1$. These two values are among the most popular in the literature.

Note that $a = \frac{2}{3}$ is below $a_{\rm crit}$ for both nucleon and gamma-ray reactions. Accordingly, there is a single solution for $E_{\rm th}$ from $\epsilon < 0$ and none from $\epsilon > 0$. The $\epsilon < 0$ solution lowers $E_{\rm th}$ below the classical threshold. On the other hand, the $a = 1$ value is again below $a_{\rm crit}$ for the nucleon reaction, but above $a_{\rm crit}$ for the gamma-ray reaction. Thus, the $a = 1$ gamma-ray distribution shows the nearly-classical threshold, as well as the irrelevant higher-energy solution.

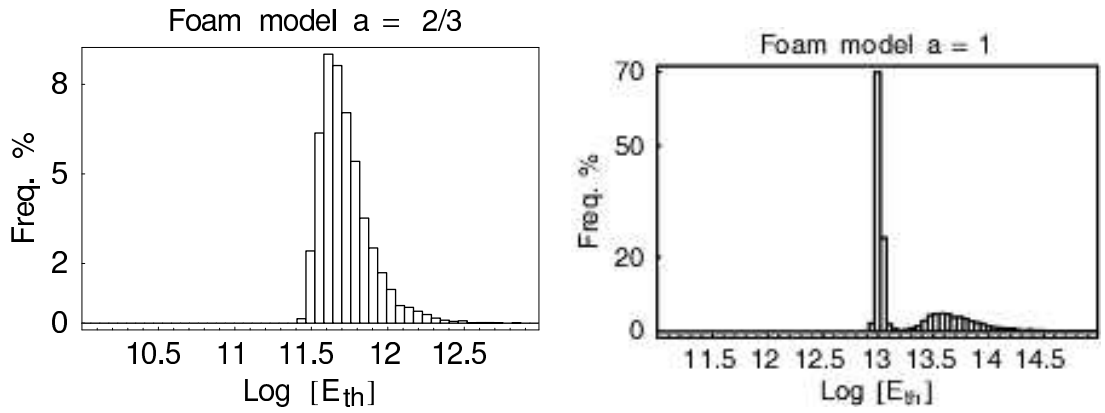

Figure 10: Threshold Distributions for γ rays (energy in eV)

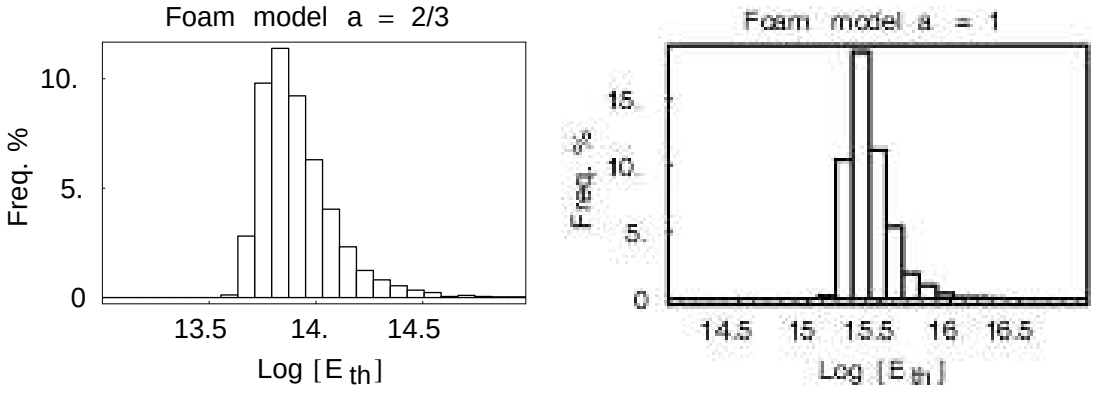

Figure 11: Threshold Distributions for UHECRs (energy in eV)

2.5 An Asymmetric Foam Model that Does Extend the Spectra

We have shown that one can only lower the reaction thresholds when fluctuations to negative ϵ are allowed. We have also shown that positive ϵ fluctuations raise the threshold energy by at most a factor of two when $a > a_{\rm crit}$, but yield no physical solution for $E_{\rm th}$ when $a < a_{\rm crit}$. Thus, there is but a single way to raise the reaction thresholds: the stochastic variable ϵ must be restricted to positive values, and a must be below $a_{\rm crit}$; the absence of a physical threshold in this case means that the absorption reaction cannot happen at all.

To postulate that $a < a_{\rm crit}$ seems acceptable. After all, the values for a suggested by modelers are small, as we have discussed. The concomitant requirement that stochastic $\epsilon > 0$, i.e. $p(\epsilon) = 0$ for all $\epsilon < 0$, seems harder to justify. A Gaussian distribution cannot deliver this, but any distribution of finite extent, e.g., a simple top-hat distribution or δ-function distribution, can. Perhaps Nature is this asymmetric, but single-sided distributions for fluctuations seem to us to be contrived, and we honorably choose not to pursue them here.

2.6 Discussion, with Speculations

In this section we present some additional interesting issues of the foam model.

2.6.1 TeV-scale Gravity?

The numerical results we have presented depend on the assumption that the Planck mass has its usual value 1.2×10^{28} eV. Modern thinking, inspired by the

extra dimensions available in string theory, admits the possibility that the fundamental mass of gravity may be much less than this value. One may ask what changes in our analysis with this (much) smaller mass-scale. Qualitatively, nothing changes. The construction of solutions for positive or negative ϵ values, illustrated in Fig. 5 is unchanged. Also, the relation between $E_{\rm th}^{\rm max}$ and $E_{\rm class}$ given in Eq. (II.12) is independent of M_P, and so is unchanged. So it is just the quantitative values of the new threshold energies that are changed. But the quantitative changes can be dramatic.

In our numerical work we have investigated the effect of lowering M_P. We find that, except for very small values of a, $E_{\rm th}$ cannot exceed M_P. This means that the Planck mass M_P provides an energy limit for all cosmic rays. Turning this remark around, the observation of cosmic rays above 10^{20} eV implies, in the context of this LIV model, that $M_P > 10^{20}$ eV. The bound is eight orders of magnitude below the usual 4-dimensional Planck mass. However, the bound is also incompatible with the popular TeV-scale gravity models by about eight orders of magnitude.

2.6.2 Proton and Photon "decays"

The general form of Eq. (II.11) enables us to discuss other processes forbidden by exact Lorentz invariance. Above some threshold energies, certain particle "decays" may become kinematically allowed [32]. In [32, 33], the authors discuss the two specific decays $p \to p\pi^0$ and $\gamma \to e^- e^+$ for the fixed value $a = 1$. In this section we will follow [32] and assume that energy-momentum fluctuations of the initial state particle characterize the Lorentz violation. However, we generalize their results by

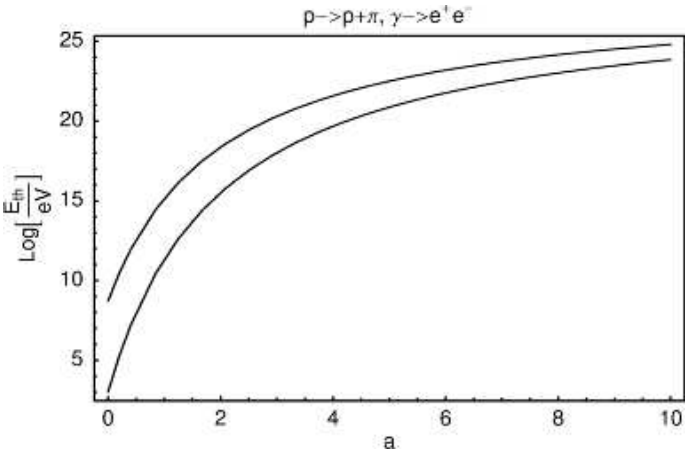

Figure 12: Threshold energies for $p \to p\pi^0$ (higher curve) and $\gamma \to e^- e^+$ (lower curve) decays as a function of parameter a.

treating a as a continuous free parameter. Following a treatment similar to that which led to Eq. (II.11), we here find the energy-threshold for the process $a \to c + d$ to be

$$E_{th} = \left\{ \left[(m_c + m_d)^2 - m_a^2 \right] \frac{(M_P)^a}{-\epsilon} \right\}^{1/(a+2)} . \tag{II.17}$$

One may invert this equation to isolate the a-parameter:

$$a = \frac{\log \left[\frac{1}{-\epsilon E_{\rm th}^2} \left[(m_c + m_d)^2 - m_a^2 \right] \right]}{\log \left(\frac{E_{th}}{M_P} \right)} . \tag{II.18}$$

It can be easily seen from the form of (II.17) that only for $\epsilon < 0$ is the threshold energy E_{th} positive and real. For $\epsilon > 0$ there is no physical solution. Furthermore, for any negative ϵ and any a, there is a unique E_{th}. We present our results in Fig. (12) for $-\epsilon = 1$. As with the scattering processes presented earlier, here too predicted thresholds are bounded from below by some simple function of particle masses (given in Eq. (II.17)), and from above by M_P. For the $a = 1$ case of [32], one obtains $E_{th} \sim 10^{15} eV$ for "pion-bremsstrahlung" by a free proton, and $E_{\rm th} \sim 10^{13} eV$ for

photon decay to e^+e^-. To hide the particle decays, one may move the threshold energies beyond the highest observed cosmic ray energies ($E_{\rm class}$) by raising the value of a. Doing this, one gets from Eq. (II.18) a lower limit for allowed values of a. To be specific, inputing 10^{20} eV for cosmic rays, and 10^{13} eV for gamma-rays, one obtains for $\epsilon = -1$ the lower bounds of 2.82 and 0.93 for the respective a's.

2.6.3 Cosmic-Ray "Knees"

We note that although our results suggest failure for the program which attempts to *raise* cosmic-ray absorption thresholds, the lowered threshold may nonetheless have application. It is conceivable that structure in the cosmic-ray spectrum, e.g., the first and second "knees", and the "ankle", are results of lowered absorption thresholds. In particular, if the parameter a itself were to trace the matter distribution, along the lines mentioned above for inhomogeneous dark energy, then $E_{\rm th}$ for galactic cosmic-rays could be much lower than for the extra-galactic component. The net result might be spectral breaks at these lower $E_{\rm th}$ values for cosmic-rays contained in our Galaxy, i.e., "knees". The argument disfavoring this remark is that Galactic cosmic rays are probably not contained long enough to undergo absorption (assuming, as we have here, that the absorption cross-section does not depend on ϵ or a).

2.6.4 A Random Walk Through Foam?

There appear to us to be conceptual problems associated with the kind of model studied here. For example, it is an assumption in the model that energy-momentum

is transferred between the particle and the foam at the point of particle interaction. However, energy-momentum transfer between a free particle and the foam must be disallowed, for this would present a random wall through Planck-sized domains, leading to, e.g., unobserved angular deflections of light. Resolution of these kinds of *ad hoc* rules, e.g., smoothing of the foam, must await a true theory of quantum gravity. In advance of a theory of quantum gravity, speculations are allowable, and in the next subsection we provide a few.

2.6.5 Energy-Momentum Non-conservation

In foam models, energy and momentum are not generally conserved in particle interactions. Non-conservation is suppressed for interactions at terrestrial accelerator energies and below, but possibly becomes noticeable for interactions of extreme-energy cosmic-rays with cosmic background fields, or with atmospheric nuclei. Obvious questions are how much energy-momentum is missing, and where does it go? To the best of our knowledge, these questions are not addressed in the literature.

In the context of the model analyzed in this work, it is simple to estimate the energy-momentum loss of the interacting quanta. As shown in Eq. (II.6), the energy-momentum added to the quanta is $\delta_{\rm Foam}$, which, obtained from Eq. (II.9), is

$$\delta_{\rm Foam} = 4\,E_b\left(1-\frac{E_{\rm class}}{E_{\rm th}}\right)\,. \tag{II.19}$$

This result makes it clear that a lowered (raised) threshold, $\delta_{\rm Foam} < 0$ ($\delta_{\rm Foam} > 0$), and some particle energy-momentum is lost (gained).

Since the numerical value of $E_{\rm th}$ depends on a, $\delta_{\rm Foam}$ too depends on a. We may

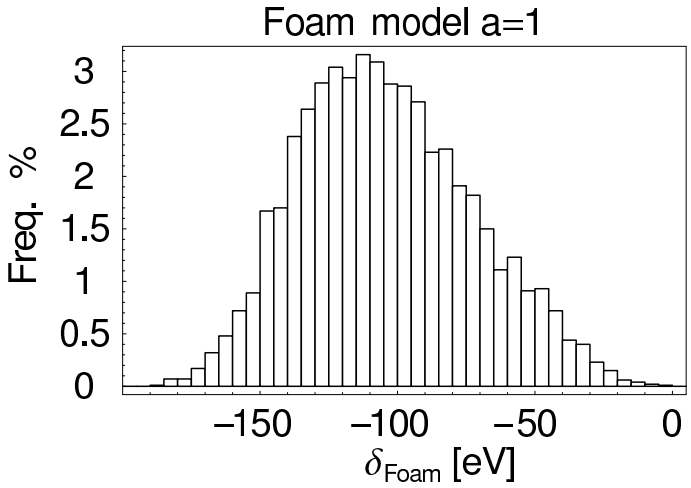

Figure 13: Energy-momentum transferred to vacuum foam, as a function of negative ϵ (the case where $E_{\rm th}$ is lowered), for $a = 1$.

see this directly by comparing Eqs. (II.9) and (II.11) and to deduce that

$$\delta_{\rm Foam} = \epsilon\, E_{\rm th} \left(\frac{E_{\rm th}}{M_P}\right)^a \left[1 - \frac{m_c^{1+a} + m_d^{1+a}}{(m_c + m_d)^{1+a}}\right] . \tag{II.20}$$

This equation also makes it explicit that the sign of $\delta_{\rm Foam}$ is the same as the sign of ϵ. Thus, particle energy-momentum is lost (gained) when $\epsilon < 0$ ($\epsilon > 0$).

We have seen that when $a < a_{\rm crit}$, there is no solution for $E_{\rm th}$ for positive ϵ, and a single solution, typically well below $E_{\rm class}$, for negative ϵ. Thus, stochastic fluctuations will on average drain energy-momentum from the interacting particles, when $a < a_{\rm crit}$. For $a > a_{\rm crit}$, $E_{\rm th}$ is very nearly $E_{\rm class}$, and there is negligible energy-momentum transfer. An example of significant energy-momentum loss is displayed in Fig. (13), where a distribution of $\delta_{\rm Foam}$ versus negative ϵ is shown for cosmic-rays, with the sub-critical value $a = 1$. The typical missing energy-momentum per interaction is ~ 120 eV, consistent with Eq. (II.19). As a fraction of the interaction energy-momentum, this loss is tiny. From Eq. (II.19), when $E_{\rm th} \ll E_{\rm class}$ one has for

the fractional loss, $\delta_{\rm Foam}/E_{\rm class} = -4\,E_b/E_{\rm th} \sim 10^{-18}(E_b/E_{\rm CMB})({\rm PeV}/E_{\rm th})$, far too small to ever be detected by direct cosmic-ray measurements.

Where the missing energy-momentum goes is a difficult question. Without a theory of quantum gravity, one is reduced to speculation. Perhaps the vacuum of the Universe itself recoils in the interaction (similar to Bragg diffraction, or the Mössbauer effect). In an isotropic Universe, the net three-momentum transferred will be zero, after averaging over many interactions. So our Universe is not running away from us. However, the net energy in the vacuum will grow with each interaction. Perhaps an integration over the interaction history provides the observed "dark energy" of the Universe, with equation of state $\frac{p}{\rho} = -1$.

Or perhaps the missing energy-momentum is not homogeneously distributed. For example, cosmic ray interactions with galactic matter may deposit missing energy-momentum into the vacuum of galaxies. Then one might expect dark energy to exhibit some "clustering" around large-scale matter distributions. Such a dark energy over-density might appear to be "dark matter".

An alternative point of view is that the missing particle energy is simply not missing. For example, since $\delta_{\rm Foam} \equiv \frac{1}{2}\,(\delta E - \delta p)$, perhaps $\delta E = 0$ and only momentum is lost in the interaction. The formalism in this chapter goes through unchanged in such a case. As for the momentum, even though momentum is lost from the particles in each interaction, the isotropy of the Universe guarantees that after averaging over momenta directions from many interactions, no net momentum is gained or lost by the vacuum. Thus, there may be no net transfer of energy-momentum to the vacuum.

Particle physics in the expanding Universe may provide a useful focus for thought. In the expanding Universe, the momentum in a co-moving collection of particles is not conserved (it red-shifts), even though the local Einstein equations conserve the energy-momentum of interacting particles. This global non-conservation of energy is related to the lack of time-translation symmetry in the global, expanding Universe. Perhaps in the foam models, translation symmetry is sufficiently broken, or the interaction of the particles with the metric foam is sufficiently nonlocal, to make the apparent energy-momentum non-conservation palatable. Even the concept of local versus global becomes confused when the particle interaction involves the foam. If the foam fluctuation is included in the "local" environment of the interaction, then energy-momentum can be said to be locally conserved. However, if the foam is counted as part of the global vacuum, then energy-momentum is not conserved locally, and may or may not be conserved globally.

2.6.6 Relation to Modified Dispersion Equation Approach

Finally, we remark on the relation between modified interaction kinematics, as presented in this work, and related work on modified particle dispersion-relations. It turns out that the same modified threshold equation is obtained in either approach, with one significant difference: the relative sign of the stochastic variable ϵ is opposite in the two approaches [29, 30]. If one includes both modified kinematics and modified dispersion relations, then the two foamy effects cancel each other.

2.7 Conclusions

We have analyzed a family of Lorentz-violating, space-time foam models. Fluctuation amplitudes are assumed to be stochastic, Gaussian-distributed, and suppressed by the Planck mass. These models can be tested, in principle, by searching for anomalous propagation of high-energy cosmic-rays and gamma-rays. We have derived an equation for a new (modified) threshold energy, in the general case of two particle scattering. As relevant examples, we examined the modified energy-thresholds for the reactions $N + \gamma_{CMB} \rightarrow \Delta \rightarrow N' + \pi$ and $\gamma + \gamma_{IRB} \rightarrow e^+ + e^-$ affecting propagation of extreme-energy cosmic rays and TeV gamma-rays, respectively. Our threshold solutions can be parametrized by a suppression parameter a. For a given particle reaction, there exists a critical value $a_{\rm crit}$ of this parameter, beyond which foam does not alter the standard predictions. Furthermore, for $a < a_{\rm crit}$, foam does alter the reaction significantly, but always lowering, never raising, interaction thresholds. We found that $a_{\rm crit} \sim 3$ for the $N + \gamma_{CMB} \rightarrow \Delta \rightarrow N' + \pi$ reaction, and $a_{\rm crit} \sim 1$ for the $\gamma + \gamma_{IRB} \rightarrow e^+ + e^-$ reaction.

Previously, Aloisio et al. [32] investigated one model (corresponding to our $a = 1$ case) for its effect on the UHECR absorption reaction on the CMB. They found that the reaction threshold is lowered to a most probable value of $E_{\rm th} \simeq 2.5 \times 10^{15}$ eV. Since the $a = 1$ used in [32] is below $a_{\rm crit}$, their lowered threshold is consistent with our more general results which extend their model to arbitrary values of a. Even for $a > a_{\rm crit}$, we found that the threshold can be raised only by a factor of at most two (according to Eq.(II.12)), and even then only if fluctuations are asymmetrically

distributed about zero. Thus, it appears that spacetime foam models of the kind we assessed are unable to extend the spectra of UHECRs or gamma-rays beyond their classical absorption thresholds on the CMB and IR background, respectively.

Tests of foam models by means other than anomalous cosmic-ray propagation abound in the literature. These include, but are not limited to, proton and even photon decay, neutron stabilization, anomalous UHECR shower development, ... Although a discussion of all these possible signatures is beyond the focus of this work, we did investigate the energy-thresholds above which kinematically disallowed $1 \rightarrow 2$ processes become allowed. The thresholds for these processes increase monotonically with the a-parameter. For the processes $N + \gamma_{CMB} \rightarrow \Delta \rightarrow N' + \pi$ and $\gamma + \gamma_{IRB} \rightarrow e^+ + e^-$, the energy-thresholds can be pushed beyond the observed end-points of cosmic-ray and gamma-ray spectra with a values (remarkably) similar to respective $a_{\rm crit}$ values.

We have succumbed to temptation and presented a few speculations. One is that the transfer of energy between interacting particles and foam may contribute to dark energy, or to apparent inhomogeneous dark matter. Another is that lowered thresholds in cosmic ray absorption may effect the "knees" (increase in the spectral slope) observed in the Galactic cosmic-ray spectrum.

Finally, we noted that the absorption thresholds for cosmic-rays and gamma-rays, in the context of the model, cannot exceed the Planck mass. Thus, the observation of cosmic rays with energies at 10^{20} eV necessitate a fundamental Planck mass in excess of 10^8 TeV. This model is, then, incompatible with TeV-scale gravity models, by eight orders of magnitude.

In the next chapter we move on to the discussion of another interesting problem, related to the role of the scalar field non-minimally coupled to gravity. Although, not directly related to the subject covered in this chapter, the spirit and philosophy remains the same. We will perform some numerical analysis of the frequency of the modes of the cosmological scalar fields which can be seen as an analysis of the dispersion relation modified by the presence of the non-minimal coupling of a given field to gravity. The modified dispersion relation (relation between the energy of a mode and its momentum) will once again lead us to new interesting physics.

CHAPTER III

HORIZON SIZE MODES OF COSMOLOGICAL SCALAR FIELDS

Here we discuss the role of the canonical massive scalar fields non-minimally coupled to gravity. A WKB analysis of the field modes will be performed and their role during matter and vacuum domination will be discussed. Finally we discuss how these modes could effect the processing of density perturbations. This chapter is based on a work published in Phys. Rev. D **73**, 123514 (2006).

3.1 Introduction

We begin with a summary of scalar fields coupled to gravity in an FRW universe. We then review redshift and physical wavelength formulas, after which we are in position to begin our numerical analysis. We conclude with a discussion of the implications of our results.

The interpretation and application of our results requires some comments. The Universe has expanded through a number of phases during its lifetime. We think we are now transitioning from a matter-dominated phase to a vacuum-dominated phase. Earlier there was radiation domination, and before that, inflation, which occurred some time before Big Bang nucleosynthesis, but it is not clear how much before. Our task is to follow modes through these phases.

It is unlikely that long wavelength modes can be measured directly so we are

obliged to consider indirect measurements. These involve the long-wavelength background on which CMB or other short wavelength radiation propagates, and a proper analysis would consist of comparing observation with results predicted with and without dispersion.

Our best guess for the relevant long wavelength modes that will lead to distortion of the CMB are those modes that were produced during inflation, then pushed outside the horizon during inflation, and have recently re-entered our horizon. These are the lowest ℓ modes. They will have their distortion preserved due of the fact that they have spent the time from which they left the horizon until the present epoch frozen, and so unable to grow or dissipate. Being of the order of the present horizon size, they will also display the maximum distortion. We give generic results that can be applied to any model, but since results are inflationary model dependent, a full analysis would require specifying model parameters ξ, m, etc.

3.2 Scalar fields coupled to gravity in an FRW universe

We first review the properties of a real free massive scalar fields coupled to gravity. The most general action (to first order in R) for this case is

$$S = \int d^4x\sqrt{-g}(g^{\mu\nu}\partial_\mu\phi\partial_\nu\phi - \xi\phi^2 R - m^2\phi^2)\,, \tag{III.1}$$

where R is the scalar curvature and ξ is a dimensionless coupling. We will work in FRW geometry, and use the convenient conformal parametrization of this family of spacetimes,

$$g_{\mu\nu} = C(\eta)\mathrm{diag}(1, -h_{ij}(\mathbf{x}))\,, \tag{III.2}$$

where $C(\eta) \equiv a^2(t)$ is the conformal scale factor related to a conformal time via

$$\eta(t) = \int^t \frac{c\, dt'}{a(t')}\,. \tag{III.3}$$

The spacial part of the metric is

$$h_{ij}(\mathbf{x}) = diag((1-\kappa r^2)^{-1}, r^2, r^2 \sin^2\theta)\,, \tag{III.4}$$

with $\kappa = 0, 1, -1$ corresponding to (flat), deSitter (positive) or Anti-deSitter (negative) curved spatial sections, respectively.

The action (III.1) leads to the field equation

$$\Box\phi + m^2\phi + \xi\phi R = 0\,, \tag{III.5}$$

where $\Box = \frac{1}{\sqrt{-g}}\partial_\mu(\sqrt{-g}g^{\mu\nu}\partial_\nu)$. Because of the homogeneity and isotropy of the FRW metric, the solution to the field equation factorizes to

$$\phi_k(\eta, \mathbf{x}) = C^{-1/2}(\eta) f_k(\eta) \mathcal{Y}_k(\mathbf{x})\,, \tag{III.6}$$

where $\mathcal{Y}_k$ is an eigenfunction of the spatial laplacian

$$\frac{1}{\sqrt{-h}}\partial_i\left[\sqrt{-h}h^{ij}\partial_j\mathcal{Y}_k(\mathbf{x})\right] = -\left(|\mathbf{k}|^2 - \kappa\right)\mathcal{Y}_k(\mathbf{x})\,, \tag{III.7}$$

and $k = |\mathbf{k}|$. In the massive case, the temporal part of (III.6) has to satisfy

$$\ddot{f}_k + \left[k^2 + m^2 C(\eta) + \xi - \frac{1}{6}R(\eta)C(\eta)\right] f_k = 0\,, \tag{III.8}$$

where the dot represents derivative with respect to conformal time η. One can express the scalar curvature R in terms of scale factor C and curvature constant κ in the form

$$\frac{1}{3}RC = \frac{\ddot{C}}{C} - \frac{1}{2}\left(\frac{\dot{C}}{C}\right)^2 + 2\kappa\,. \tag{III.9}$$

Thanks to this relation, equation (III.8) takes the form

$$\ddot{f}_k + \left\{ k^2 + m^2 C + 6\left(\xi - \frac{1}{6}\right)\kappa + 3\left(\xi - \frac{1}{6}\right)\left[\frac{\ddot{C}}{C} - \frac{1}{2}\left(\frac{\dot{C}}{C}\right)^2\right]\right\} f_k = 0\,. \quad \text{(III.10)}$$

The theory is conformally[1] coupled if $\xi = \frac{1}{6}$ and $m^2 = 0$. We will concentrate on two realistic cosmological regimes: vacuum (VDU) and matter (MDU) dominated epochs. In these cases (III.10) reduces to

$$\ddot{f}_k + \left[\beta^2 + m^2 C - \frac{\nu^2 - \frac{1}{4}}{\eta^2}\right] f_k = 0\,, \quad \text{(III.11)}$$

where we have introduced the index ν defined by

$$\nu^2(\xi, p) = \frac{1}{4} - (6\xi - 1)\frac{p(2p-1)}{(p-1)^2}\,, \quad \text{(III.12)}$$

with $p = 2/3$ for MDU and is also formally $2/3$ for VDU. We have also introduced a conformal wave number β, corresponding to a mode k:

$$\beta^2 = \left[\frac{4\pi^2}{\lambda_0^2} + (6\xi - 1)(\Omega_0 - 1)H_0^2\right] a^2(t_0)\,. \quad \text{(III.13)}$$

Here λ_0 denotes the physical wavelength, corresponding to the wave number k, as measured today, Ω_0 is the present ratio of matter-energy density to critical density and H_0 is the present value of the Hubble parameter. Since all current observational evidence points toward a flat universe, we set $\kappa = 0$ ($\Omega_0 = 1$) so that (III.13) reduces to

$$\beta = k = \frac{2\pi}{\lambda_0} a(t_0)\,. \quad \text{(III.14)}$$

[1] In $n+1$ dimensions we have $\xi = (n-1)/4n$.

3.2.1 Massless case

In the massless case (III.11) reduces to Bessel's equation

$$\ddot{f}_k + \left[\beta^2 - \frac{\nu^2 - \frac{1}{4}}{\eta^2}\right] f_k = 0\,. \tag{III.15}$$

The solutions to this equation can be written in terms of Hankel functions $H_\nu^{(1)}(\beta\eta)$, which in polar form are

$$H_\nu^{(1)}(\beta\eta) = A(\beta\eta)e^{-iS(\beta\eta,\nu)}\,, \tag{III.16}$$

with A and S being real valued amplitude and phase functions. These are easily expressed in terms of ordinary Bessel functions J_ν and Bessel functions of the second kind Y_ν. The phase is

$$S(\beta\eta,\nu) = \arctan\frac{\cot(\pi\nu)J_\nu(\beta\eta) - \csc(\pi\nu)J_{-\nu}(\beta\eta)}{J_\nu(\beta\eta)}\,, \tag{III.17}$$

for real $\nu(\xi,p)$, i.e., for $\xi < 3/16$ in a case of $p = 2/3$ and

$$S(\beta\eta,\nu) = \arctan\frac{\Im\left[e^{-i\nu\pi}J_\nu(\beta\eta) - J_{-\nu}(\beta\eta)\right]}{\Re\left[e^{-i\nu\pi}J_\nu(\beta\eta) - J_{-\nu}(\beta\eta)\right]}\,, \tag{III.18}$$

for imaginary $\nu(\xi,p)$,i.e., for $\xi > 3/16$ for both MDU and VDU. The amplitude is

$$A(\beta\eta,\nu) = \sqrt{J_\nu^2(\beta\eta) + Y_\nu^2(\beta\eta)}\,, \tag{III.19}$$

for real ν, and for imaginary ν we find

$$\begin{aligned} A(\beta\eta,\nu) &= |\csc(\pi\eta)|\times \\ &\times\left\{\left\{\Re\left[e^{-i\pi\nu}J_\nu(\beta\eta) - J_{-\nu}(\beta\eta)\right]\right\}^2 + \left\{\Im\left[e^{-i\pi\nu}J_\nu(\beta\eta) - J_{-\nu}(\beta\eta)\right]\right\}^2\right\}^{\frac{1}{2}} \end{aligned} \tag{III.20}$$

The instantaneous angular frequency of FRW modes associated with a wave number k is given by

$$\omega_k = \frac{\partial S}{\partial \eta}\,, \tag{III.21}$$

where S is the corresponding phase given by either (III.17) or (III.18), depending on a value of coupling ξ and choice of cosmology.

3.2.2 Massive case

We want to write (III.10) in the form $\ddot{f}_k + \omega_k^2 f_k = 0$. Therefore using a WKB analysis one finds the frequency (III.21) to second order $\ddot{f}_k + \omega_k^{(2)\,2} f_k = 0$, where $\omega_k^{(2)}$ is given [44] by

$$\begin{aligned}\omega_k^{(2)}(\eta) = \omega_k^{(0)} &+ \frac{3\xi - \frac{1}{2}}{2\omega_k^{(0)}}\left[\frac{\ddot{C}}{C} - \frac{1}{2}\left(\frac{\dot{C}}{C}\right)^2\right] \\ &- \frac{m^2}{8(\omega_k^{(0)})^3}\left[\ddot{C} - \dot{C}\frac{\dot{\omega}_k^{(0)}}{\omega_k^{(0)}} - \frac{3m^2}{4}\frac{\dot{C}^2}{(\omega_k^{(0)})^2}\right]\,,\end{aligned} \tag{III.22}$$

with

$$\omega_k^{(0)} = \sqrt{\beta^2 + m^2 C(\eta)}\,. \tag{III.23}$$

We have checked the validity of the WKB approximation (see section-3.5) by comparing with the massless limit where exact solutions are available. The zeroth order contributions to the frequency and conformal scale factor and their derivatives for the cosmological cases of interest are summarized in Table-1[2].

[2]In the following we take the value of the present energy density to be $\rho_0 = \rho_{crit} = 9.21 \times 10^{-27}\frac{kg}{m^{-3}} \Rightarrow H_0^{-1} = {a_{vac}^0}^{-1} = 4.42 \times 10^{17} s$.

Table 1: Important factors for VDU and MDU.

	$a(t)$			$\eta\,[a(t)]$	$\eta(z)$
VDU	$e^{a^0_{vac}t}$	$a^0_{vac} = \left[\frac{8\pi G_N}{3}\rho_0(w)\vert_{w=-1}\right]^{\frac{1}{2}}$	$a^0_{vac} \simeq 2.27\times 10^{-18}s^{-1}$	$\frac{c}{a^0_{vac}a(t)}$	$c\,{a^0_{vac}}^{-1}(z+1)$
MDU	$a^0_{mat}t^{\frac{2}{3}}$	$a^0_{mat} = [6\pi G_N\rho_0(w)\vert_{w=0}]^{\frac{1}{3}}$	${a^0_{mat}}^{\frac{3}{2}} \simeq 2.05\times 10^{-18}s^{-1}$	$\frac{3c}{{a^0_{mat}}^2}a(t)$	$2c\,{a^0_{mat}}^{-1}(1+z)^{-\frac{1}{2}}$

The scale factor and hence conformal time depends on the given epoch, so for power law expansions we have

$$a(t) = \left[6\pi G_N(1+w)^2\rho_0(w)t^2\right]^{\frac{1}{3(1+w)}} \tag{III.24}$$

as can be directly determined from the Friedmann equation, where w is the proportionality constant in the equation of state $P(t) = w\rho(t)$ appropriate for a given background, and $\rho_0(w)$ is a present value of critical density for a given epoch. Relevant choices of parameters for use in (III.22) and (III.24) are given in Table-1 and Table-2.

Table 2: Zeroth order result for frequency, scale factor and their derivatives, where a given epoch is characterized by: w, the proportionality constant in the equation of state $P(t) = w\rho(t)$ appropriate for a given background, as well as the exponent of a power-law type cosmologies, i.e. $a(t) \sim t^p$.

Epoch: (w,p)	$\omega_k^{(0)}$	$\dot{\omega}_k^{(0)}$	$C(\eta)$	$\dot{C}(\eta)$	$\ddot{C}(\eta)$
Vacuum: $\left(-1,\frac{2}{3}\right)$	$\sqrt{\beta^2 + m^2\left(\frac{c}{a^0_{vac}}\right)\eta^{-2}}$	$-\frac{m^2\eta^{-3}}{\omega_k^{(0)}}$	$\left(\frac{c}{a^0_{vac}}\right)^2\eta^{-2}$	$-2\left(\frac{c}{a^0_{vac}}\right)^2\eta^{-3}$	$6\left(\frac{c}{a^0_{vac}}\right)^2\eta^{-4}$
Matter: $\left(0,\frac{2}{3}\right)$	$\sqrt{\beta^2 + m^2\frac{{a^0_{mat}}^6}{81c^4}\eta^4\eta^4}$	$2\frac{m^2\eta^3}{\omega_k^{(0)}}$	$\frac{{a^0_{mat}}^6}{81c^4}\eta^4$	$4\frac{{a^0_{mat}}^6}{81c^4}\eta^3$	$12\frac{{a^0_{mat}}^6}{81c^4}\eta^2$

3.2.3 Redshift formula

The classical redshift formula in terms of frequency ν is

$$\frac{\nu_0}{\nu} = \frac{a(t)}{a(t_0)}\,. \tag{III.25}$$

We want to find the correction factor to this naive redshift formula where the correction is the result of the nontrivial modifications to the dispersion relations for long-wavelength modes i.e., wavelengths of the order of the horizon size. To do this we have to take into account of the conformal angular frequency correction [43] so that we find

$$\frac{\nu_0}{\nu} = \frac{a(t)}{a(t_0)}\frac{\omega_k(t_0)}{\omega_k(t)}\,. \tag{III.26}$$

Here for ω_k we use $\omega_k^{(0)} = \beta$ in the massless case and $\omega_k^{(2)}$, given by equation (III.22),

Table 3: Dictionary of conformal and physical variables.

	Conformal	Physical
space	x	$x_{phy} = a(t)x$
time	$\eta = \int^t \frac{c\,dt'}{a(t')}$	t
wave vector	k	$k_{phy} = \frac{k}{a(t)}$
wavelength	$\lambda = \frac{2\pi}{\lvert k\rvert}$	$\lambda_{phy} = a(t)\lambda$
frequency	$\omega = \frac{\partial S}{\partial \eta}$	$\omega_{phy} = \frac{\omega}{a(t)}$

in the massive case. In the following sections we are going to present the results for two different cosmologies. The relations between physical and conformal variables are

summarized in Tables 1 and 3. The advantage of an analysis via the WKB method is that it is simple and straightforward, and it usually gives the correct trends when the corrections are moderate ($\sim 5\%$ to $\sim 20\%$) (as we have shown in section-3.5). These observations can be verified by comparing with exact results where they exist. In the cosmological regimes of relevance (vacuum and matter domination), we find the dependence of the dispersion relations on the value of the mass of the scalar field. We formulate our discussion in terms of conformal invariance, i.e., in terms of the value of the mass and wavelength where the conformal behavior is approximately preserved.

In all cases we find $m \sim 10^{-33} eV$ (inverse Hubble size) as the mass where nonconformal behavior starts to set in. These masses should be nearly equal in the different regimes, since differences are caused by numerical factors of order one.

To proceed further, we first have to express all the parameters present in eqs. (III.23) and (III.22) in terms of redshifts

$$z = \frac{a(t_0)}{a(t)} - 1\,, \tag{III.27}$$

and the parameter b_0

$$b_0 \equiv \frac{\lambda_0}{cH_0^{-1}}\,, \tag{III.28}$$

that can be interpreted as the fractional size of the physical wavelength in the units of the present Hubble radius. We will work in units where $a(t)$ and hence $C(\eta)$ are dimensionless. The wave number β does not depend on the epoch, as can be seen from equation (III.14). We have now collected all the necessary epoch specific input needed for our numerical analysis that will be carried out in the next section.

3.3 Correction to Redshifts

In this section we are going to present corrections due to the redshift formula (III.26) originating from the coupling of the scalar fields to gravity. We consider massless as well as massive cases in two different cosmologies, i.e., vacuum and matter dominated universes. In order to see the full spectrum of possible behavior of the dispersion relations, one has to discuss both real and imaginary masses. We plot the ratio of initial to final frequencies in each epoch. Sequentially through matter and vacuum domination, we set $z_i^{mat} = 1100$, next $z_f^{mat} = z_i^{vac} = 0.4$ (using correct WMAP value of $\Omega_\Lambda = 0.73$ [55]) and finally $z_f^{vac} = 0$. In the case of vacuum domination, for

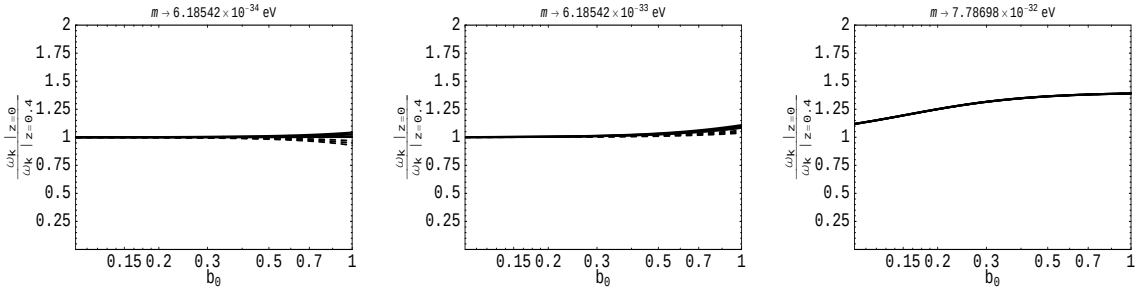

Figure 14: Vacuum Domination $m^2 > 0$ WKB: Dashed curves $\xi < 1/6$, Thick curves $\xi > 1/6$. In this and the following figures we use $\xi = \pm 3/4, \pm 1/2, \pm 1/4, 0$ for ξs.

real masses Fig.14, the deviation from the classical redshift formula is very small until length scales of the size $\sim 0.6c\,H_0^{-1}$. For imaginary mass, when $\Im(m) \lesssim 10^{-32}eV$, the ratio of frequencies exhibits similar behavior Fig.15. In both cases, as the magnitude of the mass of a scalar field gets larger than roughly 10^{-32} eV, it dominates the effects of ξ if $\xi \lesssim 1$. In the matter dominated case, both real Fig.16, and imaginary Fig.17

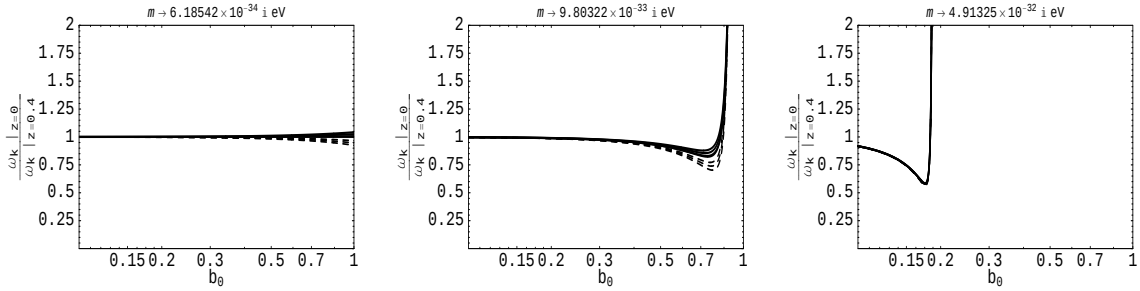

Figure 15: Vacuum Domination $m^2 < 0$ WKB: Dashed curves are for $\xi < 1/6$, and thick curves are for $\xi > 1/6$.

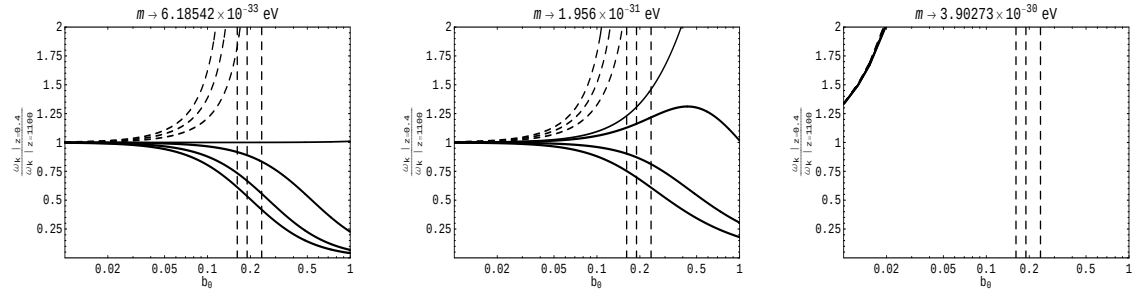

Figure 16: Matter Domination $m^2 > 0$ WKB: Dashed curves are for $\xi < 1/6$, and thick curves are for $\xi > 1/6$. On this and the following figures vertical lines show the corresponding asymptotes where the WKB approximation fails.

masses of order $\sim |10^{31}|eV$ dominate effects when $\xi \lesssim 1$. The corrections become substantial at smaller length scales $\sim 0.1c\, H_0^{-1}$.

3.4 WMAP fit and Speculations

Now let us discuss the processing of the density perturbation spectrum. As is well known, once a perturbation comes within the horizon, it begins to oscillate. This phenomenon is reflected in the observed large ℓ WMAP CMB spectrum, where the first maximum (first acoustic peak) is at $\ell \sim 200$, and higher order peaks are at larger ℓ value. The low ℓ values have not been inside the horizon long enough for

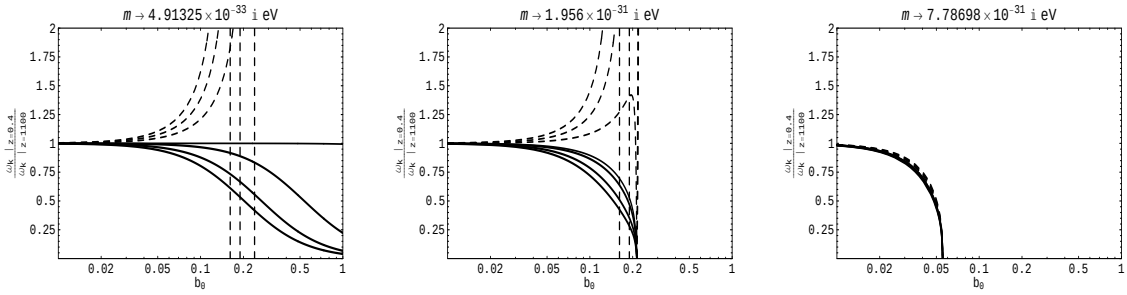

Figure 17: Matter Domination $m^2 < 0$ WKB: Dashed curves are for $\xi < 1/6$, and thick curves are for $\xi > 1/6$.

much processing to have taken place. The region from roughly $\ell = 20$ to $\ell = 200$ is just now beginning to undergo its first plasma oscillation, while for $\ell \lesssim 20$ very little has happened yet. But this is just the region of interest for the dispersive effects we have been discussing, and we are lucky that in this region ($\ell \lesssim 20$) we have a pristine, unprocessed spectrum. (Recall for large ℓ, we have short wavelengths, and so virtually no dispersion.) Hence we can confine ourselves to the analysis of perturbations with wavelengths of the order of or somewhat less than the horizon size where we do not need to worry about plasma oscillations. (There may be issues of re-ionization to consider, but at the level we are working we choose to ignore such effects.)

Perturbations that are of the order of the horizon size today have undergone an evolution from the time of their production. A typical scenario would be: Perturbations are produced during a vacuum-dominated epoch of inflation, and are pushed outside the horizon. Inflation then ends, and the universe becomes radiation dominated. Some perturbations come back inside the horizon, are processed via plasma oscillations, etc., until about $z = 1100$, when the universe becomes matter dominated.

More perturbations re-enter the horizon and are processed until around $z = 0.4$ when the universe again becomes vacuum dominated and perturbations again start to be pushed outside the horizon. Ultimately, we would like to follow the entire evolution of a perturbation from its production until today for modes that are currently near horizon size (an $\ell \lesssim 20$ mode). However, this would require a detailed model of the early universe. A less ambitious approach is to follow some (better understood) fraction of the evolution to demonstrate that dispersion can play a role in understanding the observational data, and leave it to future work, when a more detailed understanding of the early Universe including details of early Universe phase transitions are known, to follow the complete evolution of the modes. To this end we have shown in Fig.18 (where we convert wavenumber k to multi-pole moment ℓ using $k = \ell/(c\,H_0^{-1})$) the results of evolving modes from[3] $z = 1100$ until today (i.e. from $z = 1100$ to $z = 0.4$ with matter domination, and from $z = 0.4$ until today ($z = 0$) with vacuum domination), and have fit the results to the low ℓ WMAP data. Since an $\ell = 20$ mode undergoes very little processing or dispersive evolution, we have normalized our amplitude to this region of the spectrum. Once this is done, we have a single free parameter ξ for massless scalar fields ϕ. We then do a one-parameter fit, as shown in Fig.18, and find $\xi \simeq \frac{1}{6} - 0.0002$ see Fig.19. This is very close to the conformal value $\xi = \frac{1}{6}$ and can be shifted there, but only at the expense of introducing a small negative mass squared for the scalar field as can be seen from the field equation (III.11) evaluated for the

[3]For more precise z values see [56].

VDU

$$\ddot{f}_k(\eta) + \left[\beta^2 + \frac{(12\xi - 2) + (mc/a^0_{vac})^2}{\eta^2}\right] f_k = 0\,. \tag{III.29}$$

It is clear that one can introduce the effective coupling $\bar{\xi}$ such that

$$12\bar{\xi} = 12\xi + \left(\frac{mc}{a^0_{vac}}\right)^2, \tag{III.30}$$

and by setting $\bar{\xi}$ to the conformal value 1/6 we can find the value of mass m corresponding to a field ϕ with an effective conformal coupling to gravity. Our conclusion is that the evolution of large ℓ scalar modes can be used to constrain the coupling of k-essence or holographic type scalar fields to gravity, if they contribute substantially to the density perturbations. For such fields, if we set $m = 0$ we find that minimally coupled field ($\xi = 0$) is easily excluded. Our fit is merely an example of how constraints on ξ can arise. Specific models will give specific results. It is interesting that, with a few assumptions, a value of ξ can in principle be extracted from a study of the cosmic microwave background. The coupling of scalar fields to gravity have other ramifications that would need to be considered in any realistic model. Another reason for being cautious about drawing sweeping inferences from Fig.18 is that the single scalar field action given in (III.1) with $m^2 = 0$ leads to a spectral index in disagreement with the data. Perhaps what one should conclude is that we need a theory with a sufficiently complicated potential $V(\phi)$ that density perturbations can be laid down when the ϕ mass is sufficiently large (see [57]), but where the late time effective theory is nearly conformally invariant, or a theory with multiple scalar moduli field.

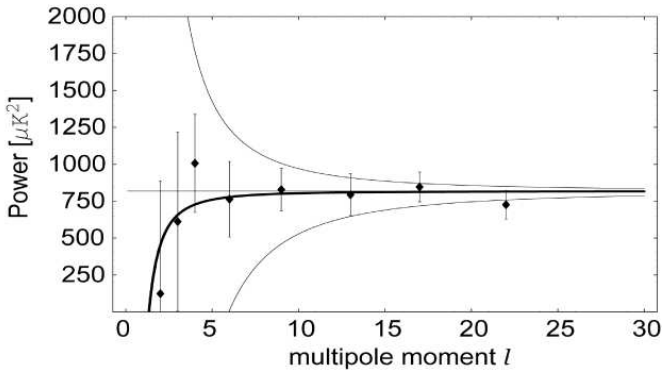

Figure 18: Fit of the low ℓ part of WMAP spectrum to scalar fields with dispersion. The thick line is for the best fit value, $\xi = 0.166434$. We have added three other curves for comparison. The upper thin line is for $\xi = 0.169492$, the flat line is for $\xi = 1/6$, and the lower thin line is for $\xi = 0.161290$.

3.5 Validity of WKB approximation

The WKB approximation works best for couplings close to the conformal case $\xi = 1/6$. For various choices of parameters, we show the percent errors of the WKB approximation relative to the exact vacuum dominated era results Fig.20(a) and Fig.21(a), and to the matter dominated universe in Fig.20(b) and Fig.21(b). In a matter domination universe represented in Fig.21(b), the WKB approximation is better (i.e. up to larger scales) for positive couplings. However, the broad range of applicability of the WKB method allows us to use the WKB approximation to draw conclusions about trends in the data.

3.6 Conclusions

In this chapter we have analyzed the role of horizon size modes of a canonical scalar field non-minimally coupled to gravity. WKB analysis of the modes were performed and implications of the existence of such modes were discussed. The following

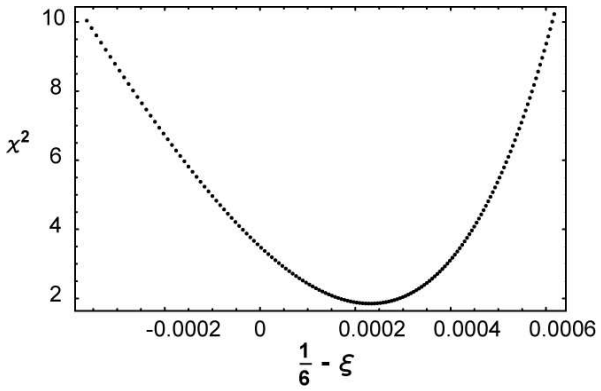

Figure 19: Deviation of ξ from the conformal value of coupling $\xi = \frac{1}{6}$ as seen on a plot of χ^2 vs. $(\frac{1}{6} - \xi)$.

picture can be drawn out of this project. Although, the precision of recent measurements of fundamental cosmological parameters is improving, the existence of massive scalar fields cannot be excluded. The masses of the fields under considerations are tiny $(10^{-33} - 10^{-34} eV)$ and their coupling to gravity is close but not equal to the conformal value.

In the next chapter we discuss more formal aspects of gravity. We give examples of black holes with extra hair related to the presence of scalar fields. Both, canonical and exotic types of scalar fields, motivated by recent discoveries in cosmology, will be included in the analysis.

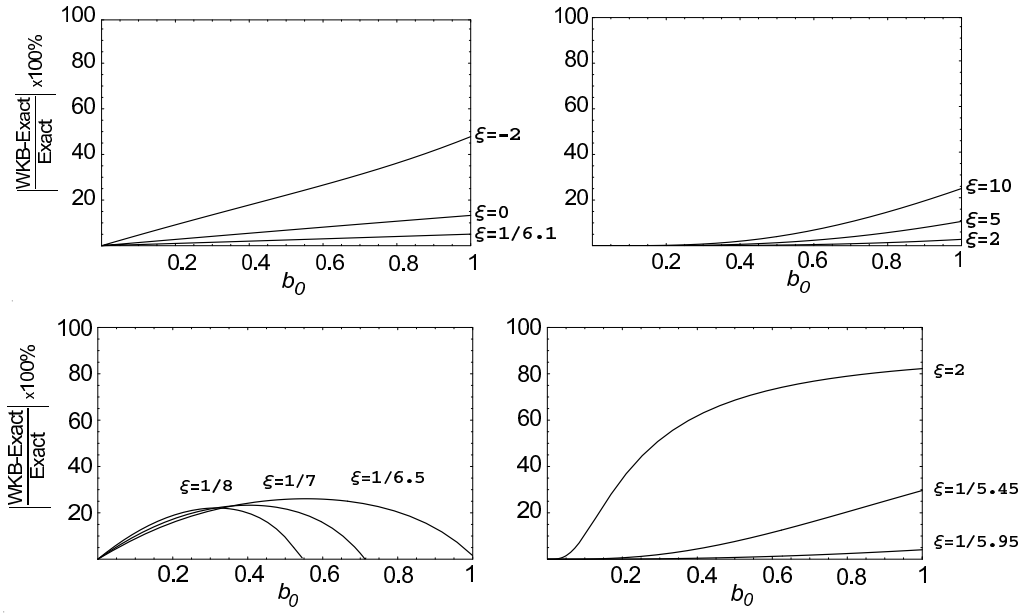

Figure 20: Percent error in VDU (a) and MDU (b) for both negative and positive values of ξ.

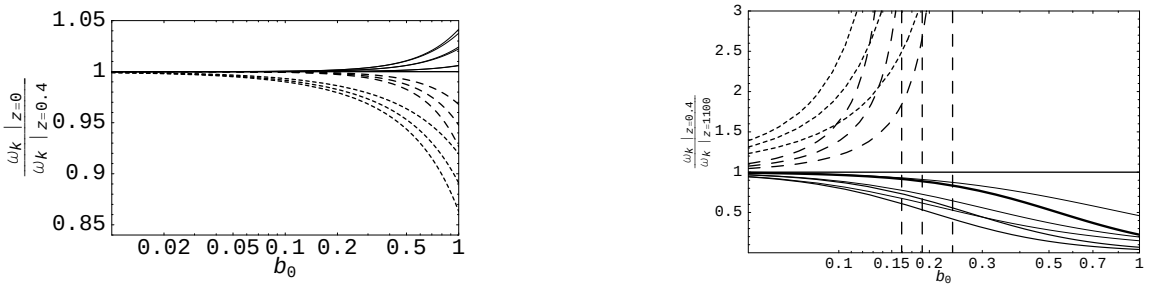

Figure 21: Comparison of exact solutions to the WKB approximation in VDU (a) and MDU (b) case. Thin (thick) lines represent exact (WKB) solutions with $\xi > 1/6$. Small (large) dashing represents exact (WKB) with $\xi < 1/6$.

CHAPTER IV

BLACK HOLES AND GENERALIZED SCALAR FIELD

4.1 Introduction

The existence or nonexistence of the scalar hair has been the topic of active research for more than three decades (see [58] for a nice review). It actually started with the famous statement by J.A. Wheeler "a black hole has no hair" [59]. This is due to the nature of stationary black holes as they are completely characterized by three conserved quantities, mass, electric charge and angular momentum, which can be measured at asymptotic infinity. This is the so called "no hair theorem" for black holes. It suggests that all matter fields present in the black hole space-time should be either radiated to infinity or vanish inside of the black hole, except the three conserved charges mentioned above. This result has been proven for the vacuum case [60], for Einstein-Maxwell theory [60] as well as for several minimally [61] and non-minimally coupled scalar field theories [62].

In recent years, there have been a number of investigations studying the black hole solutions with non-linear matter fields. The discovery of black hole solutions in Einstein-Yang-Mills theory [65], Einstein-Skyrme theory [66] , Einstein-Yang-Mills-Higgs theory [67] as well as Einstein-non-Abelian-Proca theory [68], are all examples of violation of the "no hair theorem". Also the Bronikov-Melnikov-Bocharova-Bekenstein solution [69], which corresponds to a spherically-symmetric black hole

solution with scalar field conformally coupled to gravity, is another example of scalar hair, although it was later shown that in this configuration, scalar field diverges at the horizon. This and the fact that the energy-momentum tensor of this field is ill-defined at the horizon, is enough to dismiss this as a candidate for a regular black hole solution.

The obstacle of obtaining a regular black hole solution with a self interacting scalar field, can be overcome by introducing a cosmological constant Λ and a conformal coupling [70]. For a minimally coupled scalar field, one needs to have $\Lambda < 0$ [71], which allows existence of a black hole with scalar hair and nontrivial topology on the horizon [72].

Recently, an effective scalar field theory governed by a Lagrangian with a non-canonical kinetic term ($\mathcal{L} = -V(\phi)F(X)$, where $X = -\frac{1}{2}\partial^{\mu}\phi\partial_{\mu}\phi$), has attracted considerable attention. One example of such a field is the tachyon in open string field theory [73, 74]. Such a model can lead to a late time accelerated expansion and is called "k-essence" [75, 76, 77]. It is worth noting that models such as the Generalized Chaplygin Gas (GCG) [78] which has been proposed to unify the dark matter and dark energy of the universe, may be seen as a special case of k-essence. A Lagrangian with a non-canonical kinetic term has also been investigated for an early universe inflationary scenario and is termed "k-inflation" [79].

In this letter, we study the existence of scalar hair for Lagrangians containing non-canonical kinetic terms for a static asymptotically flat spherically-symmetric black hole space-time with a regular horizon. We have considered various examples for the

Lagrangian and our study shows that with a suitably chosen Lagrangian, it is possible to have a non-trivial asymptotically flat static black hole space-time with scalar hair.

4.2 Asymptotically Flat Black Hole Solutions

We restrict ourselves to the minimally coupled case and start with a general action given by

$$\mathcal{S} = \int d^4x\sqrt{-g}\left[\frac{1}{2}R + F(X,\phi)\right], \tag{IV.1}$$

where R is the scalar curvature, $F(X,\phi)$ is a general function of matter field ϕ and $X = -\frac{1}{2}\partial^\mu\phi\partial_\nu\phi$. We have set gravitational constant $\kappa^2 = 8\pi G = 1$. We shall use a sign notation $(-,+,+,+)$ for the metric.

Next we consider the most general static, spherically symmetric black hole space-time with a regular horizon, whose exterior is given by the metric

$$ds^2 = -e^{-2\delta(r)}A(r)dt^2 + A^{-1}(r)dr^2 + r^2(d\theta^2 + \sin^2\theta d\Phi^2)\,, \tag{IV.2}$$

where $A(r)$ and $\delta(r)$ are some arbitrary functions of the radial coordinate r only. One can think of $\delta(r)$ as an additional redshift beyond the usual one resulting from the geometry of the static hypersurface.

Typically one can parametrize $A(r)$ as

$$A(r) = 1 - \frac{2m(r)}{r}\,. \tag{IV.3}$$

The existence of a regular horizon at $r = r_H$ demands that $2m(r_H) = r_H$ and $\delta(r_H)$ is finite. The condition of asymptotic flatness requires that $\mu \to 1$ and $\delta(r) \to 0$ as $r \to \infty$.

The matter field ϕ should also respect the symmetries of the space-time and hence is only a function of radial coordinate r. One can now calculate the components of the energy-momentum tensor $T^{\mu}_{\ \nu}$ for the scalar field ϕ

$$\begin{aligned} T^{t}_{\ t} &= T^{\theta}_{\ \theta} = T^{\Phi}_{\ \Phi} = F(X,\phi)\,, \\ T^{r}_{\ r} &= -2XF_X + F(X,\phi)\,, \end{aligned} \tag{IV.4}$$

where the subscript 'X' represents derivative with respect to X. Einstein's equations $G^{\mu}_{\ \nu} = T^{\mu}_{\ \nu}$ in this case become

$$\begin{aligned} A^{'}(r) &= rT^{t}_{\ t} + \frac{1 - A(r)}{r}\,, \\ \delta^{'}(r) &= \frac{r}{2A(r)}(T^{t}_{\ t} - T^{r}_{\ r})\,, \end{aligned} \tag{IV.5}$$

where the prime represents derivative with respect to r. The equation of motion is

$$\left[e^{-\delta(r)}T^{r}_{\ r}\right]^{'} = -\frac{e^{-\delta(r)}}{2A(r)r}\left[(T^{t}_{\ t} - T^{r}_{\ r}) + A(r)(2T - 3T^{t}_{\ t} - 5T^{r}_{\ r})\right]\,, \tag{IV.6}$$

which can be obtained from the Bianchi identity $T^{\mu}_{\nu;\mu} = 0$. This equation closes the system of equations for the scalar field. Here T stands for the trace of the energy momentum tensor for the scalar field.

One can use the expression for the T^{μ}_{ν}'s from above to write this equation as

$$\left[e^{-\delta(r)}T^{r}_{r}\right]' = -\frac{2e^{-\delta(r)}\phi'^{2}}{r}\left[1-\frac{3m(r)}{2r}\right]F_X(X,\phi)\,. \tag{IV.7}$$

This is a key result. This equation generalizes the previous one by Sudarsky [63] for a minimally couple scalar field with canonical kinetic energy term to one for the non-canonical kinetic term. One can see that the term inside the square bracket on a r.h.s of the above equation is always positive outside the horizon, i.e., at $r_H = 2m(r_H)$. Hence the action $F(X,\phi)$ determines whether the term $e^{-\delta(r)}T^{r}_{r}$ is an increasing or decreasing function outside the horizon. Asymptotic flatness requires that it should vanish as $r \to \infty$.

Also at $r = r_H$, $X = -\frac{1}{2}g^{rr}\phi'^{2} = 0$. We assume that, both F and F_X are regular at $r = r_H$, property which is essential for existence of a regular horizon. Further, we set $T^{t}_{t} = T^{r}_{r} = F = -\rho$ at $r = r_H$, where ρ is the energy density for the scalar field.

Hence to satisfy the Weak Energy Condition (WEC) for the scalar field $\rho > 0$ at $r = r_H$, the term $e^{-\delta(r)}T^{r}_{r}$ on the l.h.s of the above equation is negative at the horizon $r = r_H$. Hence it depends solely on the function $F(X,\phi)$ whether one can have asymptotic flatness. With $e^{-\delta(r)}T^{r}_{r} < 0$ at the horizon, this condition can be fulfilled for $F_X < 0$, as in this case, $e^{-\delta(r)}T^{r}_{r}$ will be an increasing function outside horizon and can reach zero asymptotically. On the other hand, for $F_X > 0$, function $e^{-\delta(r)}T^{r}_{r}$ will be more negative outside horizon and can not vanish asymptotically.

We shall now discuss different examples for $F(X,\phi)$ to see whether a non-trivial scalar hair exists outside of the regular horizon of an asymptotically flat black hole

space-time.

4.2.1 $F(X, \phi) = X - V(\phi)$ with positive $V(\phi)$.

This is the standard scalar field case with a canonical kinetic term, that has been widely discussed in the context of scalar hair for black holes. In this case $F_X(X, \phi) = 1$, and equation (IV.7) becomes

$$\left[e^{-\delta(r)} T^r_{\ r}\right]' = -\frac{2e^{-\delta(r)}\phi'^2}{r}\left[1 - \frac{3m(r)}{2r}\right]. \tag{IV.8}$$

As r.h.s of this equation is always negative outside the horizon $r_H = 2m(r_H)$, $e^{-\delta(r)}T^r_{\ r}$ can not vanish asymptotically and hence one can not have non-trivial scalar field outside of the horizon. This shows that for a asymptotically flat black hole with a regular horizon, one cannot have a non-trivial canonical scalar field with a non-zero potential in the space-time outside the horizon. This result, has been obtained earlier by Sudarsky [63].

In our subsequent examples, we shall show that for certain scalar field Lagrangian, it is indeed possible to have the scalar hair in a region outside of the horizon of the asymptotically flat black hole.

4.2.2 $F(X, \phi) = -X - V(\phi)$ with positive $V(\phi)$.

This is an example of a phantom field [80]. In cosmology, this kind of a field has attracted a lot of attention in recent years, since it has been shown that it can serve as a possible explanation of the present accelerating phase of the universal expansion.

The observational data predicts that the equation of state of the dark energy, i.e., $p = w\rho$, responsible for a description of the accelerating universe, has w less than -1 and phantom field with the above Lagrangian can be one such candidate for this component.

In this case as $F_X(X, \phi) = -1$, the r.h.s of equation (IV.7) is positive and one can have the asymptotic flatness condition satisfied as $e^{-\delta(r)}T^r_r$ can vanish asymptotically.

4.2.3 $F(X, \phi) = f(X) - V(\phi)$ with positive $V(\phi)$.

This kind of Lagrangian for the scalar field has been recently considered by Mukhanov and Vikman [82] to show that a non-trivial kinetic term results in substantial contributions of the gravitational waves to the Cosmic Microwave Background (CMB) fluctuations, leading to a larger B-mode CMB polarization, thereby making the prospects of detection of gravity wave in future experiments much more promising. Let us consider the case $f(X) = X^\alpha$. As $X < 0$ outside the horizon, $F_X < 0$ for α odd positive integer and for α even negative integer. Therefore in these two cases, it is possible to have asymptotically flat black hole solutions with a non-trivial scalar field outside the horizon. For α even positive integer and also for odd negative integer, $F_X > 0$, and space-time (IV.2) is not asymptotically flat.

4.2.4 $F(X, \phi) = -V\sqrt{1 - X}$ with positive $V(\phi)$.

This is the Lagrangian for a Born-Infeld tachyon field which has attracted lot of attention in cosmology recent times. It can act as dark energy as well as a potential

candidate for a unified candidate for dark matter and dark energy [76, 77]. This field has also been extensively studied for its possible role of as an inflaton candidate and in connections with tachyons in open string field theory [73, 74]. In this case $F_X = \frac{V}{2}(1-X)^{-1/2} > 0$ and hence $e^{-\delta(r)}T^r_r$ is a decreasing function outside the horizon and it is not possible to obtain a asymptotically flat solution.

4.2.5 $F(X,\phi) = -V(1-X)^\alpha$ with positive $V(\phi)$.

This is a generalized version for the tachyon Lagrangian. Where F_X can be negative for $\alpha < 0$ resulting in a increasing $e^{-\delta}T^r_r$ outside the horizon. Hence one can obtain a asymptotically flat black hole space-time.

4.3 Conclusions

Scalar fields with non-canonical kinetic terms have gained in interest in recent years. This is particularly due to their importance for cosmology. Recent investigation show that this type of scalar fields are very useful in modeling the late time acceleration of the universe, as predicted by the latest SN1a observations. Scalar fields with non-canonical kinetic terms are also common in string theory and a tachyon with Born-Infeld type action arising in open string theory is one such example.

Until now, no attempt has been made to study the existence of a scalar hair with a non-canonical kinetic term in a model independent way, for a static, spherically-symmetric black hole space-time (see [83] for such an analysis with a specific non-canonical kinetic energy term). This work is the first general study in this direction.

Generalizing the work by Sudarsky for a minimally coupled scalar field with a canonical kinetic term, we derive a general equation for studying the existence of scalar hair for non-canonical kinetic term. Equation (IV.7) is our main result. Using this equation, we study different examples for the Lagrangian of a scalar field containing a non-canonical kinetic term. It shows that for a tachyon with positive potential, which naturally shows up in open string theory, it is not possible to obtain a asymptotically flat black hole space-time which is the relevant boundary condition for the spherically-symmetric space-time. For other cases, existence of the asymptotically flat solutions depends on the choice of the kinetic function $F(X)$.

In the next chapter we are going to change the subject again; this time we are going to concentrate on the formalism of lattices, heavily used, for example, in string theory and conformal field theories.

CHAPTER V

LARGE C CONFORMAL FIELD THEORIES

In this chapter study the partition functions of conformal field theories and related lattices. Connections between these functions and the largest simple sporadic group, a Monster group will be drawn. The results of this chapter were published in Nucl. Phys. B **744**, 380 (2006).

5.1 Introduction and Motivation

We found an interesting set of relations between the partition functions of a certain class of theories, that potentially can be related to conformal field theories with a central charge being multiple of 24. We are going to use a language of lattices to help the reader understand often complicated mechanisms behind conformal field theories. A central charge c of a conformal field theory corresponds to a dimension of a lattice on which the conformal field theory is build on. The points in the lattice correspond to the fields of a theory.

The plan of this chapter is following. First we overview the formalism of modular transformations, and the relations between modular functions and forms and the lattices. We present lower dimensional examples of lattices and transformations between them. Then, we move on to higher dimensions, where we will deploy the formalism that we have developed. In the last sections of this chapter we present results, pub-

lished in [84]. The results can be seen as an extension of the remarkable relation between certain class of $24k$ dimensional lattices, and largest discrete sporadic group, called the Fischer-Griess Monster.

As a starting point for our considerations we choose the result obtained by Dixon et al. [86], which tells us that that the partition function $\mathcal{Z}$ of an arbitrary $c = 24$ holomorphic conformal field theory based on $\mathbb{R}^{24}/\Lambda$, where Λ could be any of the 24 even self-dual Niemeier lattices in 24 dimensions, can be written as follows

$$\mathcal{Z} = J + 24(h + 1)\,. \tag{V.1}$$

Here J is the weight zero modular function (with constant term set equal to zero), and h is a Coxeter number for a lattice solution. We will show that any Niemeier lattice Λ_1, represented in terms of the Θ-series related to the partition function (V.1), can be obtained from another Niemeier Λ_2. We accomplish this using projections that rearrange the lattice points to form a new lattice. Only for the particular combination of the projection parameters corresponding to the Coxeter numbers of the Niemeier lattices, do we have a lattice as a solution. For other combinations non-lattice solutions are obtained. Since Θ-functions of the 24 dimensional lattices are modular forms of weight 12, and partition functions are modular invariant (weight zero), a natural question to ask is, which object is (more) physical? The answer to this question depends on the system being investigated.

Any Niemeier lattice can be used as a starting point, i.e., any Θ-function corresponding to a lattice can be used for the initial Θ-function Z_0^0. The role of the transformation parameters is simple, they rearrange vectors in a lattice, e.g., by rescaling.

The number of transformation parameters depends strictly on an initial choice of the Θ-function Z_0^0, and hence on the number of different conjugacy classes or the number of canonical sublattices in a lattice. For example, for E_8^3, which is one of the Niemeier lattices, we have initially three parameters, one for each $SO(16)$ spinor conjugacy class. In the case of $D_{16} \times E_8$ we will have 4 parameters, that build up the sublattice. However, in these examples, upon constructing the new Θ-series (or partition function), the initial number of parameters can be reduced to a single independent parameter, leading to the Θ-function related to (V.1) with h being represented by the last free transformation parameter.

Parametrization of the twisted sector has been used to obtain new theories from 16 dimensional even self-dual lattices [87], [88]. These include theories that were already known, like supersymmetric $E_8 \times E_8$, nonsupersymmetric but non-tachyonic $SO(16) \times SO(16)$, and nonsupersymmetric and tachyonic $E_8 \times SO(16)$, etc. We generalize the analysis of [87], [88], to 24 dimensional lattices and also relax the constraints on the transformation parameters, i.e., we will no longer be working with just $\mathbb{Z}_2$ actions acting on the conjugacy classes, but rather with more complicated actions.

The plan of the chapter is as follows. In section-5.1.1 we review the formalism of modular forms and functions. We also define modular transformations. In section-5.1.2 we show some two dimensional examples of lattices. In section-5.1.3 we move on to discussion of $16D$ lattices. Section-5.1.4 introduces our transformation procedure for $c = 24$ theories. We are going to derive equation (V.1) and demonstrate some

specific patterns of lattices that can be obtained by this method. Most of our new results are contained in section-5.2 where we provide examples with $c = 24k$ via a composition construction of k modular invariant $c = 24$ partition functions. The Leech lattice is an extremal case for $k = 1$ where the coefficient of q^2 vanishes and where all other coefficients in the q-expansion decompose into irreducible representations of the Fischer-Griess Monster sporadic group. We show that when $k \geq 1$, the coefficients of the analog extremal cases also decompose into Monster group representations. Furthermore, we demonstrate interesting periodicities in k. The symmetry due to this higher dimensional Monster Moonshine leads us to conjecture that the extremal examples will correspond to lattices and corresponding CFTs. The final section contains this conjecture and a discussion.

5.1.1 Modular Space, Forms and Functions

We want to introduce a space where the points of the lattices under consideration are naturally defined. We know what we want, we just need a proper (useful) parametrization of the points of the lattices.

We start with some basic definitions [90].

First, let's define a modular form of weight k, to be a function that satisfies following conditions:

- f is analytic in the upper half-plane H (of a complex plane C) also known as Teichmüller space,

- $f\left(\frac{a\tau+b}{c\tau+d}\right) = (c\tau+d)^k f(\tau)$ whenever $\begin{bmatrix} \text{a} & \text{b} \\ \text{c} & \text{d} \end{bmatrix}$ is a member of the modular group $SL(2,\mathbb{Z})$.

The Teichmüller parameter τ is a point in the Teichmüller space such that (imaginary part of τ) $\Im\tau > 0$. This space is the space of classes of conformally inequivalent Riemann surfaces, like compactification tori for example. To define a torus on this complex space one has to make the following identification

$$z \sim z + n + m\tau \ , z \in C,\ n, m \in Z\,.$$

However, we are not quite done yet, since τ is not yet conformally invariant. The reason is that, beside of rescalings and rotations, we must also consider homeomorphisms, which leave the torus invariant but change τ. Typical example of such homeomorphisms are Dehn twists which generate all the homeomorphisms of the torus. In terms of τ, Dehn twists are given by $\tau \to \tau + 1$ and $\tau \to \frac{\tau}{\tau+1}$ as shown below.

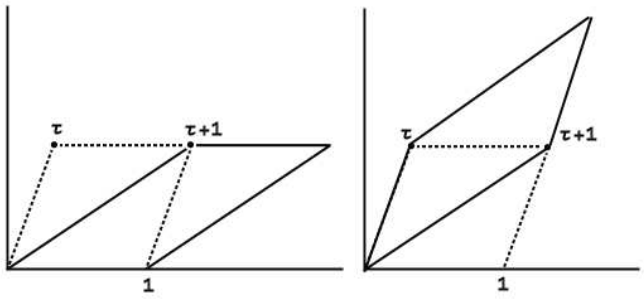

Figure 22: Dehn twists $\tau \to \tau + 1$ and $\tau \to \frac{\tau}{\tau+1}$ (solid lines) of the two dimensional torus (dotted line)

What is important for us is that the space of different possible shapes of lattices in the complex τ plane is really a quotient $H/SL(2,\mathbb{Z})$. Any function of some complex variable τ defined on this space is invariant under transformations $\tau \to \tau' = \frac{a\tau+b}{c\tau+d}$. In order to prove that a given function is invariant under transformations generated by a modular group $SL(2,\mathbb{Z})$, we are going to use the following theorem.

Thm. Let D consists of all $\tau \in \Im$ such that $-\frac{1}{2} \leq \Re\, \tau \leq \frac{1}{2}$ and $|\tau| \geq 1$. Then D is *a fundamental domain* for $SL(2,\mathbb{Z})$ in $\Im$. The $SL(2,\mathbb{Z})$ group is generated by

$$\mathbf{T} = \begin{pmatrix} 1 & 1 \\ 0 & 1 \end{pmatrix} \text{ and } \mathbf{S} = \begin{pmatrix} 0 & -1 \\ 1 & 0 \end{pmatrix} . \tag{V.2}$$

To check that some function is modular invariant under modular group $SL(2,\mathbb{Z})$, it's enough to check that it is invariant under the action of transformations S and T. It is useful to write the explicit action of $\mathbf{S}$ and $\mathbf{T}$ on τ:

$$\mathbf{S}:\ \tau \to -1/\tau\,, \tag{V.3}$$

$$\mathbf{T}:\ \tau \to \tau + 1\,. \tag{V.4}$$

In terms of T and S, Dehn twists are simply $\mathbf{S}$ and $\mathbf{TST}$. Furthermore, any element in $SL(2,\mathbb{Z})$ group can be written as $\mathbf{T}^{n_k}\mathbf{S}\mathbf{T}^{n_{k-1}}\mathbf{S}...\mathbf{S}\mathbf{T}^{n_1}$ where the n_i are integers [90].

Let us move on to some examples of modular forms, that we are going to use later in the chapter. Let us start with a formal definition of a Jacobi θ-functions:

$$\theta_3(\xi|\tau) \equiv \sum_{m=-\infty}^{\infty} e^{2mi\xi+\pi i\tau m^2}\,.$$

For us it will be enough to work with the simpler theta functions, often called θ constants, defined as:

$$\theta_2(\tau) \equiv e^{\pi i \tau/4}\theta_3(\frac{\pi\tau}{2}|\tau)\,,\ \theta_3(\tau) \equiv \theta_3(0|\tau)\,,$$
$$\theta_4(\tau) \equiv \theta_3(\tau+1)\,. \tag{V.5}$$

These functions have fantastic properties including a basically infinite web of identities which will be used later on. Most important for us, is that they have very simple modular transformation properties. Here we show their behavior under the generators of the modular group, namely under $\mathbf{S}$ we have

$$\theta_2(-1/\tau) = \left(\frac{\tau}{i}\right)^{\frac{1}{2}}\theta_4(\tau)\,, \tag{V.6}$$

$$\theta_3(-1/\tau) = \left(\frac{\tau}{i}\right)^{\frac{1}{2}}\theta_3(\tau)\,, \tag{V.7}$$

$$\theta_4(-1/\tau) = \left(\frac{\tau}{i}\right)^{\frac{1}{2}}\theta_2(\tau)\,, \tag{V.8}$$

and under $\mathbf{T}$:

$$\theta_2(\tau+1) = \sqrt{i}\theta_2(\tau)\,, \tag{V.9}$$

$$\theta_3(\tau+1) = \theta_4(\tau)\,, \tag{V.10}$$

$$\theta_4(\tau+1) = \theta_3(\tau)\,. \tag{V.11}$$

These transformation rules are easily derived using the Poisson resummation formula [91]. Finally, we introduce the modular invariant function J, which plays a very

important role in our considerations

$$\begin{aligned} J &\equiv 1/\eta^{24}\left[(\theta_3(\tau)\theta_4(\tau))^{12}+(\theta_2(\tau)\theta_3(\tau))^{12}-(\theta_2(\tau)\theta_4(\tau))^{12}\right]+24 \\ &= 1/q^2+196884q^2+21493760q^4+\mathcal{O}(q^6)+\ldots, \end{aligned} \tag{V.12}$$

with q being nome, i.e, $q=e^{i\pi\tau}$. Function J (sometimes called the J-invariant related to weight-zero modular function j by $J=j-744$) is the modular form of weight zero, as can be easily proved using transformations (V.6)-(V.11). In the denominator of (V.12) we have the 24th power of Dedekind η-function[1]

$$\eta^{24}(\tau)=\left[q^{1/12}\prod_{m=1}^{\infty}(1-q^{2m})\right]^{24}=q^2-24q^4+252q^6-1472q^8+\ldots, \tag{V.13}$$

which is the unique form of weight 12, with the following transformation rules under **S** and **T**

$$\eta^{24}(-1/\tau)=(\sqrt{-i\tau}\eta(\tau))^{24}\,,\ \eta^{24}(\tau+1)=(e^{i\pi/12}\eta(\tau))^{24}\,. \tag{V.14}$$

5.1.2 Modular Transformations and 2 Dimensional Examples

Even and self-dual lattices exist in, $d=8k$ is the lowest dimension in which we an have even and self-dual lattice. However, we can give examples of lower dimensional either even or self-dual lattices. Knowing the modular properties of theta functions, we can easily guess that any n-dimensional lattice given by θ_3^n is self-dual since θ_3^n/η^n is invariant under **S** transformation. This lattice is just an n-dimensional integer lattice, $\mathbb{Z}^n$. We present $\mathbb{Z}^2$ i.e., the square lattice as an example. The theta expansion of this

[1]Dedekind η-function itself is a modular form of weight 1/2.

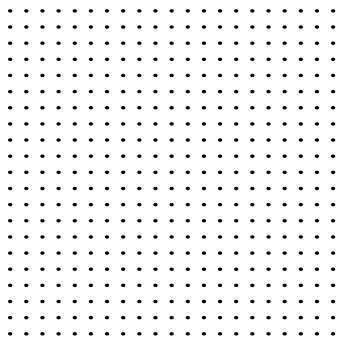

Figure 23: Square lattice and its dual.

lattice is

$$\mathrm{Z}_{\mathbb{Z}^2} = 1 + 4q + 4q^2 + 8q^5 + 4q^8 + \dots . \tag{V.15}$$

We see that this is the correct function by counting the number of neighbors at every layer. The dual lattice is obtained via a $\pi/2$ rotation and it covers the original lattice, therefore $(Z)^2$ is self-dual.

Now we want to present an example of an even lattice. From $(V.15)$, it's easy to see that after elimination of odd distances (i.e. odd powers in q) one gets even lattice. Knowing the modular properties of θ_4 and its theta expansion:

$$\theta_4 = 1 - 2q + 2q^4 - 2q^9 + 2q^{16} + \dots . \tag{V.16}$$

We conclude that

$$\mathrm{Z}_{Even} = \frac{1}{2}(\theta_3^n + \theta_4^n) \tag{V.17}$$

is an even lattice. Two dimensional example of this type of lattice is simply a checkerboard, obtained by coloring the points of $\mathbb{Z}^2$ alternatively black and white with

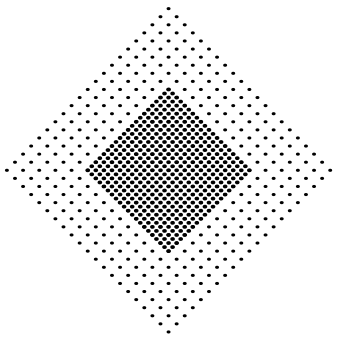

Figure 24: Two dimensional even (checkerboard) lattice, and its dual (the one with a higher density)

checkerboard coloring, and taking the black points. Again, using modular properties of θ_3 and θ_4 (V.6)-(V.8) we see that this lattice is not self-dual. The dual of a check-board lattice is simply $\frac{1}{2}(\theta_3^2+\theta_2^2)$ and that's why one cannot transform it either by rotation or translation to the original lattice.

5.1.3 Modular Transformations and 16 Dimensional Examples

We start with some basic definitions and a classic example already present in the literature [87], [88]. A formal definition of a Θ-series of an even self-dual lattice Λ is

$$\mathrm{Z}_\Lambda = \sum_{x\in\Lambda} N(m) q^m \,, \tag{V.18}$$

where $N(m)$ is a number of vectors with length squared equal to an even number m. From a mathematical point of view, Z_Λ is a modular form of weight $\dim(\Lambda)/2$. Let us recall the difference between Z_Λ and a partition function $\mathcal{Z}$. Namely, a partition function $\mathcal{Z}$ is a modular function (a modular form of weight zero). By looking at the modular properties of Z_Λ we conclude that it is related to $\mathcal{Z}$ by $\mathcal{Z} = \mathrm{Z}_\Lambda/\eta^{\dim(\Lambda)}$, where $\eta(q)$ Dedekind η-function defined in (V.13). Most of the time, we will focus

on the lattices, hence we will work with Θ-functions. However we will make some remarks about partition functions as well.

Let us investigate the relationship between $SO(32)$ and $E_8 \times E_8$ compactification lattices. The Θ-function of both can be expressed in terms of different conjugacy classes of the $SO(16) \times SO(16)$ lattice, which is a maximal common subgroup of both $SO(32)$ and $E_8 \times E_8$. $SO(2N)$ groups have four conjugacy classes namely, the *adjoint* (I_N), the *vector* (V_N), the *spinor* (S_N), and the *conjugate spinor* (C_N). They can be expressed in terms of Jacobi-θ functions as follows [89]:

$$I_N \equiv \frac{1}{2}(\theta_3^N + \theta_4^N)\,,\ V_N \equiv \frac{1}{2}(\theta_3^N - \theta_4^N)\,, \tag{V.19}$$

$$S_N \equiv \frac{1}{2}\theta_2^N\,,\ C_N \equiv \frac{1}{2}\theta_2^N\,, \tag{V.20}$$

where N is the rank of $SO(2N)$. Both *spinor* and *conjugate spinor* have the same Θ-expansions.

We will make a use from the transformation rules for Jacobi-θ functions (V.6)-(V.11). We have the following **S**-transformed conjugacy classes

$$\mathbf{S}(I_N) = \frac{1}{2}(I_N + V_N + S_N + C_N)\,,\ \mathbf{S}(V_N) = \frac{1}{2}(I_N + V_N - S_N - C_N)\,, \tag{V.21}$$

$$\mathbf{S}(S_N) = \frac{1}{2}(I_N - V_N)\,,\ \mathbf{S}(C_N) = \frac{1}{2}(I_N - V_N)\,, \tag{V.22}$$

and **T**-transformations acting on **S**-transformed conjugacy classes of $SO(2N)$ give

$$\mathbf{TS}(I_N) = \frac{1}{2}(I_N - V_N + S_N + C_N)\,,\ \mathbf{TS}(V_N) = \frac{1}{2}(I_N - V_N - S_N - C_N)\,, \tag{V.23}$$

$$\mathbf{TS}(S_N) = \frac{1}{2}(I_N + V_N)\,,\ \mathbf{TS}(C_N) = \frac{1}{2}(I_N + V_N)\,. \tag{V.24}$$

We will use a **TS** transformation to restore the modular invariance of the new partition functions resulting from the construction presented below.

Now consider the Θ-function of the $SO(32)$ lattice, which is given in terms of $SO(16) \times SO(16)$ conjugacy classes by

$$\mathrm{Z}_{SO(32)} = (I_8^2 + V_8^2 + S_8^2 + C_8^2)\,, \tag{V.25}$$

where squares are just a short-hand notation for (I_8, I_8), etc. A $\mathbb{Z}_2$ action on the conjugacy classes means we have to multiply a given conjugacy class by ± 1. If one chooses to act with transformations that flip the sign of the vector and conjugate spinor representations of the second $SO(16)$ [88], as shown in table 4 one gets a new

Table 4: A $\mathbb{Z}_2$ transformation applied to $\mathrm{Z}_{SO(32)}$.

	I_8	V_8	S_8	C_8
First $SO(16)$	+	+	+	+
Second $SO(16)$	+	−	+	−

Θ-series

$$\mathrm{Z}_1 = (I_8^2 - V_8^2 + S_8^2 - C_8^2)\,. \tag{V.26}$$

It is obvious that Z_1 is not modular invariant as can be seen from its q-expansion. I.e., some of the coefficients are negative. In order to restore wanted modular properties,

one has to add the **S** and the **TS** transformed forms of Z_1:

$$\mathbf{S}\mathrm{Z}_1 = I_8 S_8 + S_8 I_8 + C_8 V_8 + V_8 C_8 \,, \tag{V.27}$$

$$\mathbf{TS}\mathrm{Z}_1 = I_8 S_8 + S_8 I_8 - C_8 V_8 - V_8 C_8 \,. \tag{V.28}$$

Adding partition functions (V.25)-(V.28), and also taking into account the overall normalization, one obtains the Θ-function of the dual $E_8 \times E_8$ theory, namely

$$\frac{1}{2}\left(\mathrm{Z}_{SO(32)} + \mathrm{Z}_1 + \mathbf{S}\mathrm{Z}_1 + \mathbf{TS}\mathrm{Z}_1\right) = \mathrm{Z}_{E_8 \times E_8} = (I_8 + S_8)^2 \,. \tag{V.29}$$

5.1.4 Transformation Model in 24 dimensions

Now we move on to 24 dimensional lattices. We begin by writing the $D_{16} \times E_8$ Niemeier lattice represented in terms of $D_8 \times D_8 \times D_8$ conjugacy classes[2]. We follow the standard notation (see for example [86]), where Z_0^0 is the initial untwisted sector, Z_0^1 is a projection, $\mathrm{Z}_1^0 = \mathbf{S}\mathrm{Z}_0^1$ and $\mathrm{Z}_1^1 = \mathbf{T}\mathrm{Z}_1^0$ are modular transformed (twisted) sectors. Therefore

$$\mathrm{Z}_0^0 = (I^2 + V^2 + S^2 + C^2)(I + S) \,, \tag{V.30}$$

which, after evaluation of conjugacy classes in terms of Jacobi-θ functions, can be expanded into a q-series

$$\mathrm{Z}_0^0 = 1 + 720q^2 + 179280q^4 + \mathcal{O}(q^6) \,. \tag{V.31}$$

[2]We omit subscript "8" in the notation.

Now let us make a projection, which in the most general way, can be written as

$$\mathrm{Z}_0^1 = (I^2 + a\ V^2 + b\ S^2 + c\ C^2)(I + e\ S)\,, \tag{V.32}$$

where a, b, c and e are projection parameters, that change the signs and/or scale the conjugacy classes. We also evaluate the q-expansion of Z_0^1 to see the influence of the projection we have just made

$$\mathrm{Z}_0^1 = 1 + 16(21 + 16a + 8e)q^2 + \mathcal{O}(q^4)\,. \tag{V.33}$$

This series is still even in powers of q, however self-duality may have been lost. Using transformation properties (V.21)-(V.22) we get twisted sectors

$$\begin{aligned}\mathrm{Z}_1^0 \equiv \mathbf{S}\mathrm{Z}_0^1 \;&=\; \frac{1}{8}\left[(I+V+S+C)^2 + a(I+V-S-C)^2 + b(I-V)^2 + c(I-V)^2\right]\times \\ &\times\;\; [I+V+S+C+e\ (I-V)]\ ,\end{aligned} \tag{V.34}$$

and

$$\begin{aligned}\mathrm{Z}_1^1 \equiv \mathbf{TS}\mathrm{Z}_0^1 \;&=\; \frac{1}{8}\left[(I-V+S+C)^2 + a(I-V-S-C)^2 + b(I+V)^2 + c(I+V)^2\right] \\ &\times\;\; [I-V+S+C+e\ (I+V)]\ .\end{aligned} \tag{V.35}$$

New transformed (orbifolded under certain circumstances) theories can be represented in the following general form

$$\mathrm{Z}_{\mathrm{new}} = \frac{1}{2}\left(\mathrm{Z}_0^0 + \mathrm{Z}_0^1 + \mathrm{Z}_1^0 + \mathrm{Z}_1^1\right)\ . \tag{V.36}$$

We have chosen **S** and **TS** transformations to restore modular invariance of a Θ-function. Neither Z_1^0 nor Z_1^1 is even. We can see this directly from the q-expansion

of Z_1^0

$$\mathrm{Z}_1^0 = \frac{1}{8}(1+a+b+c)(1+e) + 2\left[2-b-c+e-3be-3ce+a(3+e)\right]q + \mathcal{O}(q^2) \quad \text{(V.37)}$$

However, when added to Z_1^0, the **TS** transformed Θ-function eliminates terms with odd powers in q, i.e., its q-expansion is

$$\mathrm{Z}_1^1 = \frac{1}{8}(1+a+b+c)(1+e) - 2\left[2-b-c+e-3be-3ce+a(3+e)\right]q + \mathcal{O}(q^2) \quad \text{(V.38)}$$

An even self-dual lattice scaled by the appropriate power of Dedekind η-function is by definition a modular function, but modular invariance does not necessarily imply we have a lattice; therefore modular invariance is a more general concept[3]. But as we see we are safe; the odd terms in the twisted sectors have cancelled.

Note, $\mathrm{Z}_{\mathrm{new}}$ is modular invariant regardless of the values of the transformation parameters. However, a q-expansion of a theory transformed in a way described above has to be properly normalized. Normalization is not yet guaranteed, since the zeroth order term in the q-expansion is given by

$$1 + \frac{1}{8}(1+a+b+c)(1+e)\,. \quad \text{(V.39)}$$

For $e = 1$, we are left with only one combination of the parameters a, b and c, such that normalization of the zeroth order term is fixed to 1 i.e., $a+b+c = -1$. As a result of this fixing, one is left with

$$\mathrm{Z}_{\mathrm{new}} = (I+S)^3\,. \quad \text{(V.40)}$$

[3]This is important since only even and self-dual lattices can be used as a basis for a compactification torus.

The resulting lattice corresponds to the $E_8 \times E_8 \times E_8$ isospectral[4] partner of $D_{16} \times E_8$. But there is a more interesting case. For $e = -1$ the normalization condition is already fixed, but this puts no constraints on the rest of the parameters. Moreover, the parameters (a, b, c) are found in a specific combination[5] at every order in q^2

$$x = 3a - b - c\,. \tag{V.41}$$

We show this by explicitly evaluating $\mathrm{Z}_{\mathrm{new}}$

$$\mathrm{Z}_{\mathrm{new}} = 1 + 48(13 + 2x)q^2 - 144(-1261 + 16x)q^4 + 4032(4199 + 6x)q^6 + \ldots\,, \tag{V.42}$$

which can be rewritten

$$\mathrm{Z}_{\mathrm{new}} = \left[1 + 624q^2 + 181584q^4 + 16930368q^6 + \ldots\right] + 96x\left[q^2 - 24q^4 + 252q^6 + \ldots\right] \tag{V.43}$$

where we have divided $\mathrm{Z}_{\mathrm{new}}$ into x-dependent and x-independent parts. The number of independent parameters (after one fixes e) is reduced to one. This parameter, x, can be related to the Coxeter number h of a given lattice. The relation is model dependent and depends on an initial choice of Z_0^0. For the case at hand

$$x \equiv \frac{h - 26}{4}\,. \tag{V.44}$$

We observe that the Θ-series in the first square bracket in (V.43) is an even self-dual (i.e. invariant under $\mathbf{S}$ and $\mathbf{T}$) function. It does not correspond to a lattice solution. However it can be related to the J-invariant, defined in (V.12). Terms in the second square bracket in (V.43) form a unique cusp (constant term equal to zero) form of

[4] A pair of lattices is said to be isospectral if they have the same Θ-expansion.

[5] For other values of e the analysis gets more complicated.

weight 12 [90], which can be written as the 24th power of the Dedekind η-function . Using this knowledge we can write our solution in a more compact form

$$\mathrm{Z}_{\mathrm{new}} = [J + 24(h+1)]\,\eta^{24}\,, \tag{V.45}$$

where h is a positive integer and is equal to the Coxeter number of the 24 dimensional even self-dual lattice if $\mathrm{Z}_{\mathrm{new}}$ forms a Niemeier lattice. Only for specific values of x does one get a solution that corresponds to a lattice. However, for the majority of cases, representation in terms of group lattices is not possible. Physically this means that the primary fields of the CFT do not transform under any group (there are exceptions to be discussed below, see [107]), hence one is left with $24 \cdot h$ singlets.

We now classify all solutions that can be derived by this technique. Using (V.44) in (V.45) one finds the allowed values of x form a set of 8191 elements[6]. This is true under two conditions, first we assume that all the coefficients in a q-expansion are positive integers [91], [93]. This assumption is not only reasonable but also physical, since these coefficients give us the number of states at each string mass level from the partition function point of view, and from the lattice point of view they correspond to the number of sites in each layer. The second assumption is that the kissing number for both lattices and non-lattices is an integer number which can change by one[7].

Remembering that our starting point was the $D_{16}E_8$ lattice, one can immediately see that integer values of (a, b, c) parameters correspond to "relatives"[8] of this lattice

[6]For what it is worth 8191 is a Marsenne prime.

[7]One could assume that a kissing number for a non-lattice solution is still a multiple of 24, as with lattices. Then modular properties of the Θ-series are preserved, but the number of solutions is reduced to 342.

[8]We call a pair of group lattices relatives if they share a common maximal subgroup.

Table 5: Relatives of $D_{16}E_8$ lattice, and their parametrization.

Lattice	h	x	a	b	c
D_{24}	46	5	1	-1	-1
E_8^3	30	1	1	1	1
D_{12}^2	22	-1	-1	-1	-1
$E_7^2D_{10}$	18	-2	0	1	1
D_8^3	14	-3	-1	1	-1

[91]. Table 5 shows the transformation parameters for all five relatives of $D_{16}E_8$. All except $E_7^2D_{10}$, can be gotten from the action of a $\mathbb{Z}_2$. Since E_8^3 and $D_{16}E_8$ are isospectral, we can set $a = b = c = 1$ in that case. There are three other possible "integer combinations" for x, corresponding to D_6^4, D_4^6 and A_1^{24} (table 6), that are maximal subgroups of $D_{16}E_8$. Other integer values for x that reach Niemeier lattices

Table 6: Maximal subgroups of $D_{16}E_8$ lattice, and their parametrization.

Lattice	h	x	a	b	c
D_6^4	10	-4	-1	1	0
D_4^6	6	-5	-1	1	1
A_1^{24}	2	-6	-2	1	1

cannot be expressed in terms of integer values of (a, b, c), which means that more complicated actions are needed. We list all the lattice solutions and the corresponding x parametrization in table 7.

Table 7: All lattice solutions in 24 dimensions. The second column represents the Coxeter number h. The third column shows x parametrization when $\mathrm{Z}_0^0 = \mathrm{Z}_{D_{16}E_8}$. The glue code in the explicit form is given for most of the lattices and in a generator form for A_3^8, A_2^{12}, A_1^{24} as in [91]. Numbers in this column represent conjugacy classes, + means combination of adjoint and spinor conjugacy classes, 0 stands for the adjoint, $1, 2, 3$ are vector, spinor and conjugate spinor for D_n lattices (similarly for A_n with $n-1$, and E_6, E_7 with two conjugacy classes). In the last three columns the first three coefficients in the Θ-series are listed with a_2 being a kissing number for a given lattice (except for Leech).

Lattice	Coxeter	x	Glue Code	a_2	a_4	a_6
E_8	30		+	240	2160	6720
E_8^2	30		++	480	61920	1050240
D_{16}	30		+	480	61920	1050240
D_{24}	46	5	+	1104	170064	17051328
$D_{16}E_8$	30	1	++	720	179280	16954560
E_8^3	30	1	+++	720	179280	16954560
A_{24}	25	$-1/4$	$[0] + 2([5] + [10])$	600	182160	16924320
D_{12}^2	22	-1	$[00] + 2[12] + [11]$	528	183888	16906176
$A_{17}E_7$	18	-2	$[00] + 2[31] + 2[60] + [91]$	432	186192	16881984
$D_{10}E_7^2$	18	-2	$[000] + [110] + [310] + [211]$	432	186192	16881984
$A_{15}D_9$	16	$-5/2$	$[00] + 2([12] + [16] + [24]) + [08]$	384	187344	16869888
D_8^3	14	-3	$[000] + 3([011] + [122]) + [111]$	336	188496	16857792
A_{12}^2	13	$-13/4$	$[00] + 4([15] + [23] + [46])$	312	189072	16851744
$A_{11}D_7E_6$	12	$-7/2$	$[000] + 2[111] + 2[310] + 2[401] + 2[511] + [620]$	288	189648	16845696
E_6^4	12	$-7/2$	$[0000] + 8[1110]$	288	189648	16845696
$A_9^2D_6$	10	-4	$[000] + 4([121] + [132] + [240] + [341]) + 2[051] + [552]$	240	190800	16833600
D_6^4	10	-4	$[0000] + 12[0123] + [1111] + [2222] + [3333]$	240	190800	16833600
A_8^3	9	$-17/4$	$[000] + 6([114] + [330] + [122] + [244]) + 2[333]$	216	191376	16827552
$A_7^2D_5^2$	8	$-9/2$	$[0000] + 4([0211] + [1112] + [2202] + [3312] + [2411]) + 8[1301] + 2[0422] + [4400]$	192	191952	16821504
A_6^4	7	$-19/4$	$[0000] + 24[0123] + 8([1112] + [1222] + [2223])$	168	192528	16815456
$A_5^4D_4$	6	-5	$[00000] + 6[00331] + 24([00121] + [12231]) + 8([02220] + [11130]) + [33330]$	144	193104	16809408
D_4^6	6	-5	$[000000] + 45[000011] + 18[111111]$	144	193104	16809408
A_4^6	5	$-21/4$	$[000000] + 60[001122] + 40[111222] + 12[011111] + 12[022222]$	120	193680	16803360
A_3^8	4	$-11/2$	$[3(2001011)] +$ *cyclic permutations of* (2001011)	96	194256	16797312
A_2^{12}	3	$-23/4$	$[2(11211122212)] +$ *cyclic permutations of* (11211122212)	72	194832	16791264
A_1^{24}	2	-6	$[1(000001010011001101011111)] +$ *cyclic permutations of* $(000001010011001101011111)$	48	195408	16785216
Leech	0	$-13/2$	*None*	0	196560	16773120

Other values of (a, b, c) give the other Niemeier lattices and non-lattices solutions. As a second example, we choose another Niemeier lattice E_8^3 with a Θ-function

$$\mathrm{Z}_0^0 = (I + S)^3. \tag{V.46}$$

where the projected sector is

$$\mathrm{Z}_0^1 = (I + a\ S)(I + b\ S)(I + c\ S)\,. \tag{V.47}$$

Again to restore modular invariance we introduce twisted sectors Z_1^0 and Z_1^1. As a result a new modular invariant Θ-function is obtained, and can be written in the form (V.45), except that the relation between Coxeter number and transformation parameters is different. For example, after fixing $b = c = -1$ we are left with one free parameter $a = (h - 22)/8$, which tells us that the space of the values of the a parameters reaches all 8191 solutions.

If one restricts parameters (a, b, c) to ± 1 one gets a family of simple $\mathbb{Z}_2$ actions transforming the original lattice into the relatives $D_{16}E_8$ and $D_8D_8D_8$ of E_8^3.

Let us finish this section with a following simple observation. The $\mathbb{Z}_2$ orbifold actions are the actions which break/restore symmetry in a special way. If Λ_1 and Λ_2 have a common maximal subgroup then there is a $\mathbb{Z}_2$ action that transforms Λ_1 into Λ_2. This is not the case when Λ_1 and Λ_2 do not have a common maximal subgroup. Therefore, this is possible for only a few pairs of Niemeier lattices (see table 8). This result follows the lines of the procedure discussed by Dolan et al. in [92].

We want to emphasize that the main point of this section was to introduce trans-

Table 8: Patterns of lattices obtained by $\mathbb{Z}_2$ actions.

$$
\begin{array}{ccccccccc}
E_8D_{16} & \rightarrow & D_8^3 & & & & & & \\
 & & \downarrow & & & & & & \\
E_8^3 & \rightarrow & D_8^3 & \rightarrow & D_4^6 & \rightarrow & A_1^{24} & \rightarrow & \text{Leech} \\
D_{24} & \rightarrow & D_{12}^2 & \rightarrow & D_6^4 & \rightarrow & A_3^8 & & \\
E_7^2D_{10} & \rightarrow & A_7^2D_5^2 & & & & & &
\end{array}
$$

formations between extant lattices, and hence between known partition functions of their holomorphic conformal field theories. We do not claim that the other class of solutions we found (namely non-lattices) are new CFTs. They are however modular functions and can be generated from the choice of the projection parameter which corresponds to the analog of a Coxeter number of the non-existent Niemeier lattice, so they remain CFT candidates. We delay further discussion of these theories until we reach the discussion section. In the next section we discuss the generalization of these results to $k > 1$. The examples in this section will serve as a basis for construction of potential higher dimensional CFTs based on generalizations of Niemeier lattices, and in particular on generalized extremal Θ-functions or partition functions. The list of physical requirements which has to be imposed on a one-loop partition function of a conformal field theory was given for example in [93, 94]. All of these constraints are satisfied by any 'candidate CFT' build on even self-dual lattice presented in this section and known earlier in the literature [86]. Following this line of reasoning we proceed to focus on potential classes of CFTs build on extremal even self-dual lattices in dimensions $24k$ if and when they exist, or if not, on extremal even self-dual Θ-series

with $c = 24k$. This avoids possible (or almost certain) complications of constructions based on non-lattice objects.

5.2 $c = 24k$ Extremal Θ Series and Fischer-Griess Monster Group

In this section we generalize our procedure to higher dimensions. We concentrate on $c = 24k$ Θ series which are in some cases $24k$ dimensional lattices. Their Θ-functions can be expressed in terms of positive integer[9] powers of Z_{new} given in (V.45). For example, one can use them in the construction of the lattices with dense packing in 48 dimensions and the highest packing in 24. These lattices are build on the so called extremal Θ-functions. For $k = 1$ the kissing number (so the first non-zero coefficient in the q-expansion of the lattice) of the lattice with the highest packing is obtained as follows. The coefficients a_2 and a_4 in the q-expansion $1 + a_2q^2 + a_4q^4 + ...$ are constrained by the equation $24a_2 + a_4 = 196560$ (see below). From this we see that the maximum packing corresponds to the choice $a_2 = 0$ and $a_4 = 196560$.

In general, the equivalent of a 24 dimensional even self-dual lattice, i.e. modular invariant lattice, can be obtained from

$$\eta^{24}(J + 24 + a_2) = 1 + a_2q^2 + (196560 - 24a_2)q^4 + 252(66560 + a_2)q^6 + ... \quad \text{(V.48)}$$

where a_2 is a positive integer. The extremal $a_2 = 0$ case is a Leech lattice. In order to preserve wanted properties we have to put constraints on values of the integer a_2. It is easy to see that $a_2 \in [0, 8190]$, generates q-expansion with positive entries. The same kind of constraint can be imposed in 48 dimensions, where a modular invariant

[9] However, one can generalize this procedure to other dimensions ($8k$) as well.

Θ-series is written in the general form

$$\begin{aligned}\eta^{48}(J+24+a)(J+24+b) &= 1+(a+b)q^2+\left[2\cdot 196560-24(a+b)+ab\right]q^4+\\ &+ 12\left[2795520+16401(a+b)-4ab\right]q^6+... \quad \text{(V.49)}\end{aligned}$$

By rewriting the expression as

$$1+a_2q^2+a_4q^4+(52416000+195660a_2-48a_4)q^6+... \quad \text{(V.50)}$$

we see that a dense packing with kissing number 52416000 is obtained if one chooses $a_2=a_4=0$. It is the P_{48} lattice [91]. In 72 dimensions[10] we have

$$1+a_2q^2+a_4q^4+a_6q^6+(6218175600+57091612a_2+195660a_4-72a_6)q^8+.. \quad \text{(V.51)}$$

In this case one would expect a lattice corresponding to the extremal Θ-series would be obtained by setting a_2, a_4 and a_6 to zero so that the corresponding kissing number would be 6218175600 except for the fact that this Θ-series is not known to correspond to a lattice [95]. The extremal Θ-series in $24k$ dimensions obtained from this procedure is gotten by the requirement that all of the coefficients $a_2,...,a_{2k}$ vanish[11]. We can find in principle the number of solutions with this parametrization, i.e., sensible Θ-functions in $24k$ dimensions. In 24 dimensions the values of a_2 were constrained. In the rest of the cases, i.e., $k>1$, the number of independent parameters is k. However again the parameter space is finite. Using this information one can calculate the number of possible Θ-functions in any dimension. For example in 48 dimensions we

[10] All of the numerical calculations throughout this work were performed with a help of Wolfram Mathematica 4.2/5.0/5.1 .

[11] Alternatively, we can use the bound known in from the lattice theory [96], that the minimal norm of n-dimensional unimodular lattice is $\mu \leq \left[\frac{n}{24}\right]+2$.

find 806022416786149 Θ-series. In this plethora of possibilities, we expect only some small fraction can be interpreted as lattices, which can be related to CFT[12].

Finally the partition function for any $24k$ dimensional theory contains a finite number of tachyons. For $k = 1$ there is a single tachyon with $(m)^2 = -1$, for $k > 1$ we have k tachyon levels in the spectrum. The most general formula of a partition function in $24k$ dimensions is

$$\mathcal{J}_k(\vec{x}) \equiv \prod_{m=1}^{k}(J + 24 + x_m) = \frac{1}{q^{2k}}\left[1 + \sum_{m=(k-1)}^{\infty} f_{2m}(x_1, ..., x_k)q^{2m-2k}\right], \quad \text{(V.52)}$$

where $\vec{x} = (x_1, ..., x_k)$ and $f_{2m} \geq 0$ are polynomials in the x_i. The lowest (tachyonic) state with $(m)^2 = -k$ is always populated by a single tachyon, and higher states are functions of $(x_1, x_2, ..., x_k)$. The x_is can be chosen in such a way that all tachyon levels above the lowest level are absent, hence the next populated level would be occupied by massless states. This choice involves the elimination of $k-1$ parameters. The final series would then depend on a single parameter x_k, more precisely the massless level is a polynomial in x_k of the order k. The remainder of the spectrum does not depend on the choice of x_k, in analogy with the 24 dimensional case. What is appealing in these models is that for $k \gg 1$ we can have a single tachyonic state with arbitrarily large negative mass square that could potentially decouple from the spectrum leaving only states with $(m)^2 \geq 0$, and the partition function of such a theory is still a well defined modular function. This may be an alternative to tachyon condensation [97].

Let us evaluate a few of examples with only a single tachyon coupled to the identity

[12]For example, there are 24^2 even self-dual CFTs constructed out of 24 dimensional Niemeier lattices. This is a subset of the even self dual lattices in $48D$. Even at $32D$ the number of even self dual lattices is known to be very large.

at q^{-2k} for $k = 1, 2, 3$ and 4, which we define as $\mathcal{G}_k = \mathcal{J}_k|_{extremal}$. These are:

$$\begin{aligned}
\mathcal{G}_1(x_1) &= 1/q^2 + (24 + x_1) + 196884q^2 + ... \\
\mathcal{G}_2(x_2) &= 1/q^4 + (393192 - 48x_2 - x_2^2) + 42987520q^2 + ... \\
\mathcal{G}_3(x_3) &= 1/q^6 + (50319456 - 588924x_3 + 72x_3^2 + x_3^3) + 2592899910q^2 + ... \\
\mathcal{G}_4(x_4) &= 1/q^8 + (-75679531032 - 48228608x_4 + 784080x_4^2 - 96x_4^3 - x_4^4) + \\
&\quad +80983425024q^2 + ...
\end{aligned} \tag{V.53}$$

The allowed values of the polynomial coefficient of q^0 are integers that run from zero to the value of the q^2 coefficient. If one changes k, then the q^2 coefficients are Fourier coefficients of the unique weight-2 normalized meromorphic modular form for $SL(2, \mathbb{Z})$ with all poles at infinity [98]. The partition functions (V.53) are examples of the replication formulas [99].

There exists an interesting alternative set of possible CFTs with partition functions [100] that we will call $\mathcal{H}_k$, where for different values of k we have

$$\begin{aligned}
\mathcal{H}_1 &= 1/q^2 + 196884q^2 + ... \\
\mathcal{H}_2 &= 1/q^4 + 1 + 42987520q^2 + ... \\
\mathcal{H}_3 &= 1/q^6 + 1/q^2 + 1 + 2593096794q^2 + ... \\
\mathcal{H}_4 &= 1/q^8 + 1/q^4 + 1/q^2 + 1 + 81026609428q^2 + ... \\
\mathcal{H}_5 &= 1/q^{10} + 1/q^6 + 1/q^4 + 1/q^2 + 1 + 1668649287314q^2 + ...
\end{aligned} \tag{V.54}$$

Again we fix the tachyon levels by appropriate choices of the xs. Note that the q^2 coefficients for $k = 1$ and 2 coincide in (V.53) and (V.54) but not for larger k. These are characters of the extremal vertex operator algebra of rank $24k$ (if it exists)

Table 9: Decomposition of the coefficients of j into irreducible representations of the Monster group (for more see [101], [102]).

	J-invariant	Monster
j_2	196884	$1 + 196883$
j_4	21493760	$1 + 196883 + 21296876$
j_6	864299970	$2 \cdot 1 + 2 \cdot 196883 + 21296876 + 842609326$
j_8	20245856256	$3 \cdot 1 + 3 \cdot 196883 + 21296876 + 2 \cdot 842609326 + 18538750076$
j_{10}	333202640600	$4 \cdot 1 + 5 \cdot 196883 + 3 \cdot 21296876 + 2 \cdot 842609326 + 18538750076$ $+19360062527 + 293553734298$
j_{12}	4252023300096	$3 \cdot 1 + 7 \cdot 196883 + 6 \cdot 21296876 + 2 \cdot 842609326 + 4 \cdot 19360062527$ $+293553734298 + 3879214937598$

[100]. These characters were obtained by requiring $24k + \sum_{m=1}^{k} x_m = 0$ (so that the $-(k-1)$ state is empty), all other coefficients of tachyon levels up the to massless states are fixed to one.

The extremal 24 dimensional case has been shown to be related to the Fischer-Griess Monster group. In fact $\mathcal{G}_1(x_1)$ is the modular function j when $x_1 = -24$. j has the expansion

$$j = 1/q^2 + 196884q^2 + 21493760q^4 + 864299970q^6 + 20245856256q^8 + ... \quad \text{(V.55)}$$

and the coefficients of this expansion decompose into dimensions of the irreducible representations of the Monster (see table 9), where we use the notation

$$j = 1/q^2 + j_2 q^2 + j_4 q^4 + ... \quad \text{(V.56)}$$

Table 10: Coefficients of $24k$ dimensional extremal partition functions $\mathcal{G}_k$ in terms of coefficients j_{2n} of modular function j.

k	g_2	g_4	g_6	g_8	g_{10}	g_{12}
2	$2j_4$	$2j_8 + j_2$	$2j_{12}$	$2j_{16} + j_4$	$2j_{20}$	$2j_{24} + j_6$
3	$3j_6$	$3j_{12}$	$3j_{18} + j_2$	$3j_{24}$	$3j_{30}$	$3j_{36} + j_4$
4	$4j_8$	$4j_{16} + 2j_4$	$4j_{24}$	$4j_{32} + 2j_8 + j_2$	$4j_{40}$	$4j_{48} + 2j_{12}$
5	$5j_{10}$	$5j_{20}$	$5j_{30}$	$5j_{40}$	$5j_{50} + j_2$	$5j_{60}$
6	$6j_{12}$	$6j_{24} + 3j_6$	$6j_{36} + 2j_4$	$6j_{48} + 3j_{12}$	$6j_{60}$	$6j_{72} + 3j_{18} + 2j_8 + j_2$
$\vdots$	$\vdots$	$\vdots$	$\vdots$	$\vdots$	$\vdots$	$\vdots$
k	g_{14}	g_{16}	g_{18}	g_{20}	g_{22}	g_{24}
2	$2j_{28}$	$2j_{32} + j_8$	$2j_{36}$	$2j_{40} + j_{10}$	$2j_{44}$	$2j_{48} + j_{12}$
3	$3j_{42}$	$3j_{48}$	$3j_{54} + j_6$	$3j_{60}$	$3j_{66}$	$3j_{72} + j_8$
4	$4j_{56}$	$4j_{64} + 2j_{16} + j_4$	$4j_{72}$	$4j_{80} + 2j_{20}$	$4j_{88}$	$4j_{96} + 2j_{24} + j_6$
5	$5j_{70}$	$5j_{80}$	$5j_{90}$	$5j_{100} + j_4$	$5j_{110}$	$5j_{120}$
6	$6j_{84}$	$6j_{96} + 3j_{24}$	$6j_{108} + 2j_{12}$	$6j_{120} + 3j_{30}$	$6j_{132}$	$6j_{144} + 3j_{36} + 2j_{16} + j_4$
$\vdots$	$\vdots$	$\vdots$	$\vdots$	$\vdots$	$\vdots$	$\vdots$
k	g_{26}	g_{28}	g_{30}	g_{32}	g_{34}	g_{36}
2	$2j_{52}$	$2j_{56} + j_{14}$	$2j_{60}$	$2j_{64} + j_{16}$	$2j_{68}$	$2j_{72} + j_{18}$
3	$3j_{78}$	$3j_{84}$	$3j_{90} + j_{10}$	$3j_{96}$	$3j_{102}$	$3j_{108} + j_{12}$
4	$4j_{104}$	$4j_{112} + 2j_{28}$	$4j_{120}$	$4j_{128} + 2j_{32} + j_8$	$4j_{136}$	$4j_{144} + 2j_{36}$
5	$5j_{130}$	$5j_{140}$	$5j_{150} + j_6$	$5j_{160}$	$5j_{170}$	$5j_{180}$
6	$6j_{156}$	$6j_{168} + 3j_{42}$	$6j_{180} + 2j_{20}$	$6j_{192} + 3j_{48}$	$6j_{204}$	$6j_{216} + 3j_{54} + 2j_{24} + j_6$
$\vdots$	$\vdots$	$\vdots$	$\vdots$	$\vdots$	$\vdots$	$\vdots$
k	g_{38}	g_{40}	g_{42}	g_{44}	g_{46}	g_{48}
2	$2j_{76}$	$2j_{80} + j_{20}$	$2j_{84}$	$2j_{88} + j_{22}$	$2j_{92}$	$2g_{96} + j_{24}$
3	$3j_{114}$	$3j_{120}$	$3j_{126} + j_{14}$	$3j_{132}$	$3j_{138}$	$3j_{144} + j_{16}$
4	$4j_{152}$	$4j_{160} + 2j_{40} + j_{10}$	$4j_{168}$	$4j_{176} + 2j_{44}$	$4j_{184}$	$4j_{192} + 2j_{48} + j_{12}$
5	$5j_{190}$	$5j_{200} + j_8$	$5j_{210}$	$5j_{220}$	$5j_{230}$	$5j_{240}$
6	$6j_{228}$	$6j_{240} + 3j_{60}$	$6j_{252} + 2j_{28}$	$6j_{264} + 3j_{66}$	$6j_{276}$	$6j_{288} + 3j_{72} + 2j_{32} + j_8$
$\vdots$	$\vdots$	$\vdots$	$\vdots$	$\vdots$	$\vdots$	$\vdots$
k	g_{50}	g_{52}	g_{54}	g_{56}	g_{58}	g_{60}
2	$2j_{100}$	$2j_{104} + j_{26}$	$2j_{108}$	$2j_{112} + j_{28}$	$2j_{116}$	$2j_{120} + j_{30}$
3	$3j_{150}$	$3j_{156}$	$3j_{162} + j_{18}$	$3j_{168}$	$3j_{174}$	$3j_{180} + j_{20}$
4	$4j_{200}$	$4j_{208} + 2j_{52}$	$4j_{216}$	$4j_{224} + 2j_{56} + j_{14}$	$4j_{232}$	$4j_{240} + 2j_{60}$
5	$5j_{250} + j_{10}$	$5j_{260}$	$5j_{270}$	$5j_{280}$	$5j_{290}$	$5j_{300} + j_{12}$
6	$6j_{300}$	$6j_{312} + 3j_{78}$	$6j_{324} + 2j_{36}$	$6j_{336} + 3j_{84}$	$6j_{348}$	$6j_{360} + 3j_{90} + 2j_{40} + j_{10}$
$\vdots$	$\vdots$	$\vdots$	$\vdots$	$\vdots$	$\vdots$	$\vdots$

Table 11: Periodicity of the coefficients g_n for $c = 24k$ extremal partition functions $\mathcal{G}_k$, and for h_n coefficients of characters of the extremal vertex operator algebras $\mathcal{H}_k$ in terms of coefficients the j_{2n} of the modular function j ($k = 6$ case for h_n is not displayed since it is long but it has period 24).

$k=2$	$k=2$	$k=2$	$k=2$
g_{4i+2}	$2j_{2(4i+2)}$	h_{4i+2}	$2j_{2(4i+2)}$
g_{4i+4}	$2j_{2(4i+4)} + j_{2(2i+2)}$	h_{4i+4}	$2j_{2(4i+4)} + j_{2(2i+2)}$
$k=3$	$k=3$	$k=3$	$k=3$
g_{6i+2}	$3j_{3(6i+2)}$	h_{6i+2}	$3j_{3(6i+2)} + j_{6i+2}$
g_{6i+4}	$3j_{3(6i+4)}$	h_{6i+4}	$3j_{3(6i+4)} + j_{6i+4}$
g_{6i+6}	$3j_{3(6i+6)} + j_{2i+2}$	h_{6i+6}	$3j_{3(6i+6)} + j_{2i+2} + j_{6i+6}$
$k=4$	$k=4$	$k=4$	$k=4$
g_{8i+2}	$4j_{4(8i+2)}$	h_{8i+2}	$4j_{4(8i+2)} + 2j_{2(8i+2)} + j_{8i+2}$
g_{8i+4}	$4j_{4(8i+4)} + 2j_{2(2i+4)}$	h_{8i+4}	$4j_{4(8i+4)} + 2j_{2(2i+4)} + 2j_{2(8i+4)} + j_{8i+4} + j_{4i+2}$
g_{8i+6}	$4j_{4(8i+6)}$	h_{8i+6}	$4j_{4(8i+6)} + 2j_{2(8i+6)} + j_{8i+6}$
g_{8i+8}	$4j_{4(8i+8)} + 2j_{(8i+8)} + j_{2i+2}$	h_{8i+8}	$4j_{4(8i+8)} + 2j_{(8i+8)} + j_{2i+2} + 2j_{2(8i+8)} + j_{8i+8} + j_{4i+4}$
$k=5$	$k=5$	$k=5$	$k=5$
g_{10i+2}	$5j_{5(10i+2)}$	h_{12i+2}	$g_{12i+2} + 3j_{3(12i+2)} + 2j_{2(12i+2)} + j_{12i+2}$
g_{10i+4}	$5j_{5(10i+4)}$	h_{12i+4}	$g_{12i+4} + 3j_{3(12i+4)} + 2j_{2(12i+4)} + j_{12i+4} + j_{6i+2}$
g_{10i+6}	$5j_{5(10i+6)}$	h_{12i+6}	$g_{12i+6} + 3j_{3(12i+6)} + 2j_{2(12i+6)} + j_{12i+6} + j_{4i+2}$
g_{10i+8}	$5j_{5(10i+8)}$	h_{12i+8}	$g_{12i+8} + 3j_{3(12i+8)} + 2j_{2(12i+8)} + j_{12i+8} + j_{6i+4}$
g_{10i+10}	$5j_{5(10i+10)} + j_{2i+2}$	h_{12i+10}	$g_{12i+10} + 3j_{3(12i+10)} + 2j_{2(12i+10)} + j_{12i+10}$
		h_{12i+12}	$g_{12i+12} + 3j_{3(12i+12)} + 2j_{2(12i+12)} + j_{12i+12} + j_{6i+6} + j_{4i+4}$
$k=6$	$k=6$		
g_{12i+2}	$6j_{6(12i+2)}$		
g_{12i+4}	$6j_{6(12i+4)} + 3j_{3(6i+2)}$		
g_{12i+6}	$6j_{6(12i+6)} + 2j_{2(4i+2)}$		
g_{12i+8}	$6j_{6(12i+8)} + 3j_{3(6i+4)}$		
g_{12i+10}	$6j_{6(12i+10)}$		
g_{12i+12}	$6j_{6(12i+12)} + 3j_{3(6i+6)}$ $+2j_{2(4i+4)} + j_{2i+2}$		

For $24k$ one can expand the q^{2n} coefficients of $\mathcal{G}_k$ in terms of j coefficients which in turn can be expanded in terms of the dimensions of irreducible representations of the Monster. Table 10 demonstrates explicitly how the coefficients of the extremal $24k$ partition functions are decomposed into the coefficients of j. Observe that the pattern of the g_{2n} coefficients in the k^{th} row in table 10 is periodic with period k. The first k rows of the table of g coefficients is overall $k!$ periodic. As the periodicity holds for many coefficients, as shown in tables VII and VIII, we conjecture it continues to hold for all k. The polynomial conditions to be satisfied to find the extremal partition functions for large k become increasingly more difficult to solve with increasing k, so we do not have results for $k > 6$. Table 11 give the general periodicity.

To summarize, when $k = 1$ it is known via standard Monster Moonshine that the coefficients of j decompose into Monster representations [99]. The related extremal lattices are Leech in 24 and P_{48} in 48 dimensions. The fact that all the higher k coefficients also decompose into Monster representations indicates that they have large symmetries containing the Monster and the fact that they have these symmetries may indicate that they are related to $24k$ dimensional lattices, and this increases the probability that one can construct CFTs from these extermal partition functions.

5.3 Discussion, Conclusions and New Results

In the discussion section of [86] it is argued that by using $\mathbb{Z}_2$ twists of the 23 Lie type Niemeier lattices one gets holomorphic conformal field theories that are not graded isomorphic to any of the untwisted theories based on Niemeier lattices. What we have shown is that there exists a family of transformations, not necessarily of the simple $\mathbb{Z}_2$ form, that connects the members of the class of holomorphic conformal field theories, i.e., the Niemeier lattices. Furthermore these transformations connect non-Niemeier modular invariant $c = 24$ Θ-functions. These results generalize to any $c = 24k$ case (in particular, when the resulting parametrization corresponds to $24k$ dimensional lattice). We also found interesting patterns of periodicity related to the Monster Moonshine.

It is not clear what some of the non-lattice structures are. For instance, if we transform a subcomponent of a lattice by multiplying by a constant C it changes the number of points in the layers of that subcomponent. If we require the number

of points in a layer to be an integer (and the spacing between points in each layer to be uniform), then C must be a rational fraction. If we start with a lattice built from a set of Jacobi-θ functions, then we can change the number of points in sets of layers by multiplying the Jacobi-θ's by C_i's, with the only requirement that the coefficients in a q-expansion of a lattice are positive integers. We can also change the number of points on a lattice by adding (discrete amounts of) curvature, positive (negative) curvature reduces (increases) the number of points. So the transformation of a subcomponent of a lattice by multiplying by a rational fractional is in some sense equivalent to adding curvature. This will in general not be compatible with maintaining the integrity of the lattice, although we could still generate a perfectly acceptable partition function. Indeed in 24 dimensions, if we start with a Niemeier lattice, we can make many fractional transformation that lead to an even self-dual partition function, but most of these are not lattices (since we know there are only 24 Niemeiers). We expect the same to be true if we start with a $24k$ dimensional lattice and transform. There will be a large number of modular invariant partition functions generated, but only a limited number will correspond to even self-dual lattices.

In 24 dimensions there is one extremal partition function, corresponding to a Leech lattice, whose q-expansion coefficients can be written in the form of a linear combinations of dimensions of the irreducible representations of the Monster group; this relationship is at the core of the Monster Moonshine. The decomposition is possible only in the extremal case, since in all other cases a non-zero constant term in the q-expansion would be present. The presence of this term in the expansion would

imply the introduction of an enormous unnatural set of singlets in the decomposition. We believe a similar situation occurs at $24k$ where we have extended this argument. Instead of a Leech lattice we have to deal with higher dimensional extremal partition functions (but note that there is more than one type of extremal partition function in 24k dimensions). Existence of $24k$ extremal lattices for $k > 2$ is however only a conjecture [91], but our results are consistent with and provides supporting evidence for this conjecture. One can use our generalized version of Monster Moonshine to postulate that we already have the q-expansion of higher dimensional extremal lattices, and that the symmetry provided by the Monster decomposition can be used to learn more about these lattices.

Some of the results obtained here (related to the transformations between $c = 24$ CFTs) are already present in the literature [92], [106]. For example the $\mathbb{Z}_2$ patterns (in table 8) were explained in [106]. Also it was shown that from any even-self dual lattice it is always possible to construct one untwisted and twisted conformal field theory. However in our case it is enough to start from just a single even self-dual lattice to obtain all other lattice solutions by a proper choice of projection parameters. Finally there are a number of interesting open questions. For instance, is there any relation between solutions found here (including non-lattice solutions) and other solutions corresponding to higher level Kac-Moody algebras classified in [107, 108, 109].

As for new CFTs, we suggest that the extremal $\mathcal{G}$ partition functions will generate new $c = 24k$ CFTs. We know the first at $k = 1$ corresponds to the Leech lattice, the second $k = 2$ case also corresponds to the known lattice P_{48}, and since the

Table 12: Θ-functions (modular forms of weight 12) corresponding to 47 theories with a non-Abelian spin-1 algebra in Schellekens [107]. The second column represents our x parametrization of isospectral cases, when $\mathrm{Z}_0^0 = D_{16}E_8$. Coefficients a_i are the first three terms in the q-expansion of the corresponding Θ-function.

Lattice	x	a_2	a_4	a_6
$E_{8,2}B_{6,1}$	$-11/4$	360	187920	16863840
$B_{12,2}$	$-29/8$	276	189936	16842672
$C_{10,1}B_{6,1}$	$-15/4$	264	190224	16839648
$(A_{8,1})^3$, $C_{8,1}(F_{4,1})^2$, $E_{7,2}B_{5,1}F_{4,1}$	$-17/4$	216	191376	16827552
$D_{9,2}A_{7,1}$	$-9/2$	192	191952	16821504
$D_{8,2}(B_{4,1})^2\,(C_{6,1})^2B_{4,1}$	$-19/4$	168	192528	16815456
$E_{6,2}C_{5,1}A_{5,1}$, $E_{7,3}A_{5,1}$	-5	144	193104	16809408
$(B_{6,2})^2$	$-41/8$	132	193392	16806384
$(A_{4,1})^6$, $(C_{4,1})^4$, $D_{6,2}C_{4,1}(B_{3,1})^2$, $A_{9,2}A_{4,1}B_{3,1}$	$-21/4$	120	193680	16803360
$A_{8,2}F_{4,2}$	$-43/8$	108	193968	16800336
$(A_{3,1})^8$, $(D_{5,2})^2(A_{3,1})^2$, $E_{6,3}(G_{2,1})^3$, $A_{7,2}(C_{3,1})^2A_{3,1}$, $D_{7,3}A_{3,1}G_{2,1}$, $C_{7,2}A_{3,1}$	$-11/2$	96	194256	16797312
$(B_{4,2})^3$	$-45/8$	84	194544	16794288
$(A_{2,1})^{12}$, $(D_{4,2})^2(C_{2,1})^4$, $(A_{5,2})^2C_{2,1}(A_{2,1})^2$, $A_{8,3}(A_{2,1})^2$, $E_{6,4}C_{2,1}A_{2,1}$	$-23/4$	72	194832	16791264
$C_{4,2}(A_{4,2})^2$, $(B_{3,2})^4$	$-47/8$	60	195120	16788240
$(A_{1,1})^{24}$, $(A_{3,2})^4(A_{1,1})^4$, $A_{5,3}D_{4,3}(A_{1,1})^3$, $A_{7,4}(A_{1,1})^3$, $D_{5,4}C_{3,2}(A_{1,1})^2$, $C_{5,3}G_{2,2}A_{1,1}$	-6	48	195408	16785216
$(C_{2,2})^6$, $D_{4,4}(A_{2,2})^4$, $F_{4,6}A_{2,2}$	$-49/8$	36	195696	16782192
$(A_{1,2})^{16}\,(A_{2,3})^6$, $(A_{3,4})^3A_{1,2}$, $A_{5,6}C_{2,3}A_{1,2}$, $(A_{4,5})^2$, $D_{5,8}A_{1,2}$, $A_{6,7}$	$-25/4$	24	195984	16779168
$(A_{1,4})^{12}$, $D_{4,12}A_6$, $C_{4,10}$	$-51/8$	12	196272	16776144

higher k cases all possess Monster symmetry we conjecture that it is likely that they correspond to CFTs constructed on extremal lattices in $24k$-dimensions. To the best of our knowledge, Monster symmetry was not known to come into play except at $k = 1$.

Finally, let us compare with [107] where all examples have $c = 24$ and a_2 (number of spin-1 fields) divisible by 12. The Niemeier cases obviously corespond to those in our work, so we only need to consider his 47 non-Niemeier cases. We make the tentative identifications shown in table 12.

To conclude, given these assignments, when we extend our analysis to larger k values we expect: (i) a set of even self dual group lattices in $24k$-dimensions which generalize the Niemeiers, (ii) an extremal $24k$-dimensions lattice that is a generalization of th Leech lattice, and (iii) a set of $c = 24k$ CFTs that generalize the Schellekens spin-1 algebra cases.

There exists a possible application of conformal field theories (with high central charge) to cosmology, since for $k \to \infty$, $(m_{tachyon})^2 \to -k \cdot M^2_{Planck} \to -\infty$, which suggests this tachyon may be the single tachyon of $\mathcal{J}(x_k)$ and lead to some variant of a tachyon condensation [97]. Also in the case of $k \to \infty$ (hence divergent central charge [103], [104]) we can get, for example, a theory with a gauge lattice $(G)^k$. Depending on the representation content of the gauge group one could potentially partially deconstruct $(G)^k$ [105] to go from $2D$ CFT to a $4D$ theory.

The natural place for theories with $c > 24$ is in condensed matter systems, since there are not enough ghosts to cancel a conformal anomaly in string theory. Nevertheless, we hope applications of the transformation techniques investigated here may lead to further/deeper understanding of dualities relating $\mathcal{N} = 2$ heterotic string theories in $2D$ [110].

Recently our result caught the interest of mathematicians. Michael Tuite [111] showed that, the periodicity property we conjectured is a consequence of classical properties of the J-invariant and *Hecke operators*. His argument goes as follows:

The Hecke operators map the space of modular forms of weight k onto itself. The Hecke operator T_n is a transformation on modular forms indexed by a fixed integer k and any positive integer n. Thus if $f_k(\tau)$ is a modular form of weight k then so is $T_n(f_k(\tau))$ defined as:

$$T_n(f_k(\tau)) = n^{k-1} \sum_{d|n} d^{-k} \sum_{b=0}^{d-1} f_k\left(\frac{n\tau + bd}{d^2}\right) \tag{V.57}$$

For a modular invariant $f_k(\tau)$ and $n = p$, where p is prime this reduces to:

$$T_p(f_k(\tau)) = p^{k-1} f_k(p\tau) + \frac{1}{p}\sum_{b=0}^{p-1} f_k\left(\frac{\tau+b}{p}\right) = \\ = p^{-1}\left[f_k(p\tau) + f_k(\tau/p) + f_k((\tau+1)/p) + ... + f_k((\tau+p-1)/p)\right] \quad \text{(V.58)}$$

For the J-invariant (modular form of weight zero) we find in general

$$T_n(J) = J(n\tau) + ... = n^{-1}[1/q^{2n} + 0 + O(q)] \quad \text{(V.59)}$$

where $q = \exp(i\pi\tau)$. Thus $nT_n(J)$ is a modular invariant with a unique pole of order $2n$ and residue 1. This is $G_k(x_i)$ of (V.53). As we said earlier, the J-invariant is the unique (up to multiplicative and additive constants) modular invariant function with a simple pole at $q = 0$, and it defines a one to one mapping between the fundamental domain for $SL(2, Z)$ and the complex plane. (Thus the fundamental domain is a Riemann sphere which is referred to as the genus zero property for $SL(2, Z)$). A consequence of this is that every modular invariant meromorphic function is a rational function in the J-invariant. This property for the J-invariant implies $T_n(J)$ is a polynomial in J of degree n, called the *Faber polynomial* P_n, defined as follows. Let

$$f(z) = z + b(1) + b(2)z^{-1} + b(3)z^{-2} + ... = z\sum_{n=0}^{\infty} b(n)z^{-n} \equiv zw(1/z) \quad \text{(V.60)}$$

be a Laurent polynomial with $b(0) = 1$. Then the Faber polynomial [113] $P_n(f)$ in $f(z)$ of degree n is defined such that

$$P_n(f) = z^n + a(n,1)z^{-1} + a(n,2)^{-2} + ... = z^n + W_n(1/z), \quad \text{(V.61)}$$

where

$$W_n(x) = \sum_{m=1}^{\infty} a(n,m)x^m \quad \text{(V.62)}$$

Writing

$$(w(x))^n = \sum_{i=0}^{\infty} b(n,i)x^i \tag{V.63}$$

for $n = 1, 2, ...$ gives the relationship

$$\begin{aligned} b(n, n+m) = \quad & a(n,m) + b(n,1)a(n-1,m) + b(n,2)a(n-2,m) + ... \\ + \quad & b(n,n-1)a(1,m) \end{aligned} \tag{V.64}$$

connecting $b(n,m)$ and $a(n,m)$. For example for $f(z) = z$:

$$P_1(z) = z,\ P_2(z) = z^2 - 2a(2,1),\ P_3(z) = z^3 - 3a(3,1)z - 3a(3,2). \tag{V.65}$$

In our case

$$P_n(J) = 1/q^{2n} + 0 + \mathcal{O}(q)\,, \tag{V.66}$$

for the J-invariant with the q-expansion

$$J = 1/q^2 + 0 + \sum_{i>0} j_{2i} q^{2i}\,. \tag{V.67}$$

Then we have

$$P_n(J) = nT_n(J) \tag{V.68}$$

This is what is called the *replication formula* by Conway and Norton and was suitably generalized for Monstrous Moonshine. Our observations follow directly from this formula. Thus one can show using the formula for T_n that

$$P_n(J) = 1/q^{2n} + \sum_{i>0} a_n(2i) q^{2i} \tag{V.69}$$

with

$$a_n(2i) = n \sum_{r|n,r|i} \frac{j_{2ni/r^2}}{r} \tag{V.70}$$

where the sum is taken over all $r > 0$ such that r divides both n and i. We then find the periodicity in the pattern of J-invariant coefficients that were discussed in [84]. Thus for $n = 6$ we find $a_6(2i)$ given by:

$$6j_{12i} \text{ for } i = 1 \bmod 6 \tag{V.71}$$

$$6j_{12i} + 3j_{3i} \text{ for } i = 2 \bmod 6 \tag{V.72}$$

$$6j_{12i} + 2j_{4i/3} \text{ for } i = 3 \bmod 6 \tag{V.73}$$

$$6j_{12i} + 3j_{3i} + 2j_{4i/3} + j_{i/3} \text{ for } i = 0 \bmod 6 \tag{V.74}$$

These are corresponding to row 6 in Table 10. The realization of Hecke operator invariants appears for example in permutation orbifold theory [112].

CHAPTER VI

WHAT HAVE WE LEARNED ... AND FUTURE WORK

We have concentrated our research on four topics: phenomenological quantum gravity through the study of models with a broken Lorentz invariance; formal studies of lattices and their relation to Monster group; numerical calculations involving scalar fields with modes of horizon size; and investigation of new/possible black hole solutions with exotic scalar hair. The conclusions as well as possible future directions based on these studies are discussed in some detail here.

6.1 Lorentz Symmetry Violating Models

This work was dedicated to the study of a large family of phenomenological models in which Planck scale size fluctuations induce breaking of Lorentz symmetry at lower energies. Models were then tested with a variety of astroparticle processes, including interaction of ultra high energy cosmic rays with cosmic microwave background photons, TeV gamma ray interactions with IR photons, and forbidden particle decays. Our investigation revealed some characteristics of the physics at the Planck scale. Together with assumed foaminess, broken Lorentz invariance, puts restrictions on the parameter space that characterizes the models that we have discussed. Moreover, it appears that space-time foam models can extend the spectra of UHECRs or gamma-rays beyond their classical absorption thresholds on the CMB and IR background,

respectively. However, the extension of the spectrum is not satisfactory (it gives at most a factor of two) and does not explain exotic events like super GZK protons. Nevertheless, this project can be seen as a promising exploration of the effects of Planck scale physics in the energy regime accessible to current and near future experiments. Moreover, some of the features of the UHECRs like the "knee" or "ankle" could potentially be explained by second order multi-thresholds resulting from the corrections induced by a high energy cutoffs. Of course what is missing is the formalism, all of the results obtained and discussed in this work were purely phenomenological, and should be treated as an intelligent guess (we set up the scale at the Planck scale). This situation obviously must change. What's needed is the insight into theoretical and experimental physics at the astrophysical energy scales ($10^{19}eV$). Proposed experiments like Auger will resolve some of the fundamental issues. We will finally be able to prove/disprove the existence of super GZK events. The situation is less optimistic from the point of view of formalism. The theory describing Planck physics does not yet exist.

6.2 Lattices and Strings

The relation between partition functions of 24 dimensional even self-dual lattices and the Fisher-Griess Monster group were demonstrated nearly twenty years ago. We have taken an additional step by relating higher dimensional lattices and the corresponding candidates for conformal field theories to the same Monster group. This project can be seen as a generalization of the Monstrous Moonshine theorem.

This project, was motivated by an investigation of relations between $\mathcal{N} = 2$ heterotic strings in two complex dimensions with bosonic modes compactified on the 24 dimensional even self-dual lattices. We quickly realized that a new direction of research could be pursuit. We learned how to construct higher dimensional analogs of high density packing lattices, corresponding to conformal field theories described by an extremal partition functions, in higher dimensions and generalizations of Monstrous Moonshine were obtained.

Our results can be, at least partially, proved using Hecke operator algebra and its relation to the modular forms. The periodicity feature seems to hold for any extremal lattice. However since the existence of extremal lattices have been only conjectured in $24 \cdot k$ for $k > 3$, one could use the relations we found to find new extremal lattices in higher dimensions. As far as we know this has not been done yet.

Obviously it would be great to find a deeper connection to physics. Mathematically we have gained some information about the higher dimensional lattices. What are their application to physics? Analysis of other families of partition functions (like $\mathcal{H}_k$ related to vertex operator algebras) including a formal proof of the existence of periodicities is worth pursuing, as it may give a deeper insight into higher dimensional vertex operator algebras and their generalizations.

However, the amazing fact is that all of the information about these complicated algebraic structures, and the enormous sets of numbers, related in a more or less clear way to physics, is contained in the Monster group.

6.3 Cosmology and Gravity

We have discussed scalar fields non-minimally coupled to gravity, and the role they play by them during matter (from $z = 1100$ till $z = 0.4$) and vacuum dominated ($z = 0.4$ till now) epochs. We have investigated both the massive and massless cases. A WKB analysis of the solutions was performed. Horizon size modes were discussed in terms of their importance in the evolution of the universe. We have briefly discussed the processing of the density perturbation spectrum. The preliminary numerical analysis indicates that the horizon size modes could play a role in the evolution of early universe. The result of this work is then twofold, namely we have shown that non-minimally coupled canonical scalar fields $\xi \lesssim 1/6$ are allowed by current cosmological observations, which indicates that the universe is not conformally flat, and there is still the possibility for the existence of cosmological massive scalars non-minimally coupled to gravity. It is amazing that even today with all our knowledge and extremely well measured cosmological parameters we still cannot fully exclude such a possibility. What is also interesting is that massless scalars minimally coupled to gravity seems to be disfavored by cosmological data.

There are a couple of related research directions one could pursue. There is an ambiguity in the ξ parametrization of the massive non-minimally coupled scalar field, namely one can in principle always shift the value of ξ to a conformal value at the price of introducing small tachyonic mass term in the Lagrangian. Moreover, one could study other more exotic scalar field configurations, like Born-Infeld tachyons motivated by string theory or k-essence/phantom fields non-minimally coupled to

gravity.

We performed some studies in the area of black hole physics. We were engaged into a study of additional hair related to the presence of various, often exotic types of scalar fields. We have shown that for some scalar field configurations, like canonical scalars and Born-Infeld tachyons there are no asymptotically flat spherically symmetric black hole solutions. There are however examples of the fields that permit these kind of solutions. Some of the results were just a confirmation of earlier studies, known in the literature. This research proposal was merely an attempt to categorize possible extensions of the no-hair theorem in a more systematic fashion. We were motivated by the existing interest in the exotic scalars in modern cosmological models inspired by string theories and pure phenomenology. But even more general treatment of the problem can be proposed, where one would consider taking functionals of multiple scalar fields interacting with each other, and so a new hierarchy of solutions would be obtained.

Further research can be performed, for example into a direction of finding extra dimensional solutions, were more exotic topological solutions are known to exists, like black rings in five dimensions. One could in principle study no-hair theorem involving these exotic solutions in the presence of scalars resulting from compactifications of string degrees of freedom. One could in principle study the existence of nontrivial hair being a product of nontrivial couplings of gauge potentials (three/five forms) to gravity. Another possibility is to study dualities between asymptotically flat spherically symmetric black holes with a more or less complicated scalar hair and black

holes in the presence of cosmological constant (Einstein-de Sitter black holes). It is known that in this case, even canonical scalar hair is permitted. Hence, there must exist a condition which relates that hair and cosmological constant. The hair would asymptotically vanish in the limit of small value of Λ.

REFERENCES

[1] M.B. Green, J.H. Schwarz and E.Witten: Superstring Theory (Cambridge University Press, Cambridge 1984)

[2] J. Polchinski: String Theory (Cambridge University Press, Cambridge 1998)

[3] J. Schwarz: Lectures on Superstring and M theory Dualities (hep-th/9607201)

[4] D.L*ü*st and S. Theisen: Lectures on String Theory (Springer, Berlin Heidelberg, 1989)

[5] E. Kirtsis: Introduction to Superstring Theory (hep-th/9709062)

[6] C. Rovelli, Living Rev. Rel. **1**, 1 (1998) [arXiv:gr-qc/9710008].

[7] L. Bombelli, J. H. Lee, D. Meyer and R. Sorkin, Phys. Rev. Lett. **59**, 521 (1987).

[8] J. Ambjorn, A. Dasgupta, J. Jurkiewicz and R. Loll, Nucl. Phys. Proc. Suppl. **106**, 977 (2002) [arXiv:hep-th/0201104].

[9] R. Penrose and M. A. H. MacCallum, Phys. Rept. **6**, 241 (1972).

[10] A. H. Chamseddine and A. Connes, Phys. Rev. Lett. **77**, 4868 (1996).

[11] T. Kaluza, Sitzungsber. Preuss. Akad. Wiss. Berlin (Math. Phys.) **1921**, 966 (1921).

[12] O. Klein, Z. Phys. **37**, 895 (1926) [Surveys High Energ. Phys. **5**, 241 (1986)].

[13] S.Perlmutter et al., Ap.J.,565 (1999), J.L. Tonry et al, astro-ph/0305008

[14] S. L. Glashow, Nucl. Phys. **22**, 579 (1961).

[15] S. Weinberg, Phys. Rev. Lett. **19**, 1264 (1967).

[16] J. C. Pati and A. Salam, Phys. Rev. D **10**, 275 (1974).

[17] G. 't Hooft and M. J. G. Veltman, Nucl. Phys. B **44**, 189 (1972).

[18] V. A. Kostelecky, arXiv:hep-ph/0412406.

[19] M. Takeda *et al.*, Astropart. Phys. **19**, 447 (2003).

[20] Auger Collaboration, Proceedings 29^{th} ICRC, Puna, India **10** 115 (2005), astro-ph/0604114.

[21] R.U. Abbasi *et al.*, Phys. Rev. Lett., **92**, 151101 (2004).

[22] R.U. Abbasi *et al.*, Astropart. Phys **23**, 157 (2005).

[23] B. M. Connolly, S. Y. BenZvi, C. B. Finley, A. C. O'Neill and S. Westerhoff, "Comparison of the ultra-high energy cosmic ray flux observed by AGASA, HiRes and Auger," Phys. Rev. D **74**, 043001 (2006) [arXiv:astro-ph/0606343].

[24] R. Lehnert, "CPT- and Lorentz-symmetry breaking: a review," arXiv:hep-ph/0611177.

[25] V. Faraoni, "Inflation and quintessence with nonminimal coupling," Phys. Rev. D **62**, 023504 (2000) [arXiv:gr-qc/0002091].

[26] N. Makino and M. Sasaki, "The Density perturbation in the chaotic inflation with nonminimal coupling," Prog. Theor. Phys. **86**, 103 (1991).

[27] R. Borcherds, "Monstrous moonshine and monstrous Lie superalgebras," Invent. Math. **109**, 405-444 (1992).

[28] Kissing number problem. (2006, October 23). In Wikipedia, The Free Encyclopedia. Retrieved 22:14, November 25, 2006, from http://en.wikipedia.org/w/index.php?title=Kissing_number_problem&oldid=8313660

[29] G. Amelino-Camelia, T. Piran, Phys. Rev. D64 036005 (2001).

[30] Y.J. Ng, D. Lee, M. Oh, H. van Dam, Phys. Lett. B507 236-240 (2001).

[31] Y.J. Ng and H. van Dam, gr-qc/9906003.

[32] R. Aloisio, P. Blasi, A. Galante, P. Ghia, A. Grillo, Astropart.Phys. 19 (2003) 127-133; R. Aloisio, P. Blasi, P. Ghia, A. Grillo, astro-ph/0001258; R. Aloisio, P. Blasi, A. Galante, A. Grillo, astro-ph/0304050.

[33] R. Le Gallou, astro-ph/0304560.

[34] J. Alfaro and G. Palma, Phys. Rev. D67, 083003 (2003) [hep-th/0208193].

[35] R. Lehnert, gr-qc/0304013.

[36] M. Harwit, R.J. Protheroe, P.L. Biermann, Astrophys. J. 524, L91 (1999).

[37] M. Takeda *et al.*, Phys. Rev. Lett. 81, 1163 (1998); N. Gupta, astro-ph/0309421.

[38] T. Jacobson, S. Liberati, D. Mattingly, Phys. Rev. D67. 124011 (2003); Y.J. Ng, gr-qc/0305019;

G. Amelino-Camelia, astro-ph/0209232; G. Amelino-Camelia, Y. J. Ng, H. Van Dam, gr-qc/0204077; G. Amelino-Camelia, gr-qc/0309054; H. Vankov and T. Stanev, Phys. Lett. B538, 251 (2002) [astro-ph/0202388]; F. Stecker, Astropart. Phys. 20, 85 (2003) [astro-ph/0308214]; F. Stecker and S. Glashow, Astropart. Phys. 16, 97 (2001) [astro-ph/0102226]; J.R. Chisholm, E.W. Kolb, hep-ph/0306288.

[39] J. Ellis, N. Mavromatos, D. Nanopoulos, Phys. Rev. D61, 027503 (2000) [gr-qc/9906029].

[40] M. Jankiewicz, R. V. Buniy, T. W. Kephart and T. J. Weiler, "Space-time foam and cosmic-ray interactions," Astropart. Phys. **21**, 651 (2004) [arXiv:hep-ph/0312221].

[41] E. W. Kolb, S. Matarrese, A. Notari and A. Riotto, arXiv:hep-th/0503117; D. H. Coule, Class. Quant. Grav. **22**, R125 (2005) [arXiv:gr-qc/0412026]. L. Knox, arXiv:astro-ph/0503405; D. f. Zeng and Y. h. Gao, arXiv:hep-th/0503154; D. L. Wiltshire, arXiv:gr-qc/0503099; G. Geshnizjani, D. J. H. Chung and N. Afshordi, arXiv:astro-ph/0503553. E. E. Flanagan, universe?," Phys. Rev. D **71**, 103521 (2005) [arXiv:hep-th/0503202]; C. M. Hirata and U. Seljak, acceleration of the arXiv:astro-ph/0503582; A. Notari, arXiv:astro-ph/0503715; J. W. Moffat, arXiv:astro-ph/0504004; S. Rasanen, arXiv:astro-ph/0504005. B. M. N. Carter, B. M. Leith, S. C. C. Ng, A. B. Nielsen and D. L. Wiltshire, arXiv:astro-ph/0504192; S. P. Patil, arXiv:hep-th/0504145; E. R. Siegel and J. N. Fry, arXiv:astro-ph/0504421; A. A. Coley, N. Pelavas and R. M. Zalaletdinov, arXiv:gr-qc/0504115. P. Martineau and R. H. Brandenberger, perturbations," arXiv:astro-ph/0505236; J. W. Moffat, arXiv:astro-ph/0505326; M. Giovannini, arXiv:hep-th/0505222; D. f. Zeng and Y. h. Gao, arXiv:gr-qc/0506054; V. F. Cardone, A. Troisi and S. Capozziello, arXiv:astro-ph/0506371; H. Alnes, M. Amarzguioui and O. Gron, arXiv:astro-ph/0506449; E. W. Kolb, S. Matarrese and A. Riotto, arXiv:astro-ph/0506534; D. f. Zeng and H. j. Zhao, arXiv:gr-qc/0506115; M. Giovannini, arXiv:astro-ph/0506715;

[42] C. L. Bennett *et al.*, Astrophys. J. Suppl. **148**, 1 (2003) [arXiv:astro-ph/0302207].

[43] D. Hochberg and T. W. Kephart, "Diffractive Corrections To The Cosmological Redshift Formula," Phys. Rev. Lett. **66**, 2553 (1991).

[44] D. Hochberg and T. W. Kephart, "Cosmological dispersion, the corrected redshift formula and large scale structure," Phys. Rev. D **45**, 2706 (1992).

[45] D. Hochberg and T. W. Kephart, "Energy density of nonminimally coupled scalar field cosmologies," Phys. Rev. D **51**, 2687 (1995) [arXiv:gr-qc/9501022].

[46] S. S. Feng, "Local observed time and redshift in curved spacetime," Mod. Phys. Lett. A **16**, 1385 (2001) [arXiv:hep-th/0009001].

[47] V. Faraoni and E. Gunzig, "Tales of tails in cosmology," Int. J. Mod. Phys. D **8**, 177 (1999) [arXiv:astro-ph/9902262].

[48] V. Faraoni, E. Gunzig and P. Nardone, "Conformal transformations in classical gravitational theories and in cosmology," Fund. Cosmic Phys. **20**, 121 (1999) [arXiv:gr-qc/9811047].

[49] V. Faraoni and S. Sonego, "On the tail problem in cosmology," Phys. Lett. A **170**, 413 (1992) [arXiv:astro-ph/9209004].

[50] M. Sasaki, "Large Scale Quantum Fluctuations In The Inflationary Universe," Prog. Theor. Phys. **76**, 1036 (1986).

[51] S. A. Fulling, "Remarks On Positive Frequency And Hamiltonians In Expanding Universes," Gen. Rel. Grav. **10**, 807 (1979).

[52] T. Futamase and K. i. Maeda, "Chaotic Inflationary Scenario In Models Having Nonminimal Coupling With Curvature," Phys. Rev. D **39**, 399 (1989).

[53] T. Futamase, T. Rothman and R. Matzner, "Behavior Of Chaotic Inflation In Anisotropic Cosmologies With Nonminimal Coupling," Phys. Rev. D **39**, 405 (1989).

[54] L. Parker and D. J. Toms, "Explicit Curvature Dependence Of Coupling Constants," Phys. Rev. D **31**, 2424 (1985).

[55] D. N. Spergel *et al.*, arXiv:astro-ph/0603449.

[56] W. Hu and N. Sugiyama, Astrophys. J. **471**, 542 (1996) [arXiv:astro-ph/9510117].

[57] A. R. Liddle and D. H. Lyth, "Cosmological inflation and large-scale structure," Cambridge, UK: Univ. Pr. (2000).

[58] M. Heusler, Black Hole Uniqueness Theorems, Cambridge University Press Cambridge (1996).

[59] P. Bizon, Gravitating solutions and hairy black holes, Jagellonian University Preprint (1994).

[60] R. M. Wald, General Relativity, University of Chicago Press, Chicago (1984).

[61] J. D. Bekenstein, Phys. Rev. Lett., **28**, 452 (1972); C.Teitelbolm, Phys. Rev. D, **5**, 2941 (1972); M.Heusler, J. Math. Phys. **33**, 3497 (1992).

[62] A. Saa, J. Math. Phys. **37**, 2346 (1996); N. Banerjee and S. Sen, Phys. Rev. D. **58**, 104024 (1998); S. Sen and N. Banerjee, Pramana **56**, 487 (2001); A. Mayo and J. D. Bekenstein, Phys. Rev. D **54**, 5509 (1996)

[63] D. Sudarsky, Class. Quant. Grav. **12**, 579 (1995).

[64] R. Ruffini and J. A. Wheeler, in Proceedings of the Conference on Space Physics (ESRO, Paris, 1971).

[65] P. Bizon, Phys. Rev. Lett. **64**, 2844 (1990).

[66] M. Huesler, S. Droz and N. Straumann, Phys. Lett. B. **268**, 371 (1991); P. Bizon and T. Chamj, Phys. Lett. B. **297**, 55 (1992).

[67] B. Green, S. Mathur and C. O'Neil, Phys. Rev. D. **47**, 2242 (1993).

[68] T. Torii, K. Maeda and T. Tachizawa, Phys. Rev. D **51**, 1510 (1995).

[69] N. Bocharova, K. Bronikov, and V. Melnikov, Vestn. Mosk. Univ., Ser. 3: Fiz., Astron. **6**, 706 (1970);
J. D. Bekenstein, Annals Phys. **82**, 535 (1974).

[70] C. Martinez and J. Zanelli, Phys. Rev. D **54**, 3830 (1996).

[71] T. Torii, K. Maeda and M. Narita, Phys. Rev. d **64**, 044007 (2001).

[72] C. Martinez, R. Troncoso, J. Zanelli, Phys. Rev. D **70**, 084035 (2004).

[73] A. Sen, JHEP **0204**, 048 (2002).

[74] A. Sen, JHEP **0207**, 065 (2002).

[75] C. Armendariz-Picon, V. Mukhanov and P. J. Steinhardt, Phys. Rev. D **63**, 103510 (2001).

[76] T. Padmanabhan and T. R. Choudhury, Phys. Rev. D **66**, 081301 (2002)

[77] J. S. Bagla, H. K. Jassal and T. Padmanabhan, Phys. Rev. D **67**, 063504 (2003).

[78] M. C. Bento, O. Bertolami and A. A. Sen, Phys. Rev. D **66**, 043507 (2002).

[79] C. Armendariz-Picon, T. Damour, V. Mukhanov, Phys. Lett. B **458**, 209 (1999).

[80] R. R. Caldwell, Phys. Lett. B **545**, 23 (2002) [arXiv:astro-ph/9908168].

[81] J. M. Aguirregabiria, L. P. Chimento and R. Lazkoz, Phys. Lett. B **631**, 93 (2005)

[82] V. Mukhanov and A. Vikman, arXiv:astro-ph/0512066.

[83] H. P. de Oliveira, J. Math. Phys. **36**, 2988 (1995).

[84] M. Jankiewicz and T. W. Kephart, Nucl. Phys. B **744**, 380 (2006) [arXiv:hep-th/0502190].

[85] A. Karch and L. Randall, Phys. Rev. Lett. **95**, 161601 (2005) [arXiv:hep-th/0506053].

[86] L. J. Dixon, P. H. Ginsparg and J. A. Harvey, "Beauty And The Beast: Superconformal Symmetry In A Monster Module," Commun. Math. Phys. **119**, 221 (1988).

[87] W. Lerche, D. Lust and A. N. Schellekens, "Ten-Dimensional Heterotic Strings From Niemeier Lattices," Phys. Lett. B **181**, 71 (1986); A. N. Schellekens, "Classification of ten-dimensional heterotic strings," Phys. Lett. B **277**, 277 (1992) [arXiv:hep-th/9112006].

[88] J. D. Blum and K. R. Dienes, "Strong/weak coupling duality relations for non-supersymmetric string theories," Nucl. Phys. B **516**, 83 (1998) [arXiv:hep-th/9707160]; J. D. Blum and K. R. Dienes, "Duality without supersymmetry: The case of the SO(16) x SO(16) string," Phys. Lett. B **414**, 260 (1997) [arXiv:hep-th/9707148].

[89] D. Lust and S. Theisen, "Lectures On String Theory," Lect. Notes Phys. **346**, 1 (1989); W. Lerche, A. N. Schellekens and N. P. Warner, "Lattices And Strings," Phys. Rept. **177**, 1 (1989).

[90] Tom M. Apostol, "Modular Functions and Dirichlet Series in Number Theory", Graduate Texts in Mathematics, Springer-Verlag 1990.

[91] J.H. Conway, N.J.A. Sloane, "Sphere Packings, Lattices and Groups", Springer-Verlag NY (1993).

[92] L. Dolan, P. Goddard and P. Montague, "Conformal Field Theory, Triality And The Monster Group," Phys. Lett. B **236**, 165 (1990).

[93] J. A. Harvey and S. G. Naculich, "Conformal Field Theory And Genus Zero Function Fields," Nucl. Phys. B **305**, 417 (1988).

[94] L. Dolan, P. Goddard and P. Montague, "Conformal Field Theory Of Twisted Vertex Operators," Nucl. Phys. B **338**, 529 (1990).

[95] N.J.A. Sloane, "My Favorite Integer Sequences", http://www.research.att.com/∼njas/doc/sg.pdf

[96] E. M. Rains, N.J.A. Sloane, "The Shadow Theory of Modular and Unimodular Lattices", Journal of Number Theory, **73**, 359 (1998).

[97] A. A. Gerasimov and S. L. Shatashvili, "On exact tachyon potential in open string field theory," JHEP **0010**, 034 (2000) [arXiv:hep-th/0009103].

[98] C. L. Siegel, Advanced Analytic Number Theory, Tata Institute of Fundamental Research, Bombay, 1980, pp. 249-268.

[99] T. Gannon, "Monstrous moonshine and the classification of CFT," arXiv:math.qa/9906167.

[100] G. Hoehn, Selbstduale Vertexoperatorsuperalgebren und das Baby-monster, Bonner Mathematische Schriften, Vol. 286 (1996), 1-85. http://www.research.att.com/projects/OEIS?Anum=A028520

[101] R.E. Borcherds, A.J.E. Ryba, Duke Math J. 83 (1996) no.2 435-459

[102] Y. H. He and V. Jejjala, "Modular matrix models," arXiv:hep-th/0307293.

[103] A. Bilal and J. L. Gervais, "Extended C = Infinity Conformal Systems From Classical Toda Field Theories," Nucl. Phys. B **314**, 646 (1989).

[104] E. Verlinde,"On the holographic principle in a radiation dominated universe," arXiv:hep-th/0008140.

[105] N. Arkani-Hamed, A. G. Cohen and H. Georgi, "(De)constructing dimensions," Phys. Rev. Lett. **86**, 4757 (2001) [arXiv:hep-th/0104005].

[106] L. Dolan, P. Goddard and P. Montague, "Conformal field theories, representations and lattice constructions," Commun. Math. Phys. **179**, 61 (1996) [arXiv:hep-th/9410029].

[107] A. N. Schellekens, "Meromorphic C = 24 conformal field theories," Commun. Math. Phys. **153**, 159 (1993) [arXiv:hep-th/9205072]; A. N. Schellekens and S. Yankielowicz, "Curiosities At C = 24," Phys. Lett. B **226**, 285 (1989).

[108] P. S. Montague, "Orbifold constructions and the classification of selfdual c = 24 conformal field theories," Nucl. Phys. B **428**, 233 (1994) [arXiv:hep-th/9403088].

[109] P. S. Montague, "Conjectured Z(2)-orbifold constructions of self-dual conformal field theories at central charge 24: The neighborhood graph," Lett. Math. Phys. **44**, 105 (1998) [arXiv:hep-th/9709076].

[110] H. Ooguri and C. Vafa, "N=2 heterotic strings," Nucl. Phys. B **367**, 83 (1991).

[111] November 2006, private commutation.

[112] R. Dijkgraaf, G. W. Moore, E. P. Verlinde and H. L. Verlinde, "Elliptic genera of symmetric products and second quantized strings," Commun. Math. Phys. **185**, 197 (1997) [arXiv:hep-th/9608096].

[113] Schiffer, M. "Faber Polynomials in the Theory of Univalent Functions." Bull. Amer. Math. Soc. 54, 503-517, 1948; Schur, I. "On Faber Polynomials." Amer. J. Math. 67, 33-41, 1945.